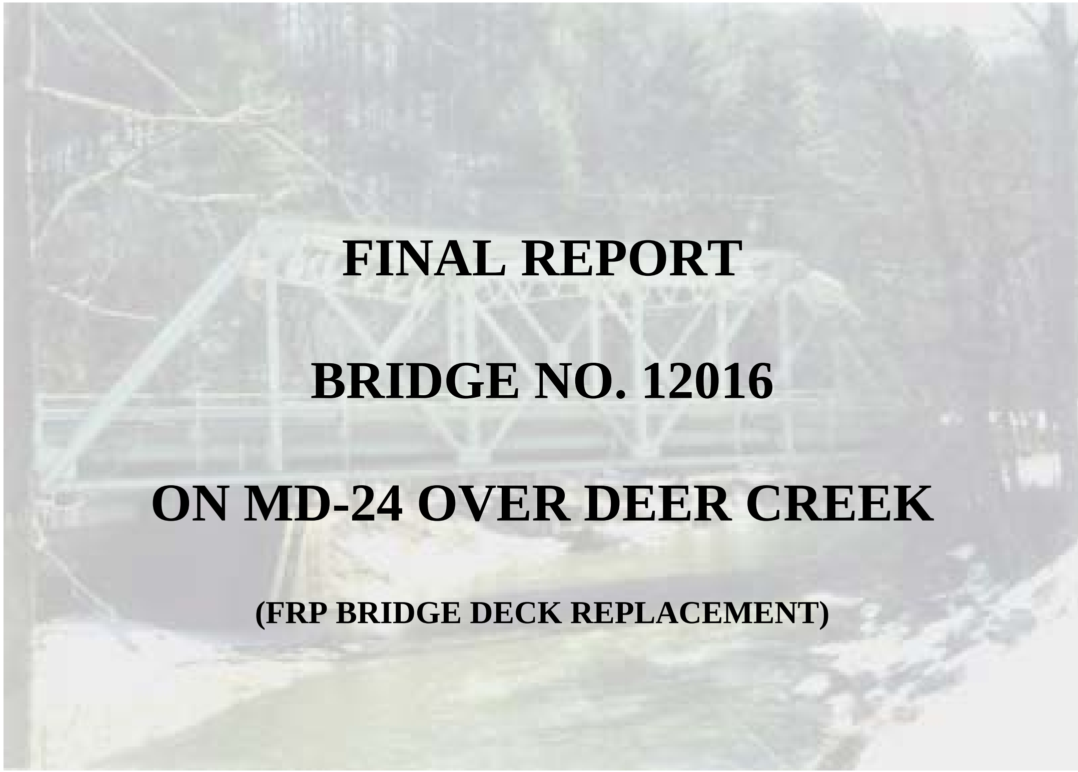

FINAL REPORT

BRIDGE NO. 12016

ON MD-24 OVER DEER CREEK

(FRP BRIDGE DECK REPLACEMENT)

Submitted to:

Maryland State Highway Administration
and
Federal Highway Administration (IBRC Program)

Prepared by

The Bridge Engineering Software and Technology (BEST) Center
Department of Civil Engineering
University of Maryland
College Park, Maryland 20742

Revision 2
December 12, 2003

Load Test Report of Bridge No. 12016 on MD-24 over Deer Creek
(FRP Bridge Deck Replacement)

TABLE OF CONTENTS

1.0 INTRODUCTION 1-1

2.0 INSTRUMENTATION AND LOAD TEST 2-1

3.0 TEST RESULTS 3-1

4.0 CONCLUSIONS 4-1

ACKNOWLEDGEMENT

Appendix A - Strain Measurement Raw Data in Graphs

Appendix B - Finite Element Model and Results in Graphs

Appendix C - Delson FRP Material Test Report provided by Martin Marietta Composites

Appendix D - Rating Factors by using LFD Method and Rating Comparisons

TABLES

Table 1.1 Description of Structure 1-1

Table 3.1 FRP Deck Properties 3-5

Table 3.2 Raw Measured Strain 3-5

Table 3.3 Calculated Neutral Axis 3-5

Table 3.4 Calculated Effective Width 3-5

Table 3.5 Verification of Test Results for Truss Members 3-6

Table 3.6 Verification of Test Results for Stringers 3-6

Table 3.7 Calculating distribution factors for interior stringers 3-7

FIGURES

Figure 1.1 Side view of MD24 over Deer Creek before Deck Replacement 1-6

Figure 1.2 Front view of MD24 over Deer Creek before Deck Replacement 1-6

Figure 1.3 Schematic of FRP Deck Panel 1-6

Figure 1.4 Concrete Abutment Diaphragm 1-7

Figure 1.5 Construction of the South End Diaphragm and the First FRP panel 1-7

Figure 1.6 Application of the Bonding Agent before the Installation of the next Panel1-7

Figure 1.7 Installation of the Mid-span Panel 1-8

Figure 1.8 Installation of the Panel at the North End 1-8
Figure 2.1 Wireless Structural Monitoring System 2-3
Figure 2.2 MD 24 Truss Bridge Instrumentation Plan 2-3
Figure 2.3 Bridge Testing Calibration 2-4
Figure 2.4 Load and Dimensional Configurations of Test Truck 2-4

1.0 INTRODUCTION

1.1 Description of the Bridge

Bridge No. 1201600 is on MD 24 over Deer Creek near Rock State Park in Harford County, Maryland (Figures 1.1 and 1.2). Description of the structure is in Table 1.1. The Federal Highway Administration's Innovative Bridge Research & Construction (FHWA-IBRC) Program awarded the Maryland State Highway Administration the first application in Maryland of a fiber reinforced polymer (FRP) bridge deck. The MD 24 bridge was chosen for the project. Most of the funding was used to acquire the FRP deck and part of the funding was used by the BEST Center, University of Maryland for the evaluation and monitoring of the bridge.

Table 1.1 - Description of Structure	
Structure Identification	Bridge #1201600
Location	MD24 over Deer Creek – in Harford County
Structure Type	5 panel steel through truss
Span Length(s)	5 panels at 24'-6" = 122'-6" c/c bearing
Truss depth	24'-6"
Skew	56-degree skew from the normal
Roadway/Structure Widths	28'-7"/33'-0"
Truss Connections	Riveted connections
Stringer Spacing	8 stringers @ 4'-1"
Members details	See attached drawings
New Deck type	7.66" FRP deck
Abutments	Concrete abutment
Structural Steel	Fy = 33 ksi, E=29,000 ksi (assumed properties)

Fiber-reinforced polymer (FRP) composites (see Figure 1.3) offer several cost-performance benefits for infrastructure applications. The material offers unique combinations of high strength-to-weight ratio, faster installation time, and reduced maintenance costs. With these benefits and years of proven performance from several pilot programs, FRP is considered as a replacement for steel, concrete, and wood used to build bridges.

The existing steel truss bridge, built in 1934, carries two lanes of traffic, provides 30′ of clear roadway, and is 123′ long. The concrete deck on this bridge was in poor condition and needed to be replaced. The Federal funding was used to replace the existing concrete deck with a fiber reinforced polymer deck and to evaluate its design, constructability, and durability. The MDSHA design team, assisted by the BEST Center, worked with manufacturers to develop plans for the replacement of the existing concrete deck with an FRP deck. When the project was near completion, the BEST Center team also installed a monitoring system to record the effects of the FRP system, including stress-strain relationships, bonding, deflection, and ultimate strength of the bridge.

1.2 Design of the FRP Deck System

The design of any bridge poses unique design challenges. Standard design details and practices must be modified to accommodate the parameters of a particular project. Working with a new design material dramatically increases the design challenges as very few standard details or practices exist to use as models.

One design challenge for this bridge was the severe roadway skew. The FRP deck panels are placed perpendicular to the stringers and act as a continuous beam between the stringer supports. A problem arises at the ends of the bridge where the skew is encountered. At this location, the edges of the panels have no bearing support. To provide this necessary support, a concrete diaphragm was placed between the existing stringers (see Figure 1.4). The installation of the concrete diaphragm also solved several of our other concerns, including how to install the compression / expansion joints, how to protect the joint and the ends of the panels from damage due to live load impacts and how to limit deflections at the ends of the bridge that cause that “uncomfortable bump” when one is driving. The diaphragm was formed such that the first 10” of the deck is concrete. This allows the compression / expansion joint to be armored with a steel angle, which protects the compression / expansion joints. It also allows for the few inches of the FRP deck to be anchored to the concrete protecting the end of the FRP deck from damage.

Another design challenge involved creating the roadway crown. The selected deck is manufactured by the protrusion method. The E-glass fiberglass strands and fabric are pulled through a die at the same time they are coated with an isophthalic polyester resin. The deck panels that are produced are perfectly flat. Therefore the accommodation of a roadway crown must be accomplished by one of two different methods. The first method is in the overlay that is applied to the FRP deck. The overlay thickness is simply varied across the deck to achieve the necessary crown and roadway cross slope. The advantage of this method is that the deck panels can be installed level without splicing the top chord of the panel, which is cheaper and quicker to install. The disadvantage of this method is that the overlay can become excessively thick and may pose problems for overhead clearance depending on the width of the bridge. It also adds weight to the deck, which lessens one of the advantages of this type of deck system – its light weight. Because the bridge did not have weight restrictions and overhead clearance was not a problem, it was decided that the roadway crown would be accommodated in the deck overlay. This would allow for a cheaper, easy installation.

The second method to accommodate the roadway crown involves cutting the top chord of the panel member at the crown location. The two halves, each side of the cut, are rotated to achieve the required crown and cross slope. This rotation opens the cut made in the top chord of the panel, which is fixed by a face sheet splice made in the field after the deck installation. It is advantageous to have the cut in the top chord of the panel member occur over a stringer to provide support, otherwise the splice must be designed for strength rather than simply closing the gap. This bridge does not have a stringer centered in the bridge cross section where the roadway crown occurs, therefore the splice would have had to be designed as a structural splice. The advantage of this method is that only a minimal overlay is required. A disadvantage is that this method is labor intensive and therefore more expensive to install. The preparation of the bridge stringers to accept the deck is also more difficult since the haunch on each stringer must be set to different elevations. Due to the added costs that served no substantial benefit for this bridge, this option was not selected.

Another design decision concerned the type of overlay to be applied over the FRP deck. An overlay is required because the surface is relatively smooth. Therefore the skid resistance is too low to meet minimum safety standards. In addition, the locations of the deck panel splices are noticeable. It has been the Maryland SHA's policy to use polymer concrete for all bridge overlays. Our objection to using asphalt is that the roadway salts used for deicing often penetrate through the asphalt and are trapped between the asphalt and the bridge deck causing deterioration of the concrete deck that cannot be seen from visual inspection. With the FRP deck, corrosion is not indicated to be a problem, therefore an asphalt overlay was acceptable for this project. Approach paving was required, thus the paving equipment would be present on site eliminating the mobilization and setup cost. The asphalt overlay is also installed much quicker and requires essentially no cure time as opposed to the polymer concrete that would require several days at a minimum. There is also a concern that a polymer concrete overlay might crack if there is any differential movement between deck panels. Several other states that have tried a polymer concrete overlay have experienced cracking at the joint locations in the FRP deck panels. Some of these cracking problems have been attributed to poor surface preparation. The Maryland SHA chose to use an asphalt deck overlay.

1.3 Advantages / Disadvantages of the FRP Deck System

FRP decks offer many advantages such as lightweight, reduced installation time, and corrosion resistance. The FRP deck installed on the MD 24 bridge weighed 25 lbs./sq. ft for the deck, connections and grout and an additional 45 lbs./sq. ft for the asphalt overlay, for a total of 70 lbs./sq. ft. This is a significant difference when compared to the 115 lbs./sq. ft for a traditional reinforced concrete deck. This large difference in dead weight allows the bridge's live load capacity to be increased. Often weight restrictions on older bridges may be removed with the installation of an FRP deck. For this bridge, the controlling loading was the HS 20 truck. Before the FRP deck installation the inventory rating was 0.92 (performed using LFD code). After installation of the FRP deck, the inventory rating was increased to 1.12 (See Appendix D for calculation).

Another advantage of FRP decks is the resistance to corrosion. The major problem with reinforced concrete decks is that cracking occurs over time allowing water and chlorides (used for roadway deicing) to penetrate the deck causing corrosion and deterioration of the concrete and steel reinforcement. This deterioration limits the life of the concrete deck to about 40 years. FRP decks have been tested in various bridge environments and corrosive environments and have experienced no deleterious effects. Ultraviolet radiation has been shown to have long term strength reductions in FRP materials. The MD 24 bridge deck will not be exposed to this radiation since it will be covered with an overlay. In addition, a protective additive has been added into the design of the FRP deck panels, which protects against any breakdown from ultraviolet radiation. This FRP deck is expected to have a design life of well over 70 years. However, this material's use in bridge decks is relatively new (less than 10 years) and therefore the life span has never been verified under actual conditions.

Another major advantage of an FRP deck is the fast installation time. An FRP deck can be installed in 1/3 the time of a conventional concrete deck. The quicker installation time can be extremely advantageous when replacing structures with high traffic volumes. Under these conditions, it is extremely important to keep traffic disturbances, delays and detours to a minimum. A cost can be associated with these delays, resulting from an increased fuel consumption and loss of time for the people sitting in the traffic. When these costs are included in a cost comparison between a concrete deck and an FRP deck, the cost of the FRP deck becomes much more competitive.

Despite all the advantages of FRP decks, there are disadvantages that must be considered in the design. One disadvantage is the proprietary nature of the product. There are only a small number of manufacturers of FRP bridge decks, all of whose systems vary in the method of production, the configuration and thickness of the deck and in the connection details used to connect the deck to the bridge. These differences present problems for projects awarded using a competitive bid process. Federally funded projects require designs to accommodate the deck systems of at least three FRP deck manufacturers or they must rely on the contractor to submit a design for the FRP deck system of his choosing for review and approval. This is not ideal because a contractor could choose an undesirable manufacturer. It is also cumbersome and costly to provide plans accommodating three different manufacturers. Therefore, neither of these options is ideal. In the future, establishing design standards could eliminate differences among FRP deck manufacturers. With set standards, contractors will become comfortable with installation procedures. This will allow the construction to be performed in much less time, resulting in reduced deck installation costs. In addition, establishing a testing agency to provide approval for manufacturing companies and their products could establish and raise standards. This would be similar to the Highway Innovative Technology Evaluation Center (HITEC) testing and review performed in the mechanically stabilized earth retaining wall industry.

Another disadvantage of this deck system is the lack of design codes / guidelines. Presently, bridge owners must rely on the manufacturers to perform designs because the engineering community lacks the education on how to design using FRP material and no AASHTO code / guidelines exist. If education were made a priority for the FRP industry, then design engineers would be more comfortable in its use. This could increase industry use that may result in a decrease in the price.

Lastly, the costs of these deck systems are currently prohibitive for wide spread use. FRP decks are usually 2 to 3 times more expensive than a conventional reinforced concrete deck. The deck on the MD 24 bridge was approximately $88/sq. ft, including the asphalt overlay, as compared to the $35/sq. ft average price for a reinforced concrete deck. This cost disadvantage can certainly be offset if life cycle costs are taken into account. However, with an increasing number of deficient bridges requiring repairs and with limited funding, State Departments of Transportation cannot easily justify rehabilitating three bridges versus ten. If other advantages are gained, such as the elimination of a weight restriction on an old bridge, then the higher cost may be justified.

1.5 Construction of the FRP Deck

The installation of the deck was easier than expected (Figures 1.5 - 1.8), but a few problems were encountered. One problem had to do with the construction of the concrete diaphragms at the abutments. These diaphragms, as mentioned, were designed to support the unsupported ends of the FRP deck panels and stiffen the deck at the expansion / contraction joints. The plan detail (see Figure 1.4) required the ends of the FRP deck panels to be anchored to the diaphragm and the last few inches of the panels to be filled with concrete. A few inches of clearance was provided between the joint angle and the end of the panels for placing this concrete within the deck panels. This space would make concrete placement difficult, but not impossible. The problem was that when all the deck panels were installed there was no clearance remaining to allow concrete to be placed within the end of the FRP deck. This was because a tight fit was not achieved at every joint. The design plans showed the joint spaces to be snug. However, in reality small gaps exist between joints resulting in a cumulative addition to length of greater than an inch. To remedy this situation, once all the deck panels were placed, the end of the deck was cut to allow adequate placement of the concrete. For future projects, the concrete end diaphragm would be made wider, allowing more room for concrete placement. In addition, the total length of the deck would take into account the growth of the panels by a small amount at each transverse panel joint.

Fortunately, Maryland SHA required a representative from the FRP deck manufacturer, involved with the design of the project to be on site during installation. This representative has valuable experience and was able to guide the contractor on how best to install the deck and offer valuable input into solving problems such as cutting of the end panels. The representative was able to arrange for the proper cutting saw to be delivered to the site immediately, in order to cut the necessary panels and properly seal the ends in a matter of hours, avoiding long delays in progress.

Figure 1.1 - Side view of MD24 over Deer Creek before Deck Replacement

Figure 1.2 - Front view of MD24 over Deer Creek before Deck Replacement

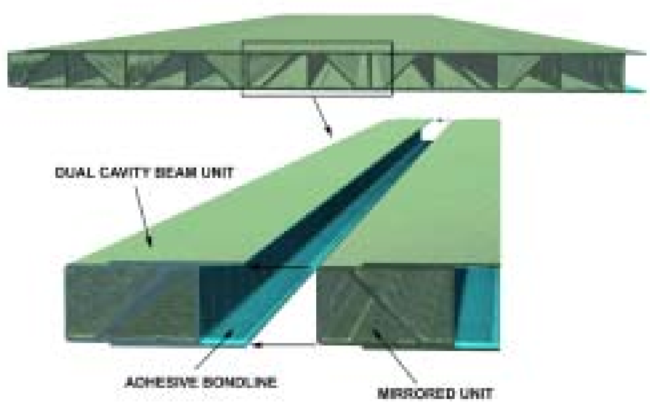

Figure 1.3 - Schematic of FRP Deck Panel

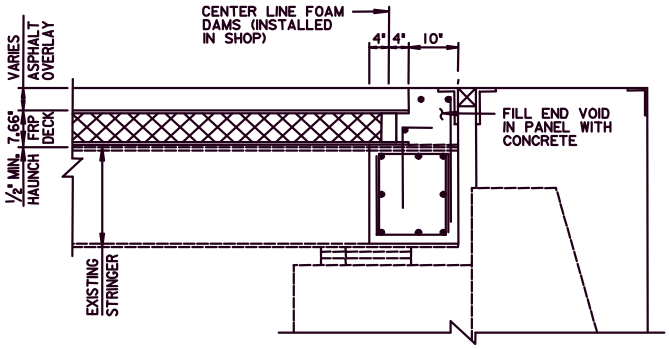

Figure 1.4 – Concrete Abutment Diaphragm

Figure 1.5 – Construction of the South End Diaphragm and the First FRP panel

Figure 1.6 – Application of the Bonding Agent before the installation of the next Panel

Figure 1.7 – Installation of the Mid-span Panel

Figure 1.8 – Installation of the Panel at the North End

2.0 INSTRUMENTATION AND LOAD TEST

2.1 Wireless Structural Monitoring System

Load tests and structural monitoring are commonly used to gain information regarding the health and performance of an existing structure. For structures using relatively new materials, such as FRP, the use of load tests can prove the structures' capacities.

Wireless structural monitoring system is a new technology developed through a previous FHWA small business innovation research (SBIR) contract to Invocon, Inc. in Conroe, Texas. This contract developed a commercially ready data acquisition system (Figure 2.1) to greatly reduce the level of effort required to instrument and obtain data from bridges. The system includes a small data acquisition and communication node connected to four strain gages that can acquire data in digital form, and relay the data to a local base receiver attached to a personal computer. Each data acquisition and communications node incorporates asynchronous two-way radio communications that operate at a "net information through-put" of 121 Kilobits/second. Also included in each node are functions for data acquisition and quantization to 16 bits, a 16-bit computer for processing and node control, and smart network control functions developed by Invocon, Inc.

In this load test, five boxes were linked in a "smart" network to control the data acquisition process and find the path of least interference for data transmission. By using this system, the effort of instrumenting a bridge was reduced by more than half compared to hard-wired systems. Besides the University of Maryland, this system is also being evaluated for bridge monitoring by researchers at FHWA, Lehigh University, and the University of Texas/Austin.

The instrumentation effort, led by Drs. Fu and Amde and assisted by Ron Nelson of the FHWA and University research assistant Hamed Al-Ayed, was conducted during the week of August 27-31, 2001. Measurements were made on various elements, including FRP deck, of the bridge under live load (Figures 2.2 and 2.3). The field tests and associated finite element analyses may provide higher confidence to the owner and users in the replaced deck of MD24 over Deer Creek Bridge and for using this new material in the future.

2.2 Instrumentation procedures

The primary goal of the instrumentation plan was to measure the live load response behavior of the bridge (truss members, floor beams, stringers, and FRP deck). All uniaxial gages CEA-06-250-UN350 installed on the bridge are produced by Measurements Group Inc. As shown in Figure 6, strain transducers were strategically located at different places to measure strains due to live load effect as follows:

- Group 1-strain transducers (1-1 and 1-2) were placed at vertical and diagonal members of the steel truss, respectively. The mission of this group was to measure the response of the mentioned members to live load.
- Group 2-strain transducers (2-1, 2-2, and 2-3) were placed at three adjacent steel stringers. These gages were useful in studying the distribution of live load between stringers at different locations (exterior and interior stringers) and the effect of the FRP deck on the distribution.
- Group 3-strain transducers (3-1, 3-2, and 3-3) were placed at the bottom of the FRP deck in the mid-span of the panel in different directions (3-1 adjacent to stringer in transverse direction, 3-2 in the middle of the distance between two adjacent stringers in transverse direction, and 3-3 adjacent to 3-2 but in the longitudinal direction). These gages can show the response of the FRP deck for live load.
- Group 4-strain transducers (4-1, 4-2, and 4-3) were placed on bottom flange, top flange of the steel stringer, and bottom of the FRP deck, respectively, in the mid-span of the panel. Using these gages, the location of neutral axis for the mentioned stringer was found, which helped to study the composite action and the contribution of the FRP in resisting compression stress. The effective width of the section could be studied too.
- Group 5-strain transducers (5-1,5-2, and 5-3) were placed at first diagonal member, bottom chord member of the steel truss, and steel floor beam, respectively. This group showed the response of those members (truss members and floor beam) to live load. This group recorded only two runs.
- Group 6 transducers (6-1, 6-2 and 6-3) were placed at the same places as 4-1, 4-2 and 4-3, respectively, but for different runs. This group recorded only one run. It was used to verify the results of group 4.
- Group 7 transducers (7-2 and 7-3) were placed at the same places as 3-2 and 3-3, respectively, but for different run. This group recorded only one run. It can be used to verify the results of group 3.

2.3 Load Test procedures

A two-axle dump truck with a gross weight of 32 Kips (Figure 2.4) was used for the controlled load test. Two paths were defined as near path (where the truck was on the side where the test instruments were installed) and far path (where the truck was on the other lane going to the other direction). Three runs were performed for each direction at different speeds. The first run was performed at a traveling speed of 10 mph for the near and far path, respectively. The second run was performed at a traveling speed of 25 mph for the near and far path. The last run for both the near and far path was performed at 47 mph traveling speed.

The transducers were installed on August 29 and 30 and the test was completed on September 6, 2001 with a vehicle provided by MD-SHA. Data was recorded continuously for each run to be processed as shown later in this report.

Figure 2.1 - Wireless Structural Monitoring System with Node Station Hard-wired to the Strain Gages but Wireless to the Base Receiver through Antenna

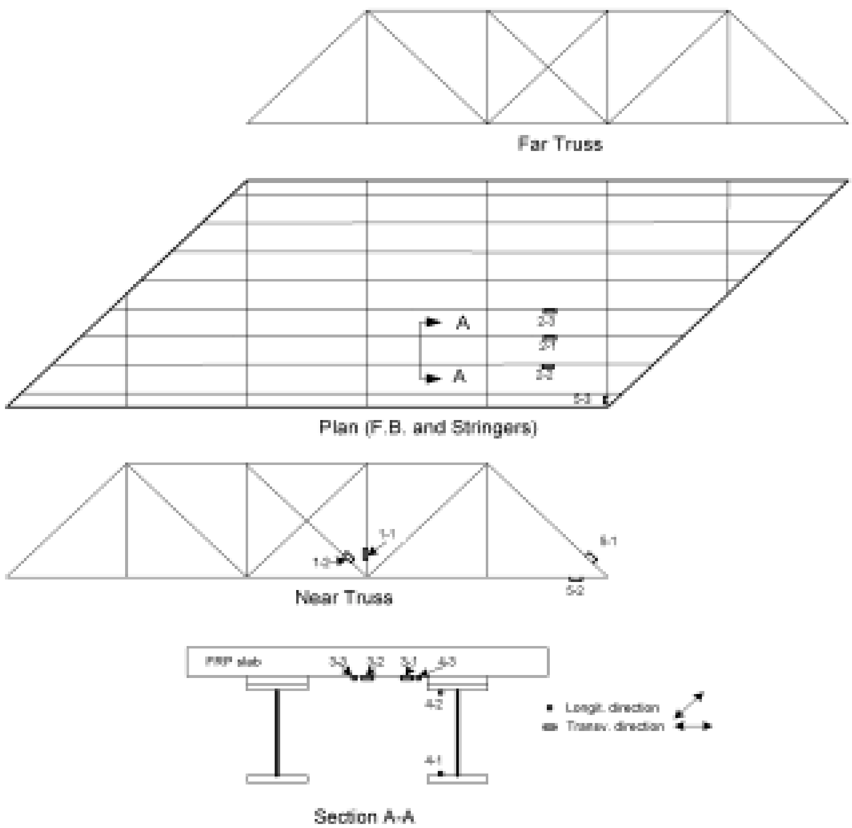

Figure 2.2 - MD 24 Truss Bridge Instrumentation Plan

Figure 2.3 - Bridge Testing Calibration of the New FRP Deck under Live Load

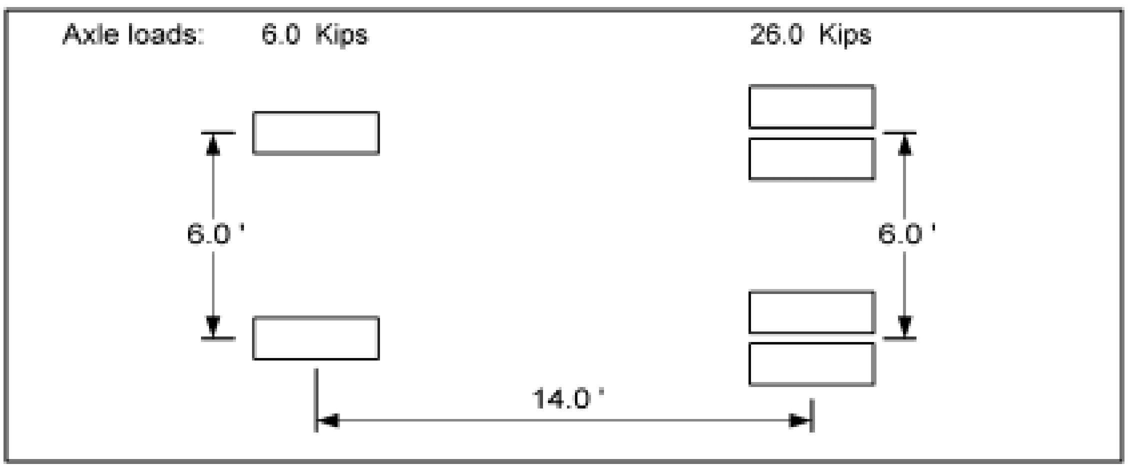

Figure 2.4 –Load and Dimensional Configurations of Test Truck

3.0 TEST RESULTS

3.1 Composite action between steel stringers and FRP deck

In order to verify the results, section and material properties had to be prepared before the final calculation. Table 3.1 shows the section properties based on the provided section and material properties provided by the manufacturer.

Table 3.2 lists the raw measured strains on the compression and tension flanges. As mentioned previously, group 4-strain transducers (4-1, 4-2, and 4-3) were placed on the bottom flange, the top flange of the steel stringer, and the bottom of the FRP deck, respectively, in the mid-span of the panel. Using these gages, location of the neutral axis for the mentioned stringer was calculated as shown in Table 3.3. For the three near runs at speed of 10, 25, and 47 mph, the neutral axis was calculated to be an average 13.77 inches above the bottom strain gage, which was placed on the top of the bottom flange of steel stringer. The neutral axis is an average 5.99 inches below the top strain gage, which was placed on the bottom of the top flange of steel stringer. Since the neutral axis is not in the middle of the stringer, this means that the FRP deck shifts the neutral axis up due to the composite action between the FRP deck and the steel stringer.

Shear studs of 2-7/8″ ϕ were provided during construction at 2-feet spacing on the top of steel stringers. Non-shrink grouting was placed in the stud pocket after welding the shear studs to give the composite action.

The next step, which is shown in Table 3.4, was to calculate the effective width of the composite section by applying equilibrium to the cross section of the steel stringer and FRP deck. Linear strain was considered along the cross section to calculate stresses and forces. The top and bottom layers of the FRP deck, which is 0.66″ in thickness each, were considered to produce force. The modulus of elasticity for the FRP, provided by Martin Marietta Composite (Appendix C), is 2800 Ksi and 29000 Ksi is used for steel. Using the linear strain, stresses were calculated for each element of the cross section. The bottom flange of the steel stringer and the steel web beneath the neutral axis produce tension. The compression is produced by the top flange of the steel stringer, the steel web above the neutral axis, and the bottom and top layers of the FRP deck. Based on the area of each element, forces produced by the steel section elements were calculated while the area of FRP elements was unknown because the width was to be calculated. By equating the tension force to the compression force of the section, the effective width of the FRP section was calculated. The effective width of the FRP section was found to be 48.85 inches where the half-space width is equal to 49 inches. Comparing the calculated effective width with the AASHTO criteria for concrete section, where the half-spacing between stringers governed in this case, the calculated width is equal to 99.7% of the effective width specified by AASHTO. The small difference (about 0.3%) can be ignored and the effective width can be considered as the half spacing between stringers.

It can be concluded that the FRP can be considered to provide forces as a composite section if the shear studs are provided as required. Also, the effective width of the FRP section can be considered as the half-spacing between stringers at least for this spacing, which is 49 inches.

3.2 FRP plate action

Longitudinal direction: As mentioned before, four transducers were located at the bottom of the FRP deck to study the plate action. In the longitudinal direction, which is parallel to the stringers, two transducers were located. The first was placed near the stringer at a distance of 7″ from the stringer web and the other was located in the middle of the FRP span between two adjacent stringers. Data was collected for these gages six times each, three of them on the near side at speeds of 10, 25, and 47 mph and the rest were on the far side at the same speeds of the former three. The data shows some inconsistency for each strain gage between readings at different speeds. The faster the speed the lower the reading is recorded for both strain gages in the longitudinal direction. In the case of the first strain gage, which was adjacent to the stringer, readings were decreased gradually as 48, 42, and 35 μs in compression at speeds of 10, 25, 47 mph, respectively. For the second strain gage, reading values recorded decreases but not gradually in this case. The recorded values were 94, 58, and 47μs at speeds of 10, 25, and 47 mph, respectively. By studying this behavior and trying to give a reasonable explanation for it, it seems that this type of transducer is not able to catch the actual strain of FRP material in the case of high speeds. Also, it can be concluded that the FRP material does not respond to load as fast as the steel or not as homogeneous and smooth as it appears, which requires using another type of transducers, maybe like the long-gage one that is used for concrete. Comparison between the readings of the two strain gages at the same speed shows another inconsistency because the second strain gage, which is in the middle between stringers, recorded higher values than the first one at all corresponding speeds, which is against expectation. Based on the measured strains, it seems there is local action along the longitudinal direction between transverse ribs due to passing of the wheels above the middle of the span.

Transverse direction: Two transducers were located in the transverse direction. The first was located adjacent to a stringer at 8″ distance from the web of the stringer where the second was located in the middle of the distance between two adjacent stringers. The two transducers recorded tension strain. The first strain gage recorded a gradually decrease of 40.5, 38.1, and 36.5 μs at speeds of 10, 25, and 47 mph, respectively. The second strain gage, which is in the middle of the span, showed a different behavior and recorded strains of 167, 106, and 115 μs at speeds of 10, 25, and 47 mph, respectively. This means that this loaded FRP span in the transverse direction is almost all under tension, which is logical that the wheels are passed above this transverse span and the adjacent transverse span has no direct load. The strain values here show that the FRP deck functions as an orthotropic plate with higher strains on both longitudinal and transverse directions between stringers.

3.3 Truss Members

Two truss members were tested successfully since saturated data results were obtained for the other two members. The two tested members were a vertical member in the middle of truss (member 16) and a diagonal member (member 18) as shown in Fig. 1. Transducers were located in the middle of the member cross section in order to eliminate any flexural effect produced by frame action due to its own weight or partial rigidity of connections. Due to symmetry of the vertical member in two directions (I –beam member), a transducer was located almost in the shear center, which coincides with the centroid; however, that could not be accomplished for the diagonal member because it is a C-channel member and has symmetry only in one direction. Direct axial loads were considered to calculate stresses and strains. A three-dimensional finite element model was developed and the ANSYS57 software program was used to perform a mathematical analysis of the bridge. Calculated and tested results are listed in Table 3.5 below. By comparing the calculated and tested results, the last column in Table 3.5 shows the percentage of difference. It is clear that the difference is small for the vertical member (3.63%). The difference for the diagonal member is larger than that for vertical member (13.73%), which means that the asymmetry in the cross section play a role here.

3.4 Stringers

Three stringers were tested to check the distribution of live load over the stringers. The tested stringers are the second, third, and fourth stringers in the first bay from the west side as shown in Fig. 1. Transducers were located on the top of bottom flanges in the middle of the span. A three-dimensional finite element model was developed and the ANSYS57 software program was used to perform a mathematical analysis of the bridge. Stringers were modeled as beam elements using BEAM4 element, which is a three-dimensional element. Each stringer was divided into two elements in order to apply loads at the midpoint of the stringer to match the tested case. Calculated and tested results are listed in Table 3.6 below. By comparing the calculated and tested results, the last column in the table shows the percentage of difference which ranges between 1.47% and 9.43%.

3.5 Distribution Factors of Stringers

The tested results of the stringers presented in section 3.4 of this report were used to calculate the distribution factors (D.F) which define the percentage of load carried by each stringer. The D.F calculated from tested results is compared with the D.F calculated using the AASHTO LRFD (1998) formula (Table 4.6.2.2.2b-1) considering the type of beams as "Concrete Deck, Filled Grid, or Partially Filled Grid on Steel or Concrete Beams …etc." Also, the D.F was calculated using the analytical results from the finite element model (ANSYS57) corresponding to the tested results and compared to D.F calculated using the AASHTO LRFD (1998) formula as mentioned above. D.F was calculated for interior stringers since the tested stringers are interiors. Comparisons are shown in Table 3.7. The maximum D.F was 0.370 and 0.383 for FEM (ANSYS57) and tested results, respectively, compared to 0.388 for the AASHTO LRFD (1998) formula. The maximum D.F was used because D.F will increase for the other two stringers if the vehicle is closer to the stringer under consideration. It is obvious that the AASHTO LRFD (1998) formula can be used as mentioned above; it gives only 4.9% and 1.3% more than FEM (ANSYS57) and tested results, respectively, which is in the conservative side.

Table 3.1 Properties

Section properties	flange thick. t_f (in)=	0.685
	haunch thick.h_t(in)=	1.87
	FRP flange thick.(in)	0.66
	Deck thick. (in) =	7.66
	bf (in) =	8.27
	tw (in) =	0.43
	spacing (in) =	49
	web height.(in) =	19.76
Modulus of Elasticity	E_{steel} (Ksi)=	29000
	E_{FRP} (Ksi)=	2800

Table 3.2 Measured strains

	Run	Comp. Strain	Tension strain
Truck on Near side	Run A	36.63	84.15
	Run C	38.37	84.66
	Run E	35.94	86.03
Average of near side		36.98	84.95
Truck on Far side	Run B	5.04	11.84
	Run D	5.84	13.77
	Run F	4.78	11.59
Average of far side		5.22	12.4

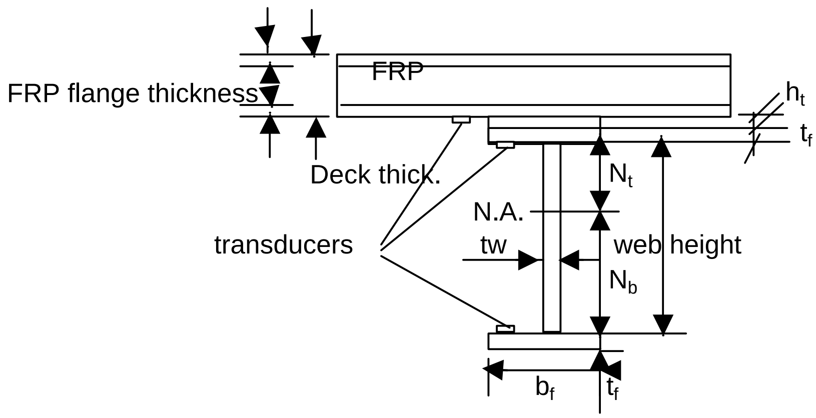

Table 3.3 Calculated Neutral Axis

	Run	Neutral Axis
Truck on Near side	Run A	13.77
	Run C	13.60
	Run E	13.94
Average of near side		13.77
Truck on Far side	Run B	13.86
	Run D	13.88
	Run F	13.99
Average of far side		13.91
N.A.above bottom flange(N_b)		13.77
N.A. below top flange (N_t)		5.99

Table 3.4 Calculated effective width

Component	Strain*10^6 in/in	Stress(Ksi)	Force (Kip)
Bottom flange	87.06	2.52	14.30
Ave. web T.	42.47	1.23	7.29
Ave. web C.	18.49	0.54	-1.38
Top flange	39.09	1.13	-6.42
Bottom FRP	54.78	0.15	to be calculated
Top FRP	97.98	0.27	
Force provided by FRP (Kips) =			13.79
Effective width of the composite section (in) =			48.85
Half-Spacing distance (in) =			49.00
% of diff. bet. calculated eff.width & half space=			0.31

Calculated Strain (bottom of FRP deck) =	52.75
Actual strain (bottom of FRP deck) =	48.00
% of diff. bet. calculated ε & measured ε =	9.89

Table 3.5 Verifying tested results with calculated results using FEM (ANSYS57) For truss members

Element	description	w/o truck	w truck	L.L. effect	Test Results*	% of Difference
16 vertical member	Axial force (Kips)	-1.2649	1.3388	2.6037		
	Stress (Ksi)	-0.08796	0.093703	0.181663		
	Strain($*10^{-6}$ in/in)	-3.03	3.23	6.26	6.5	3.63
18 Diagonal Member	Axial force (Kips)	4.2324	8.9434	4.711		
	Stress (Ksi)	0.78668	1.6623	0.87562		
	Strain($*10^{-6}$ in/in)	27.13	57.32	30.19	35	13.73

* These values were adjusted to remove the impact effect.

w/o truck : Calculated forces, stresses, and strains without the effect of truck loading.

w truck : Calculated forces, stresses, and strains with the effect of truck loading.

L. L. effect : Live load effect = w truck - w/o truck

Test Results : Tested strains recorded by testing due to truck loading.

% of Difference = [(Test Results - L. L. effect)/ Test results] * 100

Table 3.6 Verifying tested resultrs with calculated results using FEM (ANSYS57) For stringers (strains in $*10^{-6}$ in/in.)

Element	w/o truck	w/ truck	L.L. effect	Tested result	% of Difference
306	25	73	48	53	9.43
307	30	78	48		
308	27	95	68	68	1.47
309	29	95	66		
310	18	86	68	75	9.33
311	14	81	67		

* These values were adjusted to remove the impact effect.

w/o truck : Calculated forces, stresses, and strains without the effect of truck loading.

w truck : Calculated forces, stresses, and strains with the effect of truck loading.

L. L. effect : Live load effect = w truck - w/o truck

Test Results : Tested strains recorded by testing due to truck loading.

% of Difference = [(Test Results - L. L. effect)/ Test results] * 100

Table 3.7 Calculating distribution factors for interior stringers

	FEM (ANSYS57)[1]	Tested results [2]	LRFD formula [3]
Stringer 1	**0.263**	**0.270**	**0.388**
Stringer 2	**0.367**	**0.347**	**0.388**
Stringer 3	**0.370**	**0.383**	**0.388**

1- Distribution factors using results from finite element model (ANSYS57) as:

D.F @stringer j = $\dfrac{Strain@\,stringer\#\,j}{\sum_{k=1}^{n} Strain@\,k}$; where n = number of stringers.

2- Distribution factors using tested results as:

D.F @stringer j = $\dfrac{Strain@\,stringer\#\,j}{\sum_{k=1}^{n} Strain@\,k}$; where n = number of stringers.

3- Distribution factors using LRFD formula as:

D.F = $0.06+\left(\dfrac{S}{14}\right)^{0.4}\left(\dfrac{S}{L}\right)^{0.3}\left(\dfrac{k_g}{12Lt_s^3}\right)^{0.1}$; where S= spacing (ft), L=length of stringer (ft) and t_s = slab thickness (in).

4.0 CONCLUSIONS

By studying the tested results, it can be concluded that:

1. If shear studs are provided as required, FRP and the steel stringer can be considered a composite section. Non-shrink grouting can be used and placed in the stud pocket after welding the shear studs to give the composite action.
2. Effective width for FRP and steel composite sections is governed by AASHTO criteria by computing the reinforced concrete section width based on the girder spacing. However, the test result only demonstrates the calculation of the effective width for small and medium spacing between stringers (spacing for this bridge is 49”). Further tests have to be done for bridges with wider girder spacing in case other criteria, such as deck thickness or span length, govern the calculation of the effective width.
3. Local action may have an effect on plate action especially for the cases of low driving speeds. The results show that the FRP deck functions as an orthotropic plate with higher strains on both longitudinal and transverse directions between stringers.
4. FRP response to loading is not as fast as steel response. Further, the FRP material is a composite itself and may not be as homogeneous as it appears. So this type of strain gage, which is appropriate for steel, may not be the best for FRP because it may not measure the actual response at high speeds.
5. FRP slab has no negative effect on steel truss, floor beams, or stringers.
6. FRP slab has not shown any excessive deformations or unexpected responses, which increases the trust in using such material for bridges.
7. The distribution factor (D.F) can be calculated using the AASHTO LRFD (1998) formula (Table 4.6.2.2.2b-1) and considering the type of beams as “Concrete Deck, Filled Grid, or Partially Filled Grid on Steel or Concrete Beams …etc.” by taking thickness of slab as the total thickness of FRP slab.

ACKNOWLEDGEMENTS

This work was sponsored by the FHWA of US DOT and Maryland State DOT through FHWA’s Innovative Bridge Research and Construction (IBRC) Program. Thanks to William Wright and Glenn Washer of Turner-Fairbank Highway Research Center, to FHWA (TFHRC) for loaning the Invocon wireless structural monitoring system and to Ronald Nelson, also of TFHRC, for his expertise on the strain gage installation. Thanks also are due to Jeff Robert of the Maryland State DOT and project engineer of the MD24 project for his supervision and coordination and Glenn Vaughan and Jock Freedman, also of MD DOT, for the support.

Appendix A - Strain Measurement Raw Data in Graphs

- Pages A-1 & A-2: Group 1 strain transducers (1-1 and 1-2) at vertical and diagonal members of the steel truss, respectively.
- Pages A-3, A-4 & A-5: Group 2 strain transducers (2-1, 2-2, and 2-3) at three adjacent steel stringers.
- Pages A-6, A-7 & A-8: Group 3 strain transducers (3-1, 3-2, and 3-3) at the bottom of the FRP deck in the mid-span of the panel in different directions (3-1 adjacent to stringer in transverse direction, 3-2 in the middle of the distance between two adjacent stringers in transverse direction, and 3-3 adjacent to 3-2 but in the longitudinal direction).
- Page A-9: Group 7 transducers (7-2 and 7-3) at the same places as 3-2 and 3-3, respectively, but for different run. (This group recorded only one run.)
- Pages A-10, A-11 & A-12: Group 4 strain transducers (4-1, 4-2, and 4-3) on bottom flange, top flange of the steel stringer, and bottom of the FRP deck, respectively, in the mid-span of the panel.
- Page A-13: Group 6 transducers (6-1, 6-2 and 6-3) at the same places as 4-1, 4-2 and 4-3, respectively, but for different runs. (This group recorded only one run.)
- Page A-14: Group 5 strain transducers (5-1,5-2, and 5-3) at first diagonal member, bottom chord member of the steel truss, and steel floor beam, respectively. (This group recorded only two runs.)

Data1-1 A* 8.855586 -2.497729

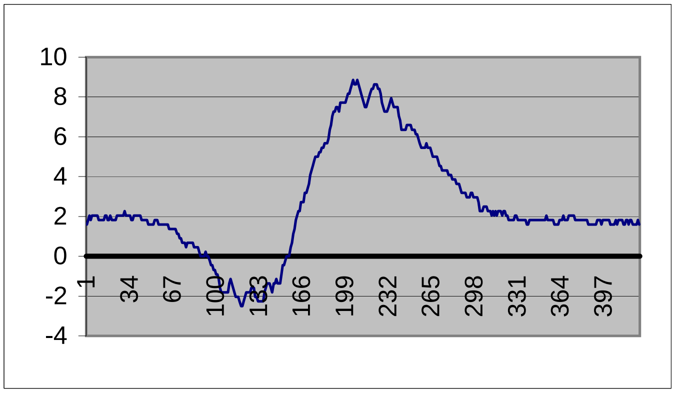

Data1-1 B* 4.087193 0

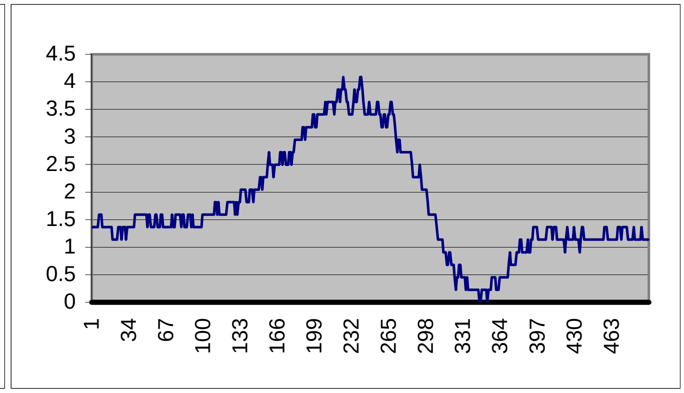

Data1-1 C* 7.493188 -5.449591

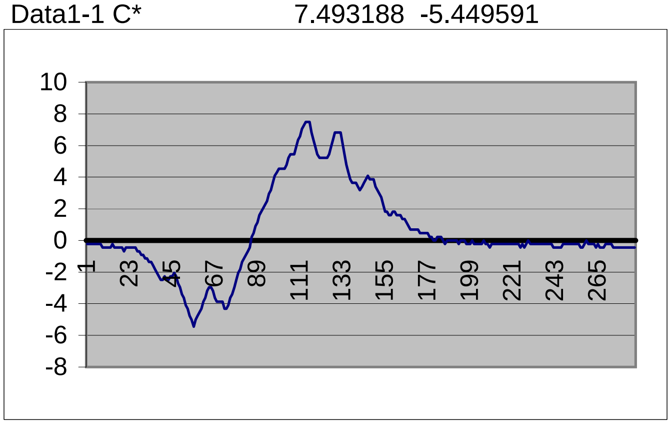

Data1-1 D* 0.227066 -3.860127

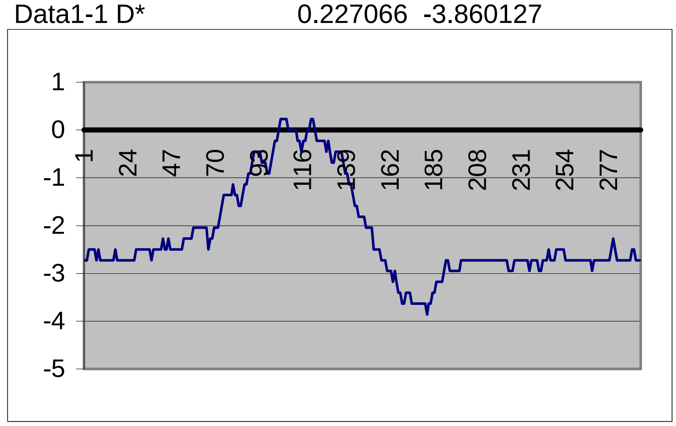

Data1-1 E* 3.633061 -8.855586

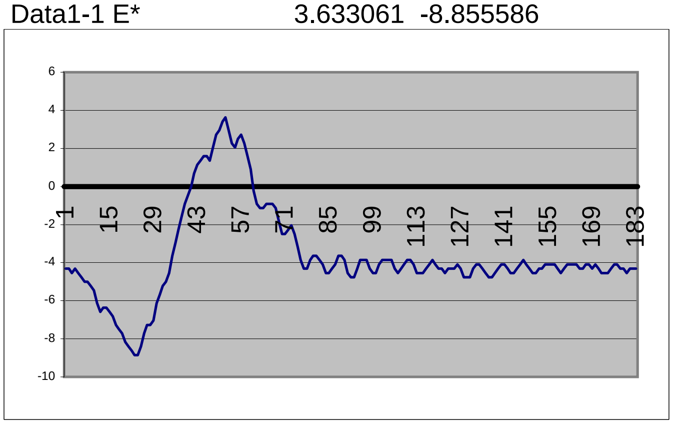

Data1-1 F* -13.85104 -21.79837

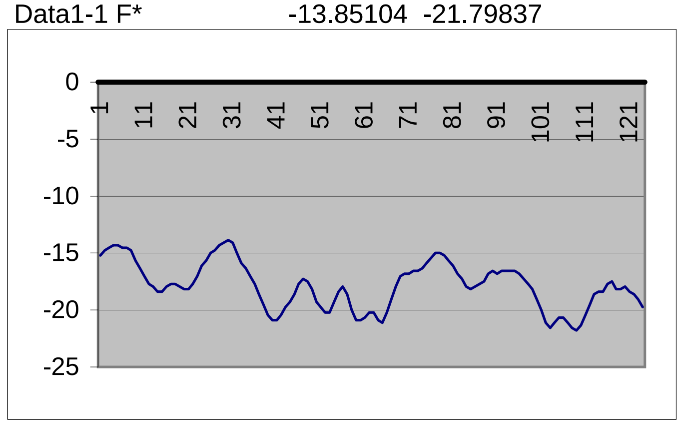

* A: Near side -10 mph speed.
B: Far side -10 mph speed.
C: Near side -25 mph speed.
D: Far side -25 mph speed.
E: Near side - 47 mph speed.
F: Far side - 47 mph speed.

Data1-2 A* 46.32153 -2.724796

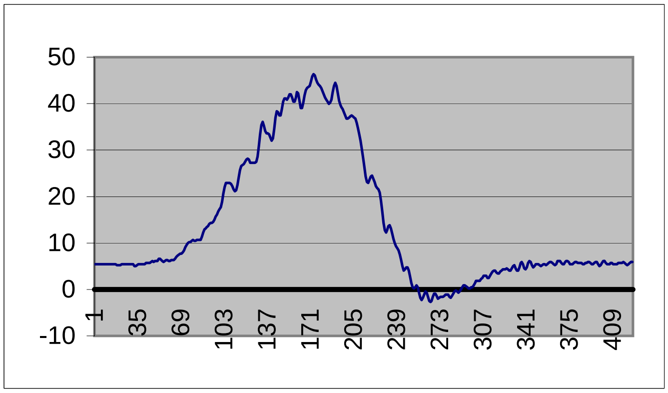

Data1-2 B* 22.9337 2.270663

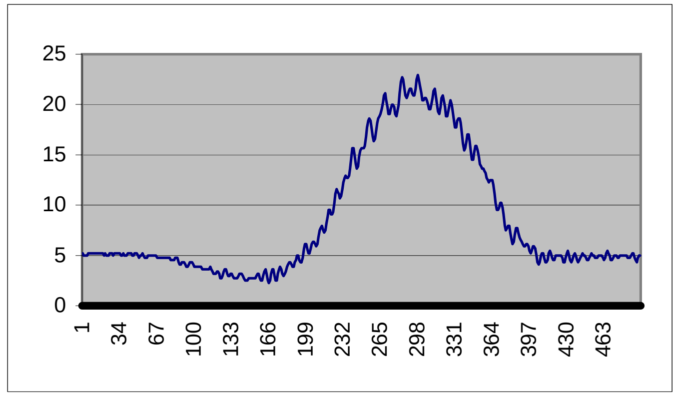

Data1-2 C* 45.64033 -4.768392

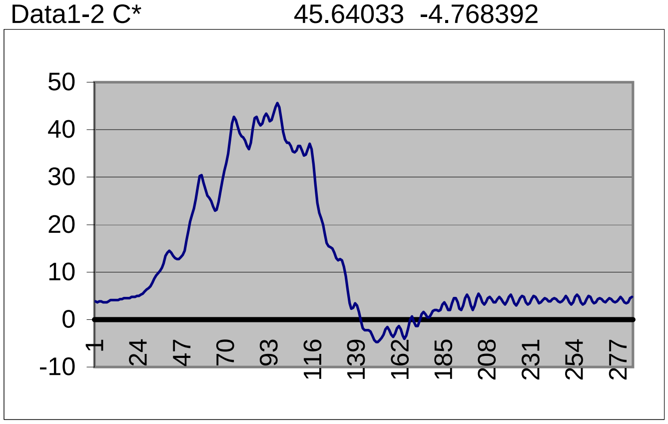

Data1-2 D* 22.02543 -1.135332

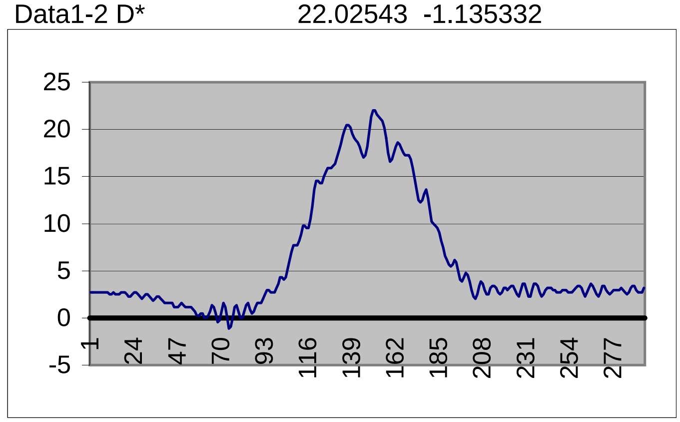

Data1-2 E* 51.77112 -8.401453

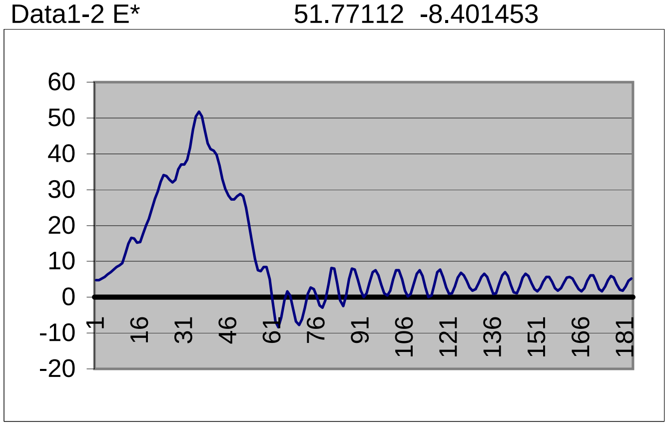

Data1-2 F* 22.70663 0.227066

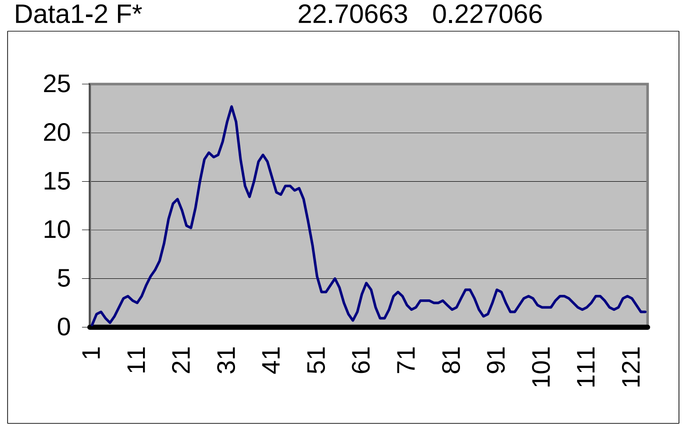

* A: Near side -10 mph speed.
B: Far side -10 mph speed.
C: Near side -25 mph speed.
D: Far side -25 mph speed.
E: Near side - 47 mph speed.
F: Far side - 47 mph speed.

Data2-1 A* 92.18892 19.30064

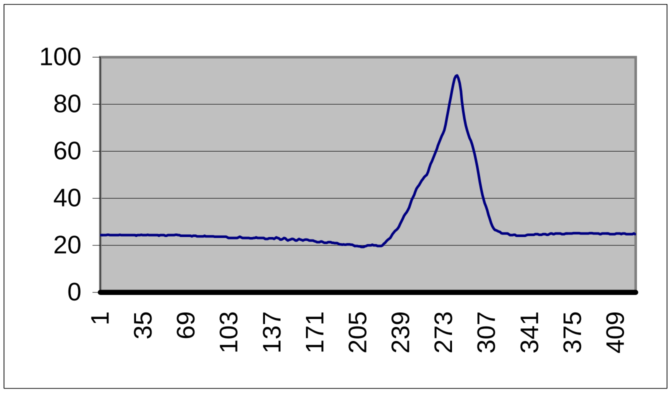

Data2-1 B* 32.69755 21.79837

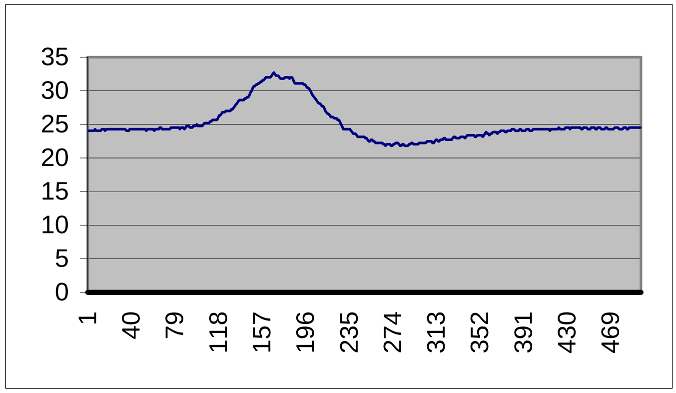

Data2-1 C* 93.55132 19.30064

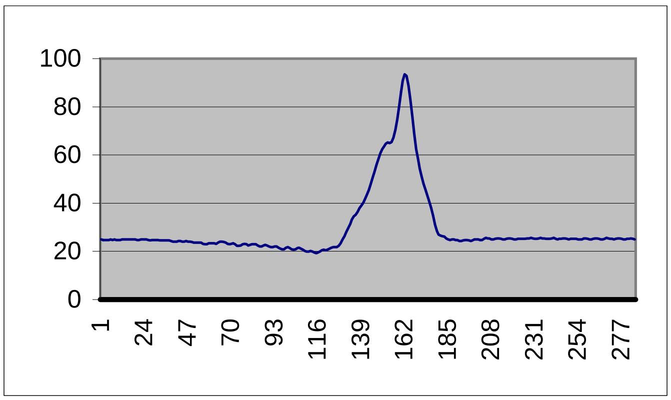

Data2-1 D* 35.87648 23.38783

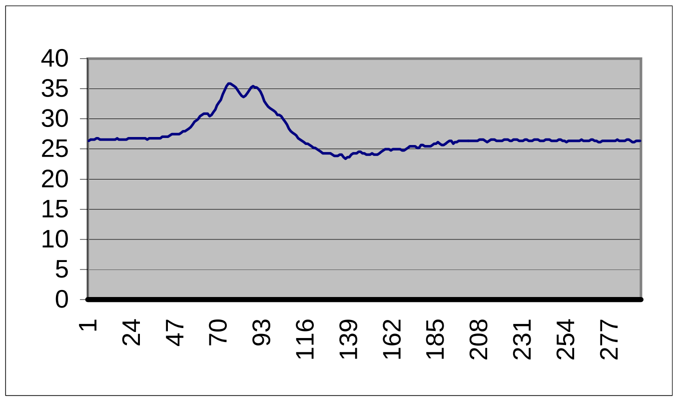

Data2-1 E* 96.27611 20.43597

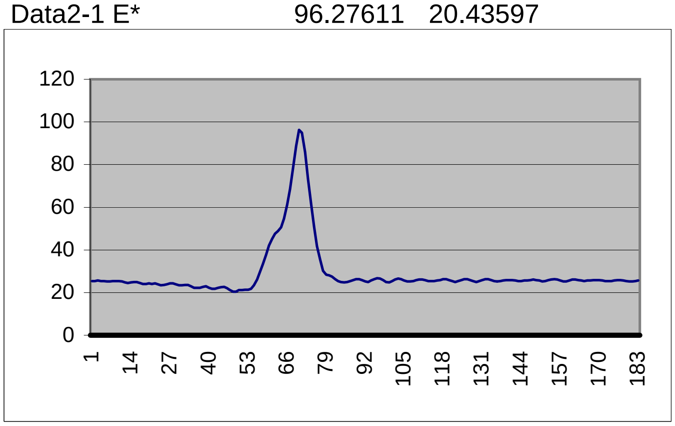

Data2-1 F* 33.83288 22.9337

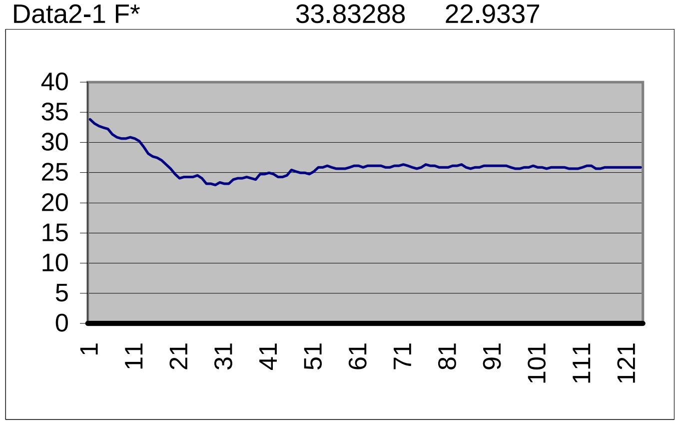

* A: Near side -10 mph speed.
B: Far side -10 mph speed.
C: Near side -25 mph speed.
D: Far side -25 mph speed.
E: Near side - 47 mph speed.
F: Far side - 47 mph speed.

Data2-2 A* 73.79655 14.98638

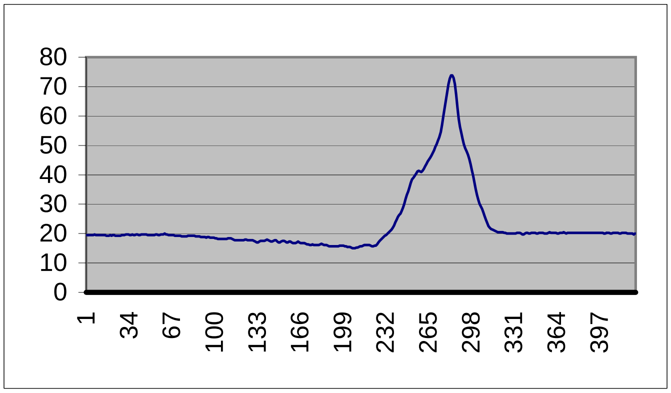

Data2-2 B* 22.9337 17.25704

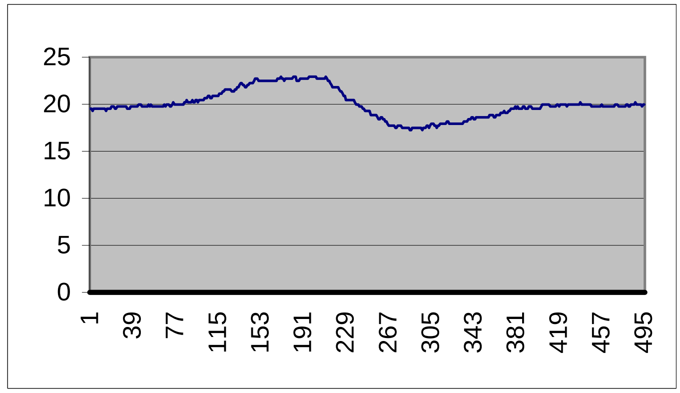

Data2-2 C* 79.92734 14.07811

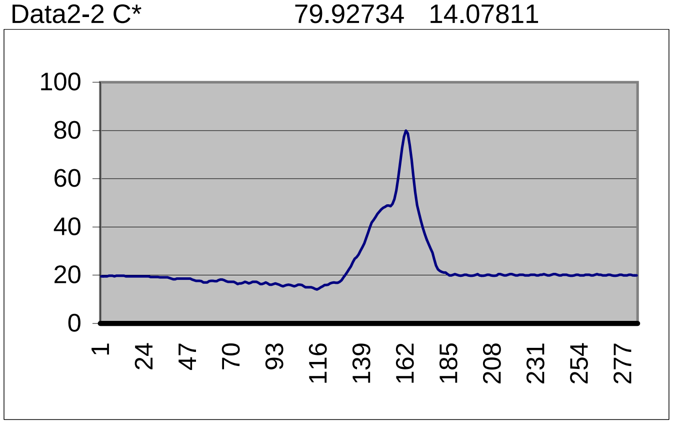

Data2-2 D* 24.97729 18.61944

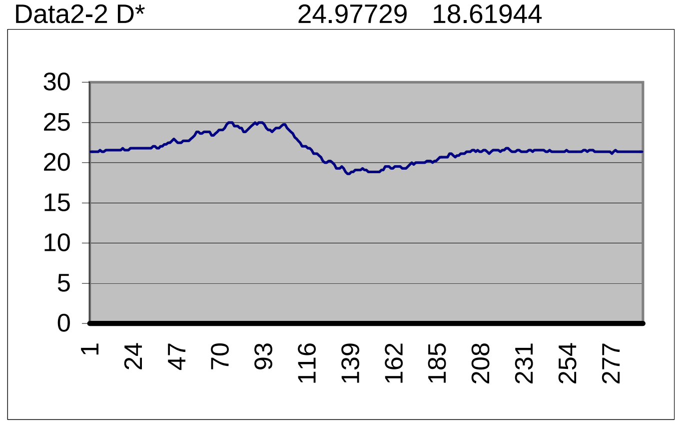

Data2-2 E* 85.14986 15.66757

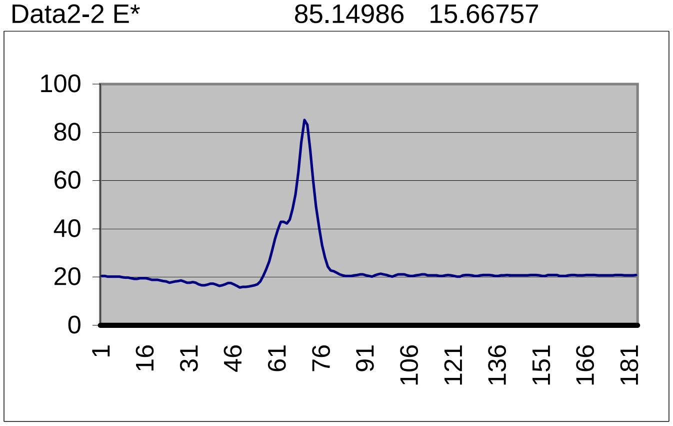

Data2-2 F* 23.84196 17.48411

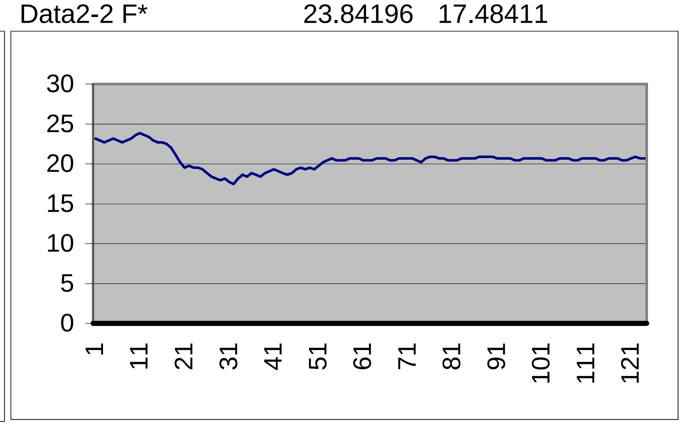

* A: Near side -10 mph speed.
B: Far side -10 mph speed.
C: Near side -25 mph speed.
D: Far side -25 mph speed.
E: Near side - 47 mph speed.
F: Far side - 47 mph speed.

Data2-3 A* 99.90917 18.39237

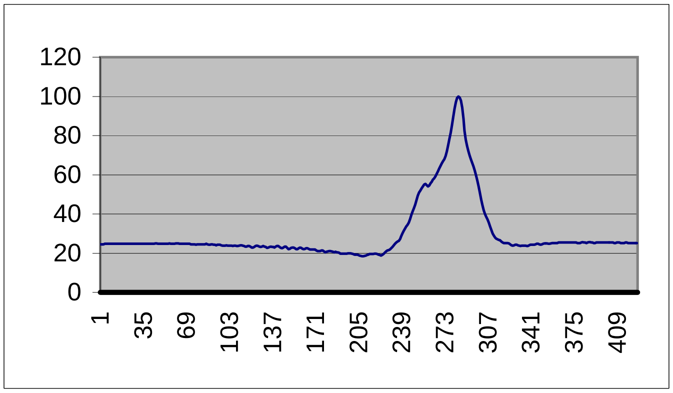

Data2-3 B* 54.72298 20.43597

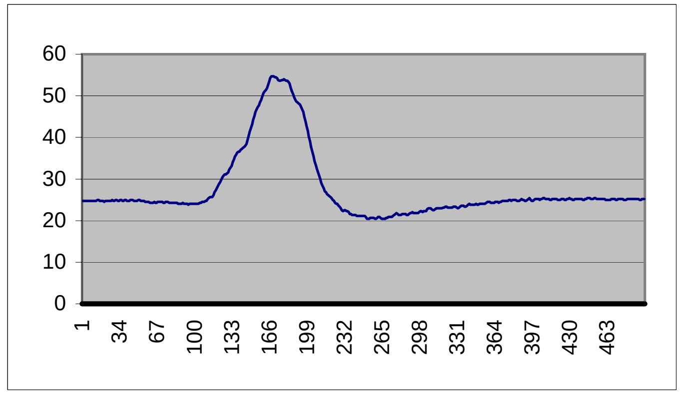

Data2-3 C* 98.54678 18.8465

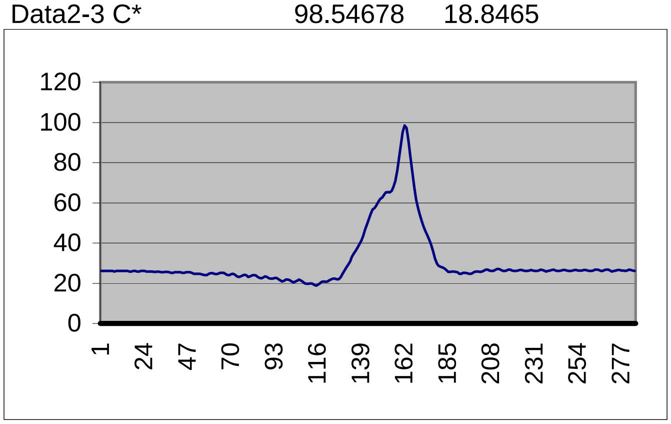

Data2-3 D* 61.3079 23.16076

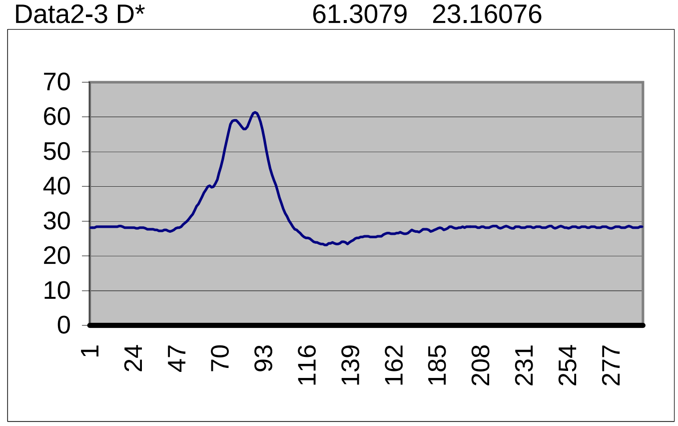

Data2-3 E* 96.04905 20.8901

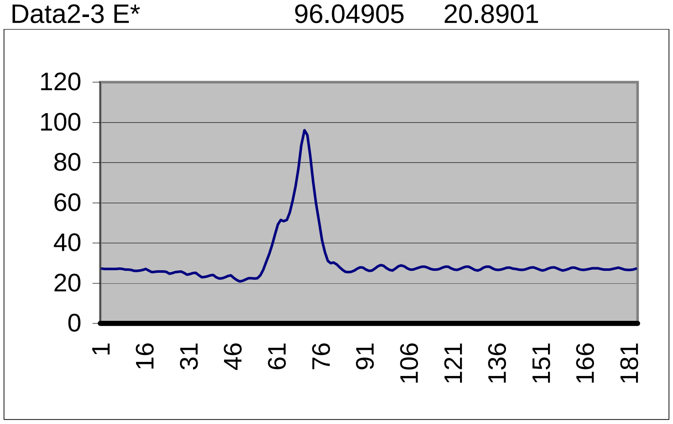

Data2-3 F* 55.17711 22.9337

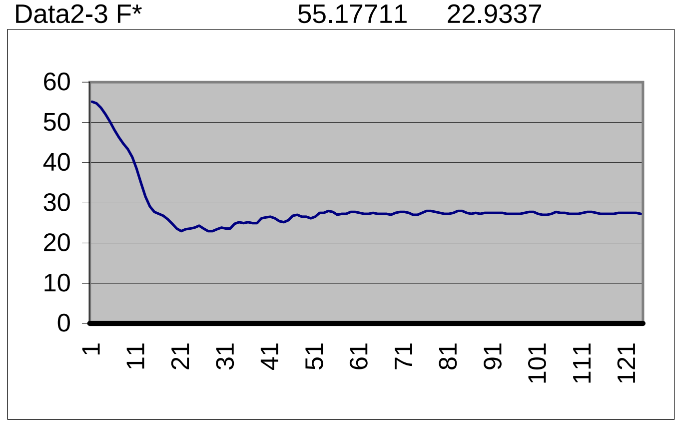

* A: Near side -10 mph speed.
B: Far side -10 mph speed.
C: Near side -25 mph speed.
D: Far side -25 mph speed.
E: Near side - 47 mph speed.
F: Far side - 47 mph speed.

Data3-1 A* 81.5168 40.87193

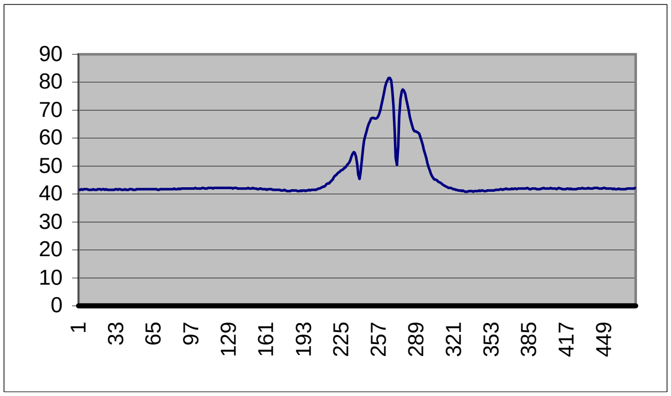

Data3-1 B* 269.9818 15.66757

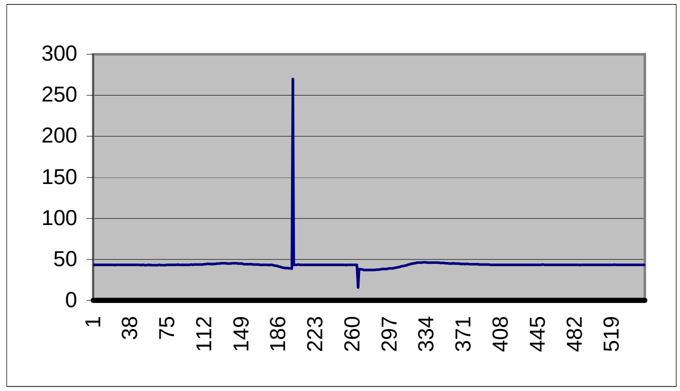

Data3-1 C* 81.06267 42.91553

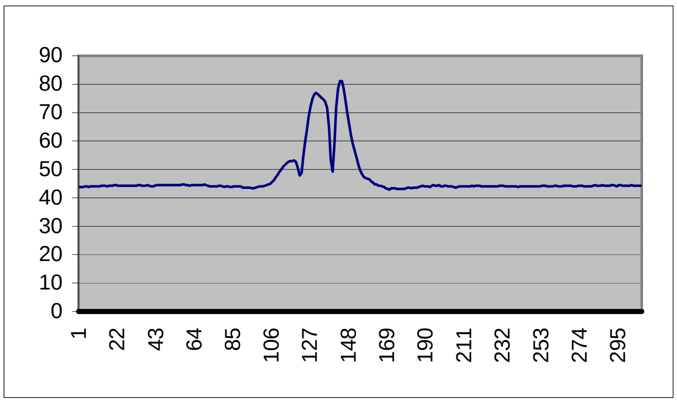

Data3-1 D* 44.505 36.10354

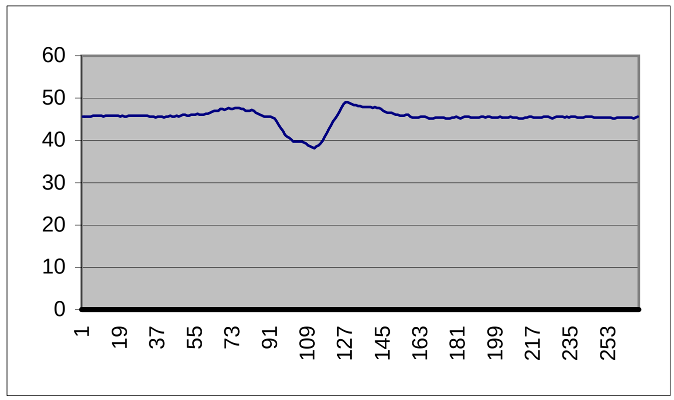

Data3-1 E* 81.5168 44.95913

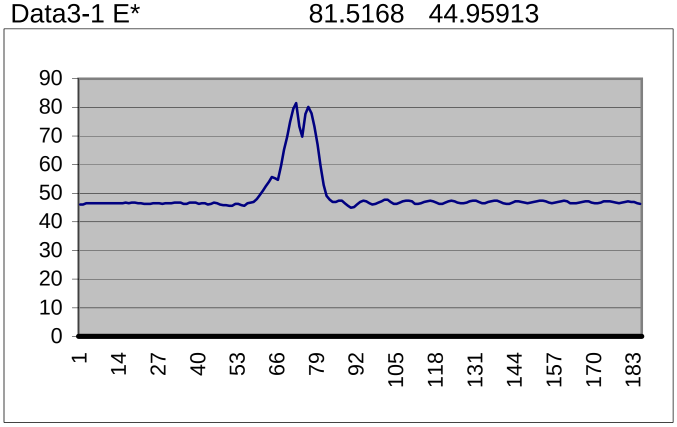

Data3-1 F* 43.59673 36.10354

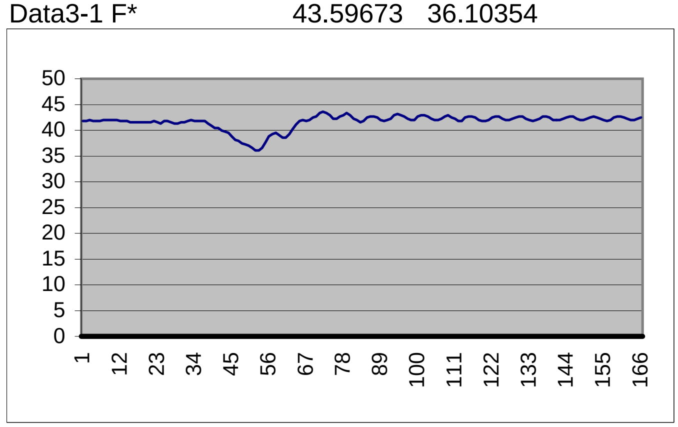

* A: Near side -10 mph speed.
B: Far side -10 mph speed.
C: Near side -25 mph speed.
D: Far side -25 mph speed.
E: Near side - 47 mph speed.
F: Far side - 47 mph speed.

Data3-2 A* 198.683 31.10808

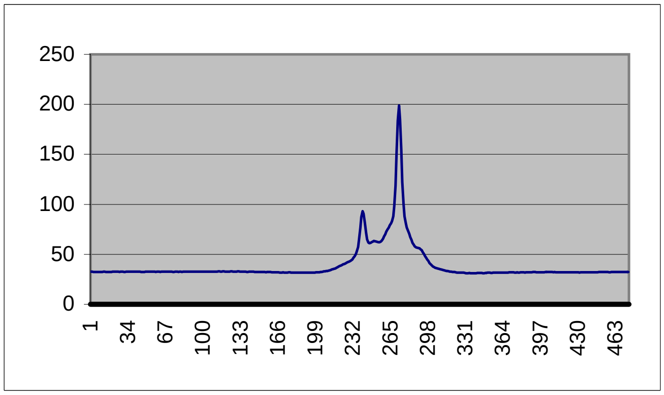

Data3-2 B* 36.78474 26.79382

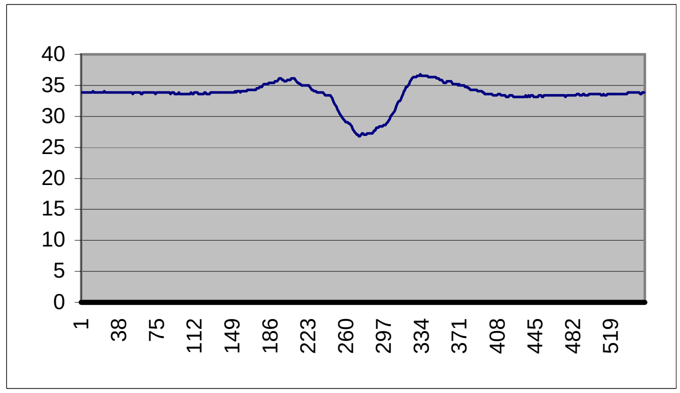

Data3-2 C* 138.9646 33.15168

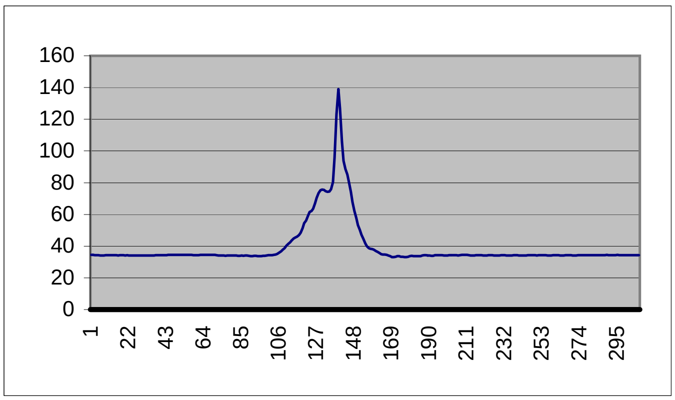

Data3-2 D* 39.96367 28.61035

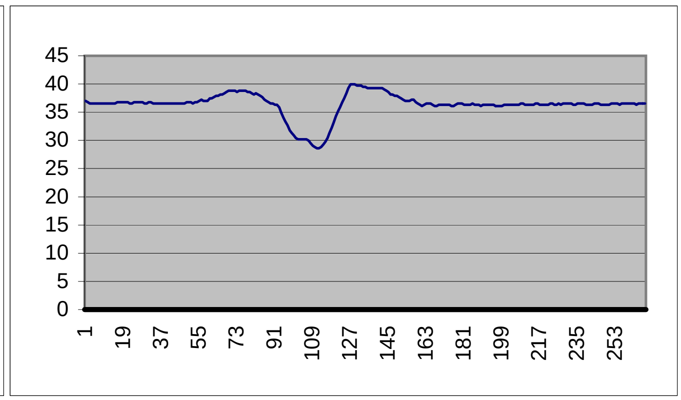

Data3-2 E* 150.545 35.64941

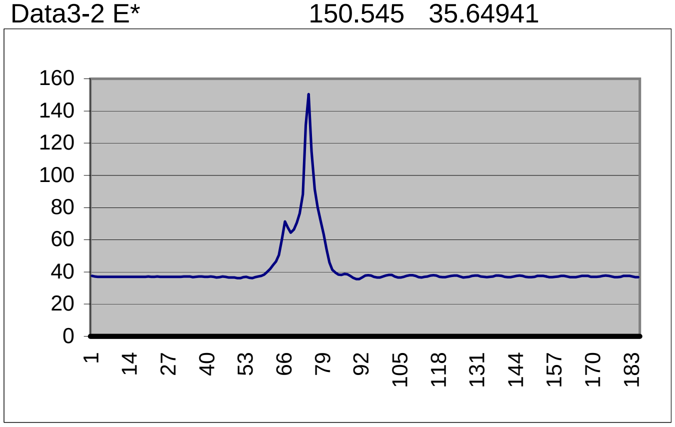

Data3-2 F* 41.32607 32.01635

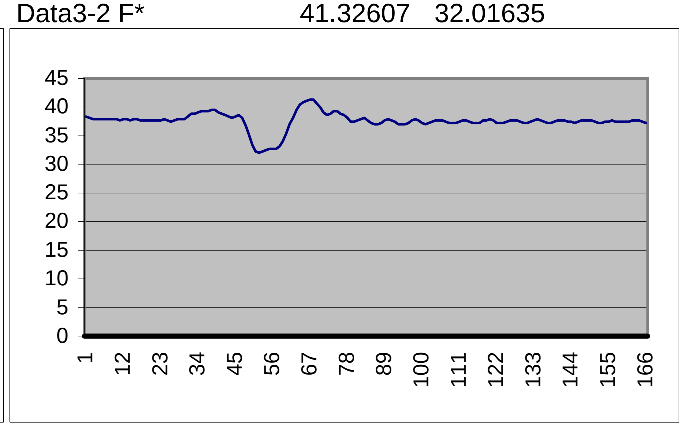

* A: Near side -10 mph speed.
B: Far side -10 mph speed.
C: Near side -25 mph speed.
D: Far side -25 mph speed.
E: Near side - 47 mph speed.
F: Far side - 47 mph speed.

Data3-3 A* 86.96639 -51.08992

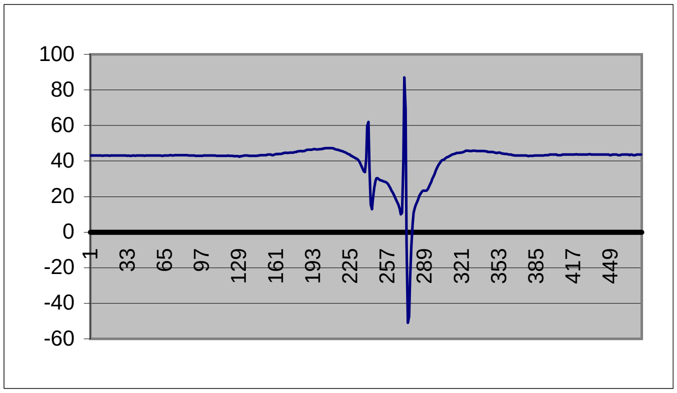

Data3-3 B* 45.18619 37.69301

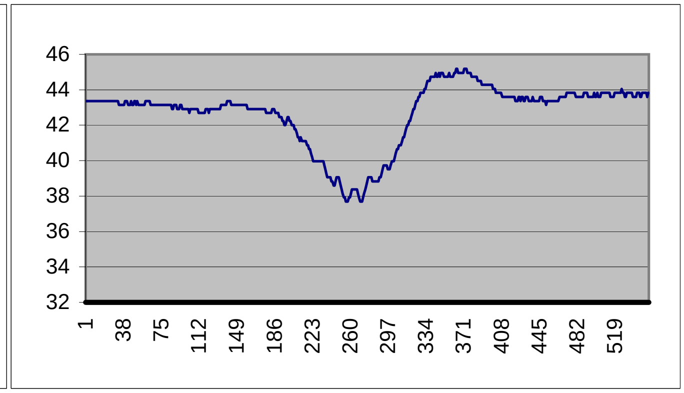

Data3-3 C* 46.54859 -15.44051

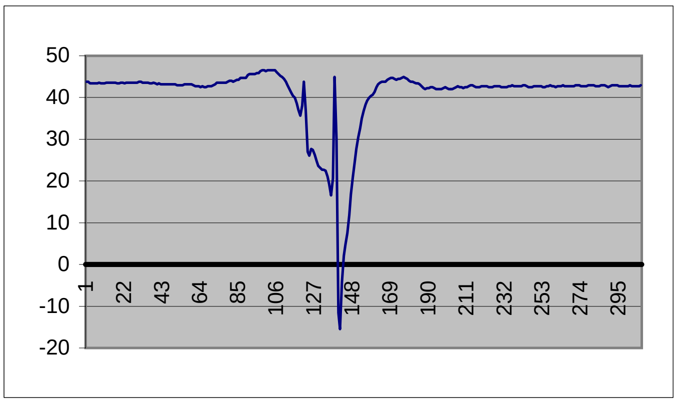

Data3-3 D* 45.86739 37.23887

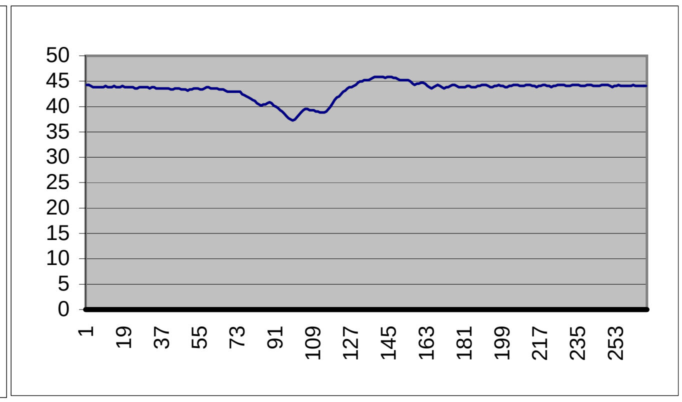

Data3-3 E* 46.77566 -3.405995

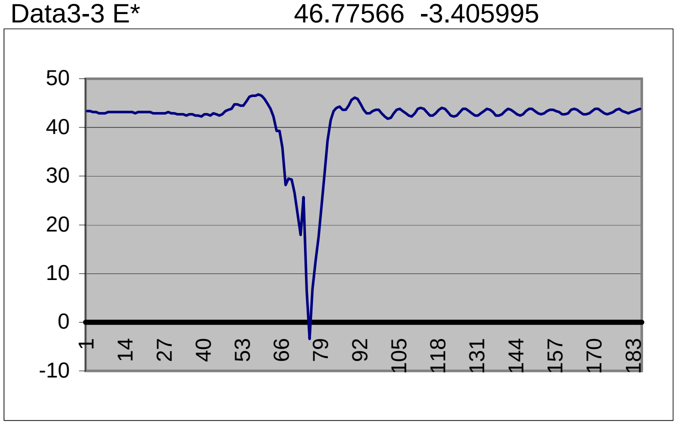

Data3-3 F* 45.41326 37.92007

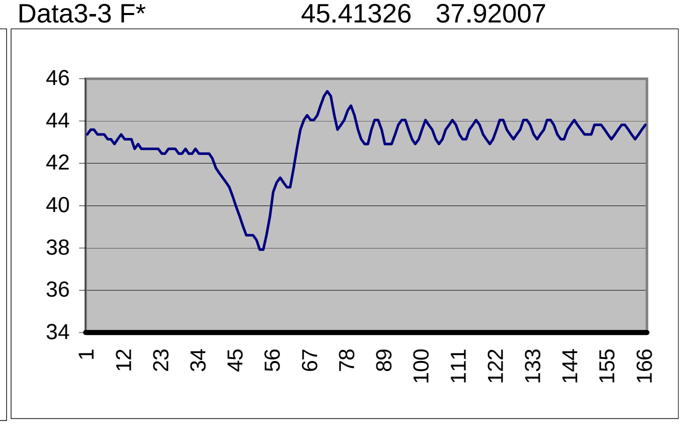

* A: Near side -10 mph speed.
B: Far side -10 mph speed.
C: Near side -25 mph speed.
D: Far side -25 mph speed.
E: Near side - 47 mph speed.
F: Far side - 47 mph speed.

Data1A-72 191.644 34.74114

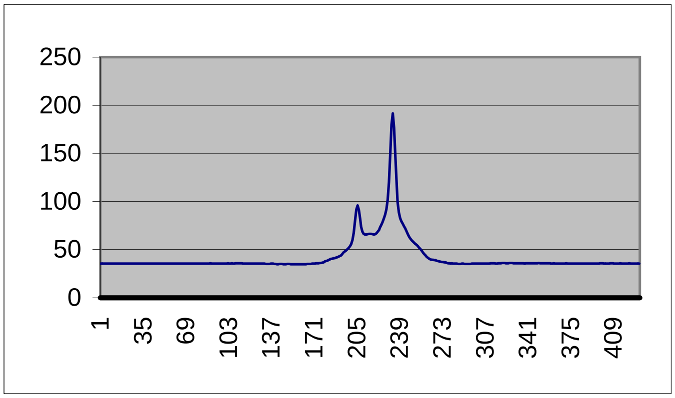

Data1A-73 46.09446 -50.40872

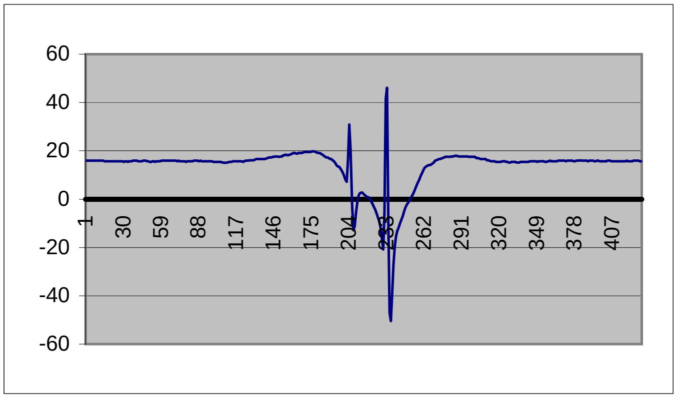

Data4-1 A* 99.45504 8.855586

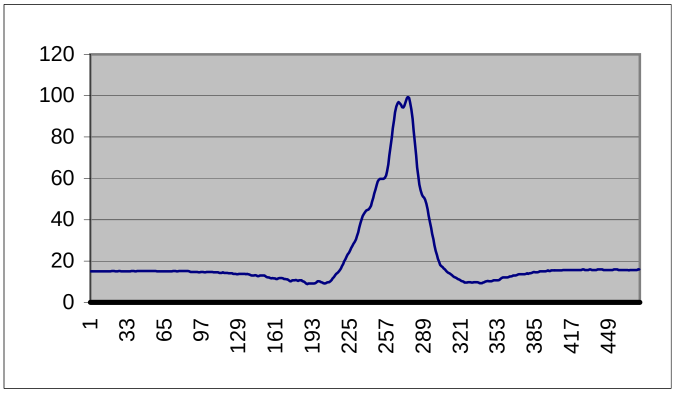

Data4-1 B* 27.47502 12.48865

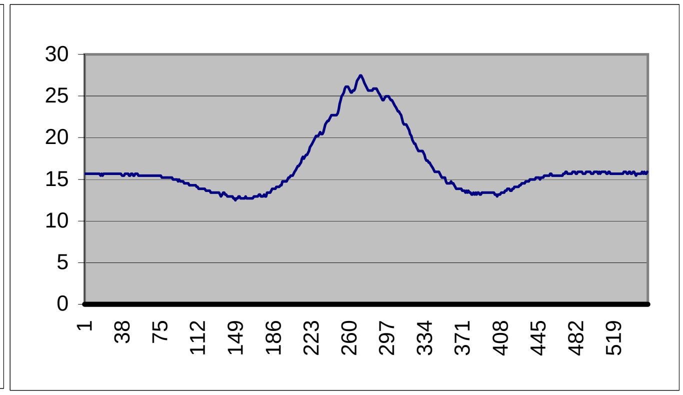

Data4-1 C* 101.2716 9.763851

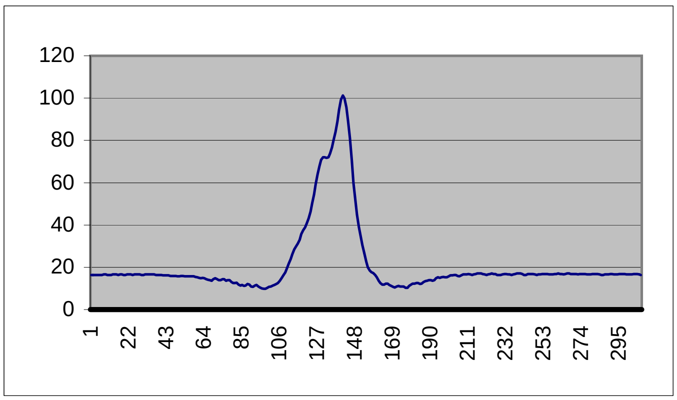

Data4-1 D* 30.88102 13.39691

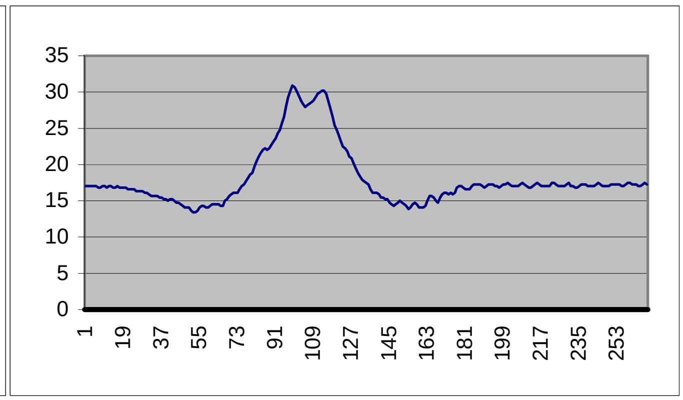

Data4-1 E* 103.3152 9.309718

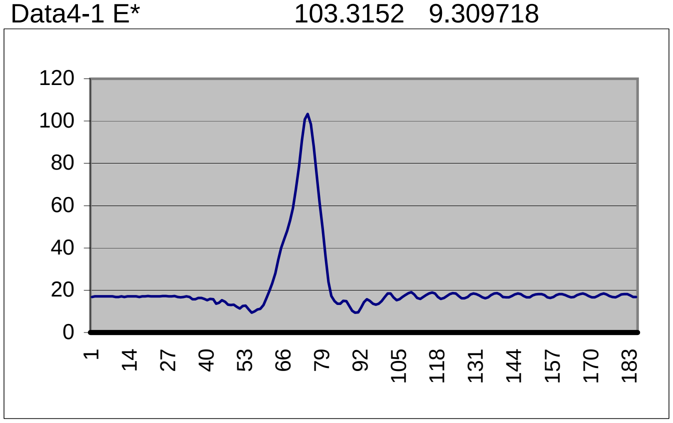

Data4-1 F* 29.51862 14.07811

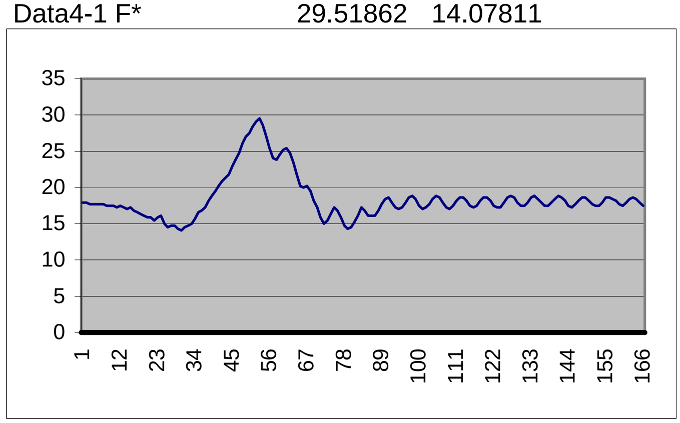

* A: Near side -10 mph speed.
B: Far side -10 mph speed.
C: Near side -25 mph speed.
D: Far side -25 mph speed.
E: Near side - 47 mph speed.
F: Far side - 47 mph speed.

Data4-2 A* 23.6149 -15.66757

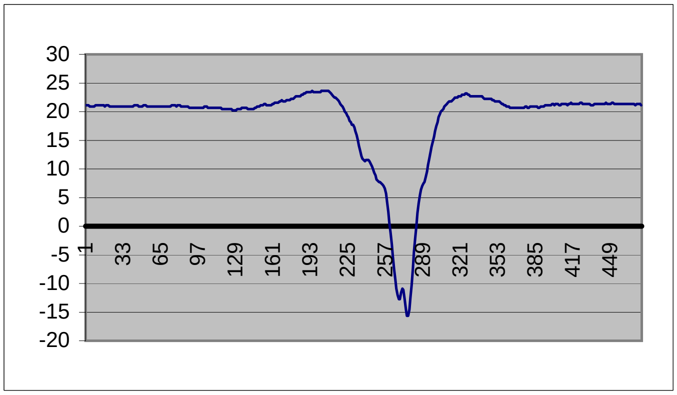

Data4-2 B* 22.9337 16.80291

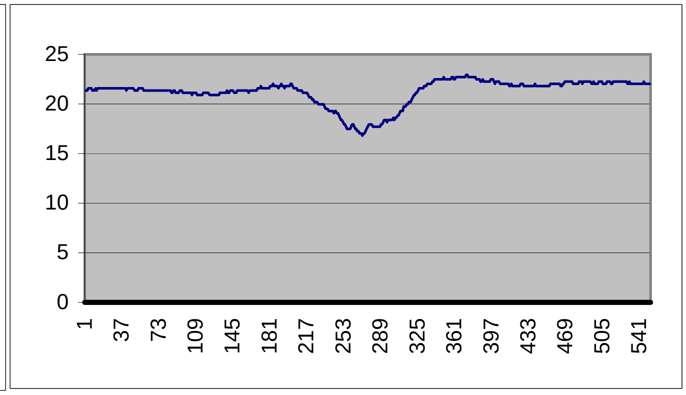

Data4-2 C* 24.75023 -13.62398

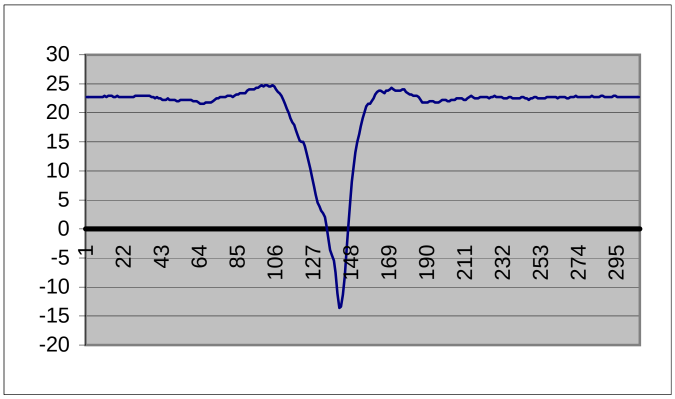

Data4-2 D* 23.84196 17.02997

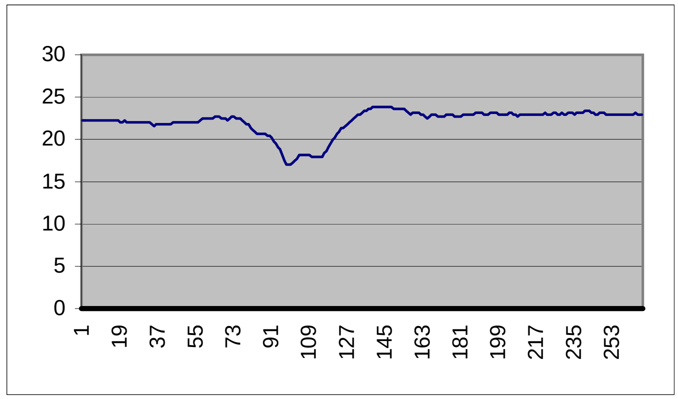

Data4-2 E* 24.75023 -13.16985

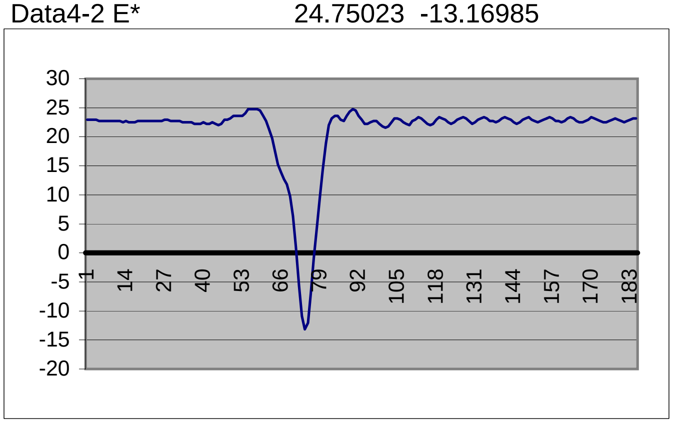

Data4-2 F* 24.52316 18.61944

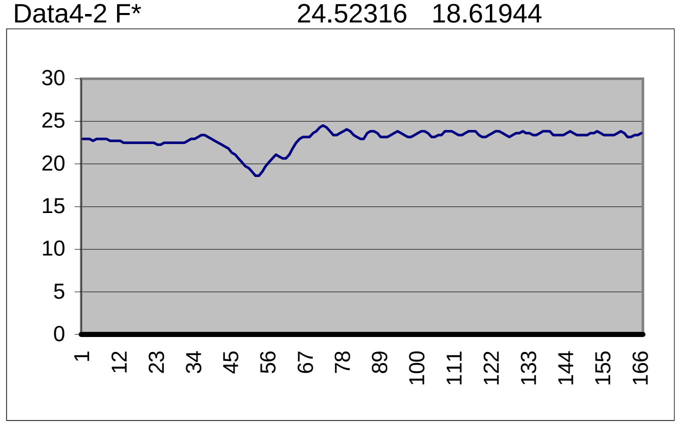

* A: Near side -10 mph speed.
B: Far side -10 mph speed.
C: Near side -25 mph speed.
D: Far side -25 mph speed.
E: Near side - 47 mph speed.
F: Far side - 47 mph speed.

Data4-3 A* 57.22071 -4.541326

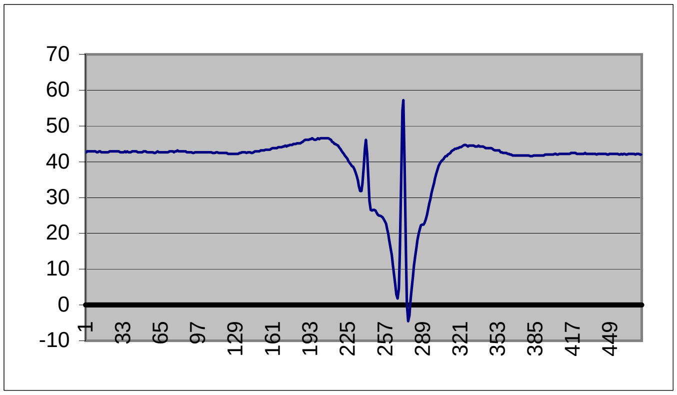

Data4-3 B* 44.27793 36.78474

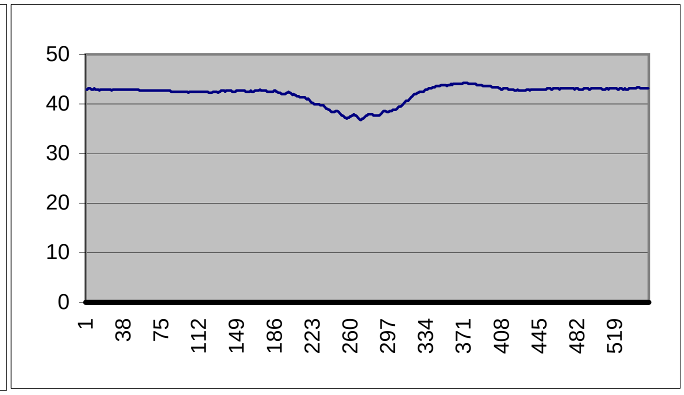

Data4-3 C* 45.18619 0.454133

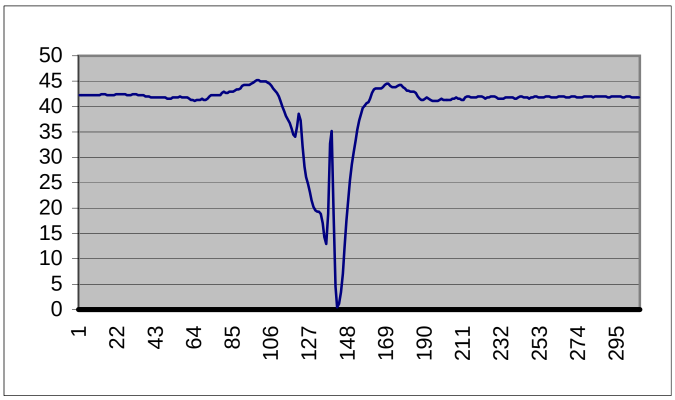

Data4-3 D* 44.505 36.10354

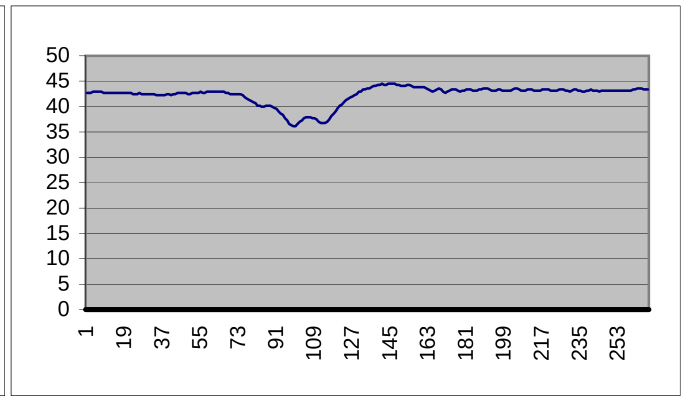

Data4-3 E* 45.41326 7.266122

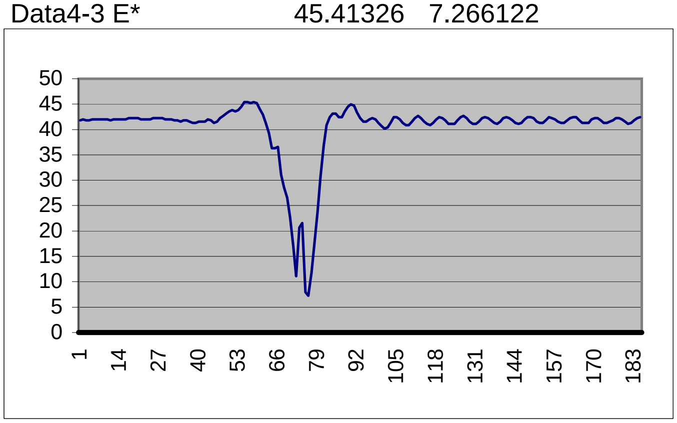

Data4-3 F* 43.59673 36.10354

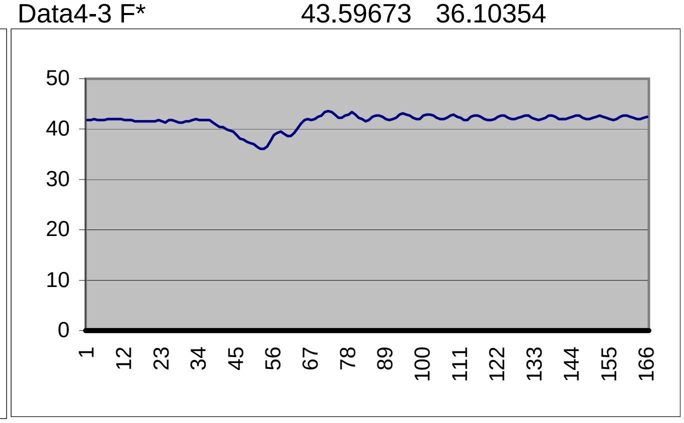

* A: Near side -10 mph speed.
B: Far side -10 mph speed.
C: Near side -25 mph speed.
D: Far side -25 mph speed.
E: Near side - 47 mph speed.
F: Far side - 47 mph speed.

Data1A-61 117.1662 22.47956

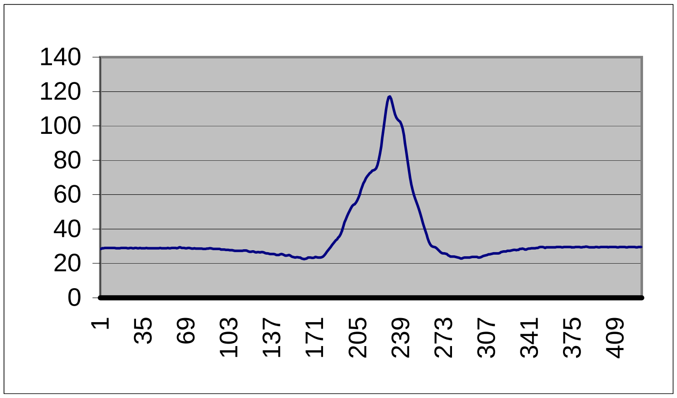

Data1A-62 38.10409 -13.94052 (* 3.228)

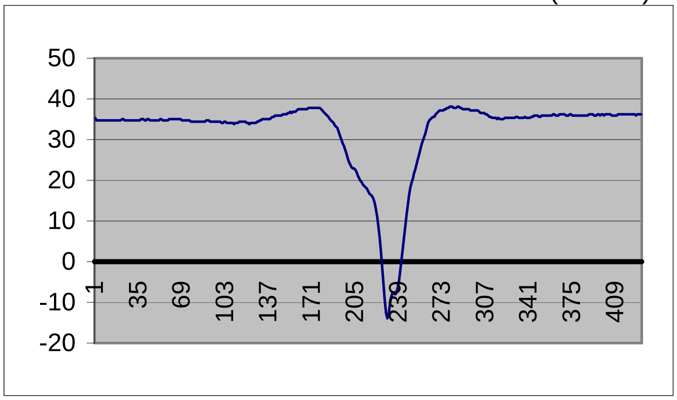

Data1A-63 2.990768 -0.411994 (*65.535)

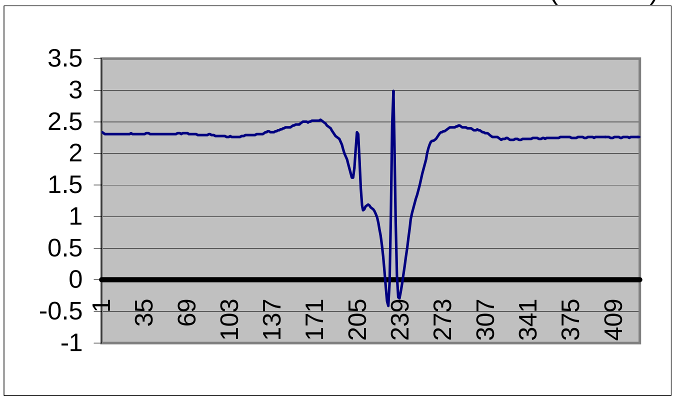

Data5-1 A* (Saturated) 1.876974 0.701958 (*65.531)

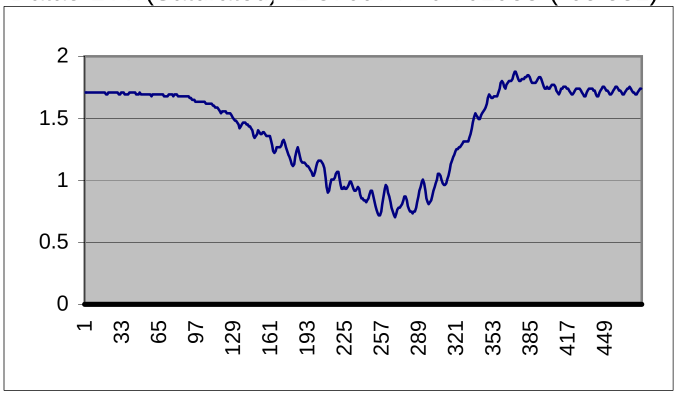

Data5-1 E* (Saturated) 2.197433 0.793518 (*65.531)

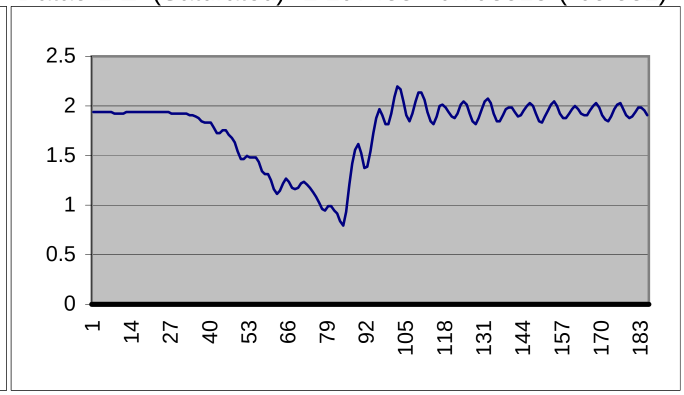

Data5-2 A* 28.38329 13.39691

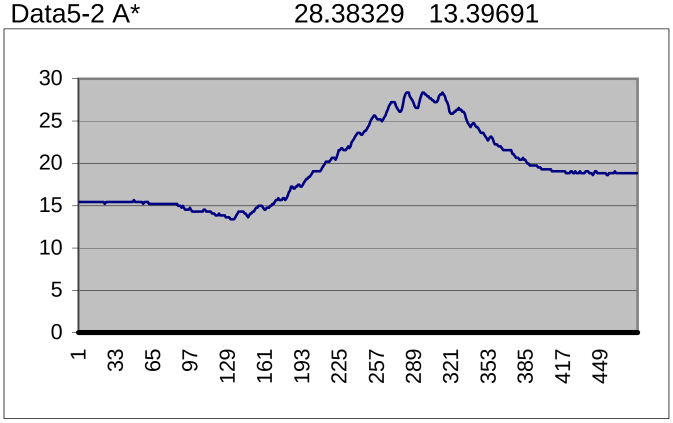

Data5-2 E* 38.60127 22.2525

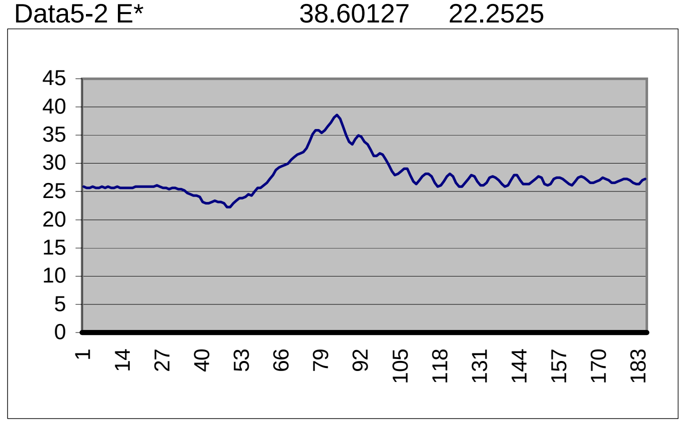

Data5-3 A* (Saturated) 162 73 (* 1.0)

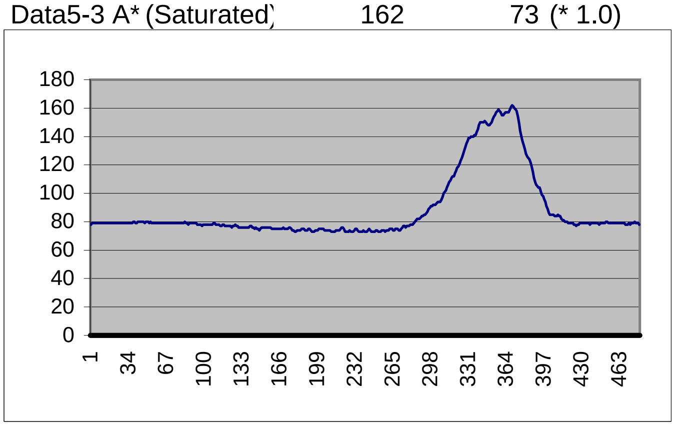

Data5-3 E* (Saturated) 225 136 (* 1.0)

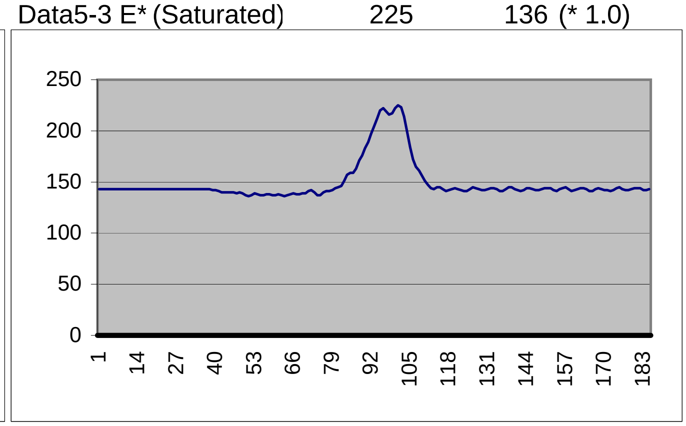

* A: Near side -10 mph speed.
E: Near side - 47 mph speed.

Appendix B - Finite Element Model and Results in Graphs

- Page B-1: ANSYS 3-D Finite Element Model perspective view
- Page B-2: ANSYS 3-D Finite Element Model displacement under dead load and live load (testing truck) applied at the mid-span
- Page B-3: ANSYS 3-D Finite Element Model stress contour under dead load and live load (testing truck) applied at the mid-span

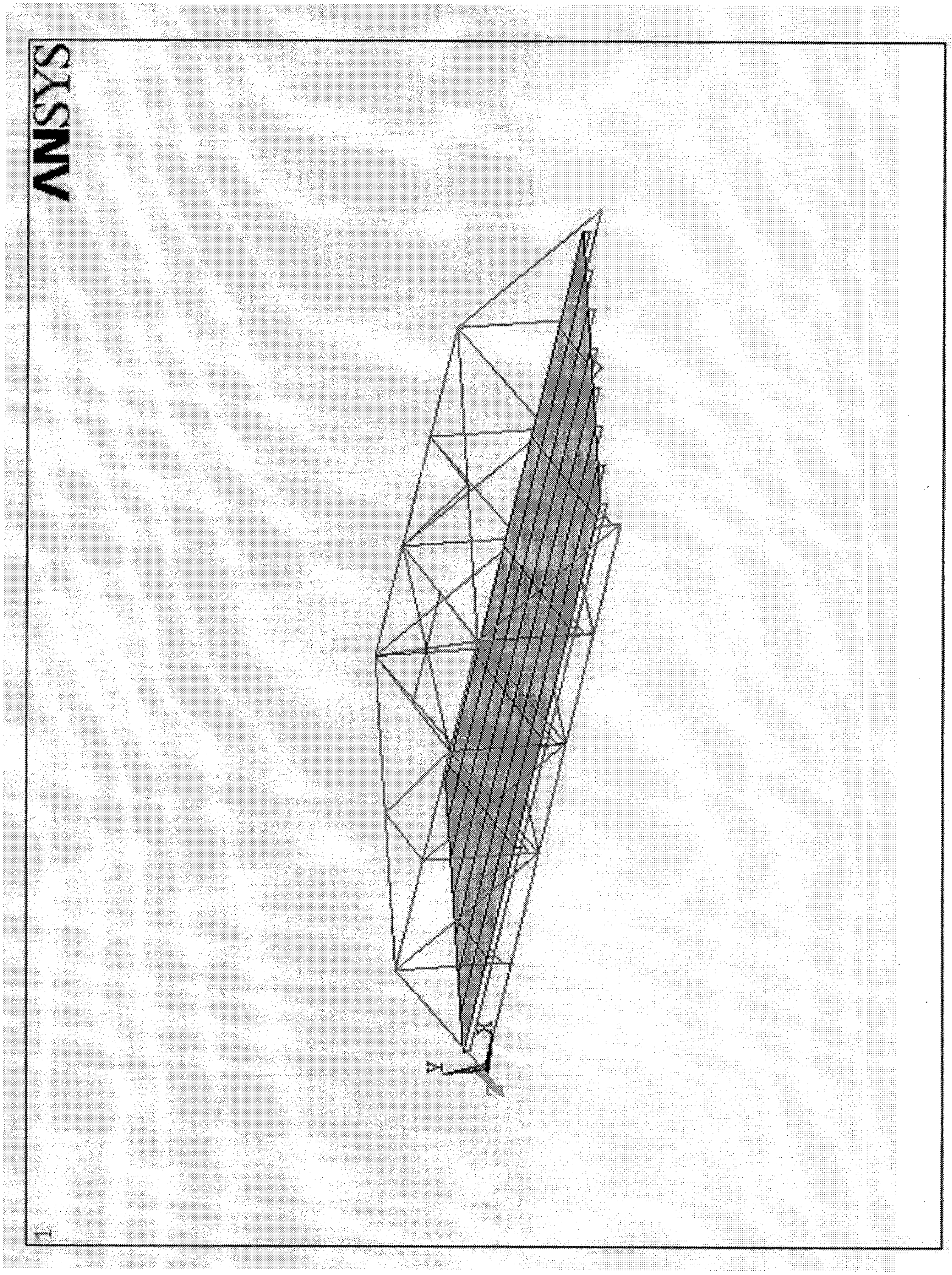
ANSYS
1
Y

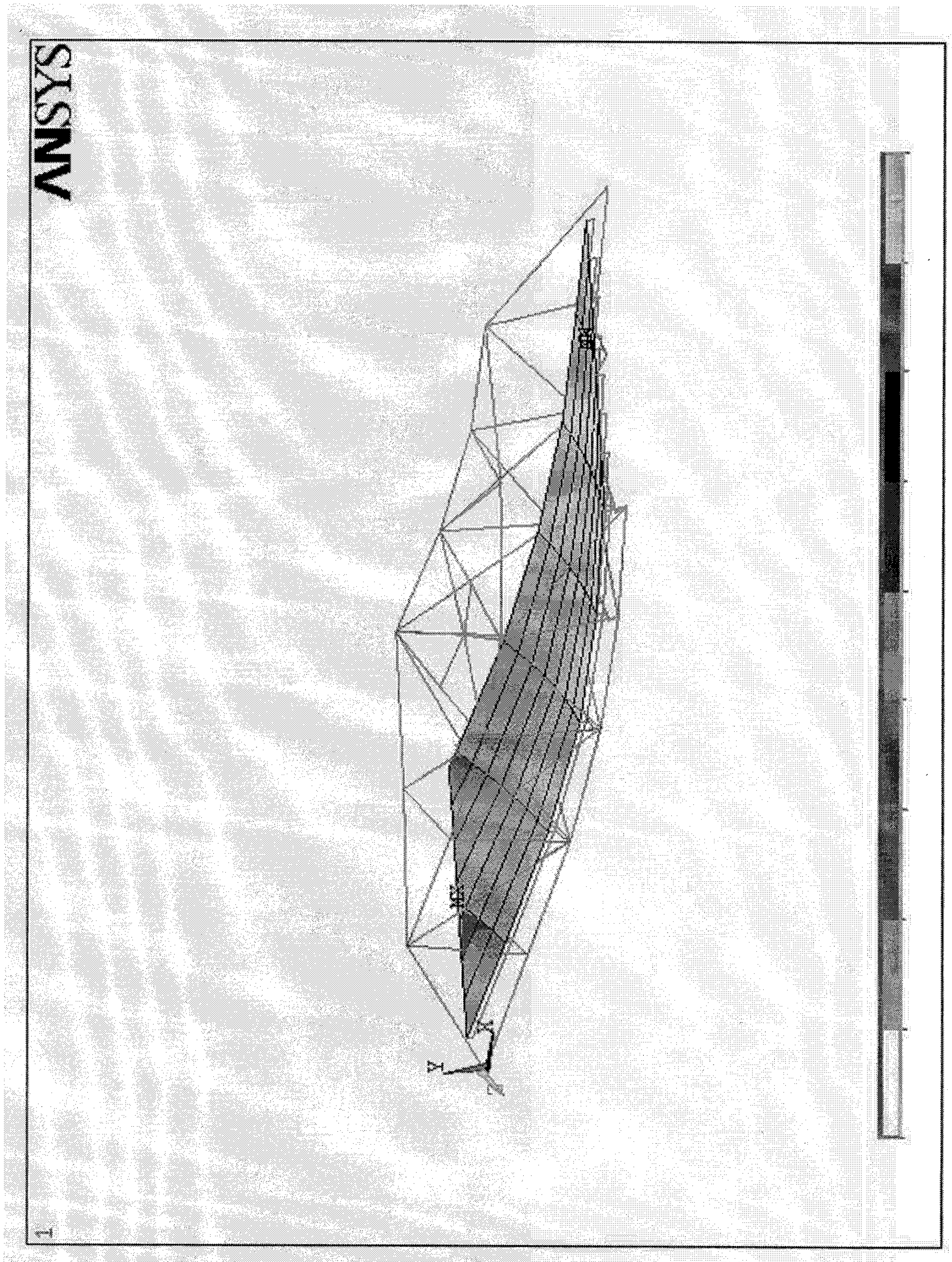
ANSYS
1

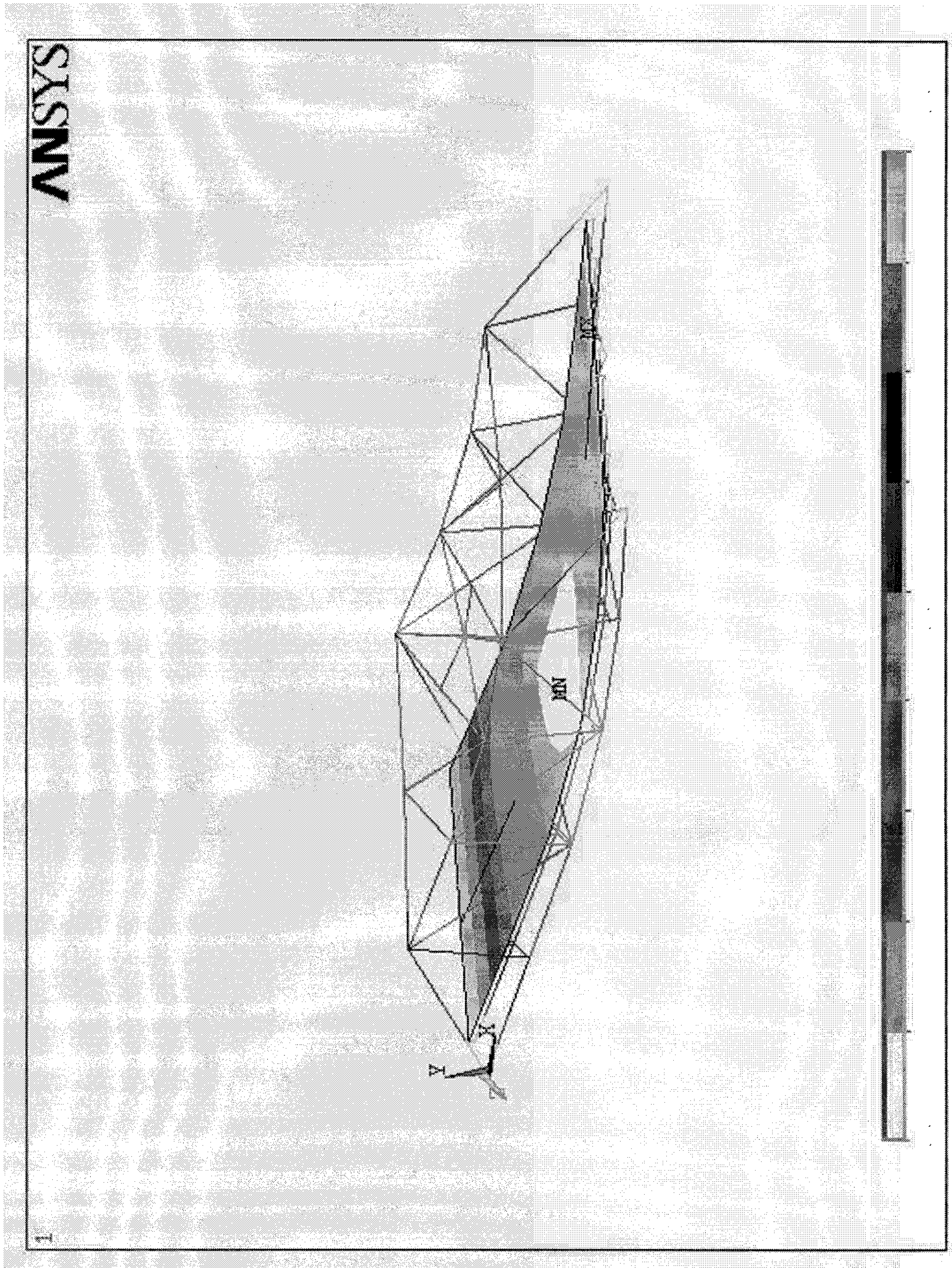
ANSYS
MX
MN

Appendix C - Delson FRP Material Test Report provided by Martin Marietta Composites

Test Method:

- Tension (ASTM D 638-99)
- Compression (ASTM D 695-96)
- Flexure (ASTM D 790-99)
- Interlaminar Shear (ASTM D 2344-84(95))
- V-notch Shear (ASTM D 695-98)
- Resin Content & Void Volume (ASTM D 792-98; Lip ASTM D 2584-94; Web ASTM D 2734-94)
- Glass Transition Temperature (ASTM D 3418-97)
- Coefficient of Linear Thermal Expansion (ASTM E 831-92)

Martin Marietta Composites

P.O. Box 30013
Raleigh, North Carolina 27622-0013
Telephone: 919.783.4679
Dan Richards, Ph.D., P.E.
Director of Composite Technology

2710 Wycliff Road
Raleigh, North Carolina 27607
Fax: 919.788.4399

October 3, 2001

Dr. C. C. Fu
Professor, Department of Civil Engineering
University of Maryland
College Park, MD 20742

Dear Dr. Fu:

The conversation with you on Tuesday, October 2, 2001, about the difficult of modeling and analyzing the DuraSpan™ 766 composite deck on the Deer Creek, Maryland Bridge is a familiar story. Fiber Reinforced Polymer (FRP) composite materials like the DuraSpan™ 766 is breaking new ground in the infrastructure world.

It was very refreshing to hear someone approach this problem of test data verses analytical models with an open mind. Martin Marietta Composites (MMC) is gaining knowledge everyday, but MMC does not pretend to know everything yet. MMC has taken the approach that the unknowns will be accepted by over designing the structures and not allowing any danger of structural integrity to be compromised for the user.

This is why, in my opinion, you are seeing the material properties that were given to you in November 2000 being smaller than the testing data is showing on Deer Creek, Maryland Bridge. Your suggestion of a magnitude of 10 seems too large for the material properties to be low. The material properties for an orthotropic plate element in a finite element model should be in the range of 1.5 or 2.0 too low. Laboratory test data is the only tool available to MMC right now, but the field-testing like you are doing is going to increase for MMC on other bridge projects in the next 3 to 4 months. This data will be a stronger measuring instrument for structural material properties of DuraSpan™ 766 to use in the future. Until then, MMC will stay with a conservative approach to protect the public using the bridge structures, which will protect MMC's customers and MMC also.

Included with this letter is a summary of the Delsen Test Report on coupon material properties for the DuraSpan™ 766. Please feel free to contact me if you have any questions concerning this data. Thanks again for your work on the Deer Creek Project.

Regards,

Dan Richards

Dan Richards
Director of Composite Technology

Cc: Greg Solomon

DELSEN
Testing Laboratories, Inc.

TEST REPORT

In account with	Date	Page
Martin Marietta Composites 2710 Wycliff Road Raleigh, NC 27607	08/25/00	Page 1 of 23 Page
	W.O. No. T 35845	P.O. No 034 053200
	Identification As noted	Shipper None

IDENTIFICATION : Four (4) sections of three foot long pultruded parts, identified by the client as DuraSpan™, (Please see photograph and drawing in Appendix I) were submitted for physical and mechanical testing.

REFERENCES :

1. Martin Marietta Purchase Order No. 034 053200
2. A fax from D. Richards of Martin Marietta to J. Moylan of Delsen, dated June 30, 2000
3. Delsen Quotation No. Q 15062, dated July 5, 2000

TEST MATRIX :

TEST TYPE	TEST METHOD	NUMBER OF TEST SPECIMENS Room Ambient Temperature
Tension	ASTM D 638-99	
0° Lip		5
90° Lip		5
0° Web		5
90° Web		5
Compression	ASTM D 695-96	
0° Lip		5
90° Lip		5
0° Web		5
90° Web		5
Flexure	ASTM D 790-99	
0° Lip		5
90° Lip		5
0° Web		5
90° Web		5

TEST TYPE	TEST METHOD	NUMBER OF TEST SPECIMENS Room Ambient Temperature
Interlaminar Shear	ASTM D 2344-84(95)	
0° Lip		5
90° Lip		5
0° Web		5
90° Web		5
V-notch Shear	ASTM D 695-98	
0° Lip		5
90° Lip		5
0° Web		5
90° Web		5
Resin Content & Void Volume	ASTM D 792-98	
Lip	ASTM D 2584-94	3
Web	ASTM D 2734-94	3
Glass Transition Temperature	ASTM D 3418-97	
Lip		1
Web		1
Coefficient of Linear Thermal Expansion	ASTM E 831-92	
0°Lip		1
90° Lip		1
0° Web		1
90° Web		1

SPECIMEN
IDENTIFICATIONS :

Test specimens were identified as follows:

{------SPECIMEN IDENTIFICATION------}
A - B - C

where A. Panel Identification ----------------- L = Lip
W = Web

B. Test Direction & Test Type -------- 0T = 0° tension
90T = 90° tension
0C = 0° compression
90C = 90° compression
0F = 0° flexure
90F = 90° flexure
0ILS = 0° interlaminar shear
90ILS = 90° interlaminar shear
0VNS = 0° V-notch shear
90VNS= 90° V-notch shear
RC = fiber content
TG = glass transition temperature
0CTE = 0° coefficient of linear thermal expansion
90CTE= 90° coefficient of linear thermal expansion

C. Specimen Number ---------------- 1, 2, 3 etc..

SPECIMEN PREPARATION :

It should be noted that in this report the 0° direction referred to the direction parallel to the pultruded direction and the 90° direction referred to the direction perpendicular to the pultruded direction, for the "Lip" and "Web" areas.

After identified the "Lip" and "Web" areas, these areas were removed from the part using a saw. The area for each test type was first mapped. Then, these mapped areas were machined. The specimens were fabricated from each designated piece, using a vertical milling machine equipped with a diamond coated abrasive wheel and using water as a coolant. The test specimens, which did not require tabs, were first cut slightly over-sized. Then, each specimen was ground to the required dimensions using a grinding machine equipped with an aluminum-oxide grinding wheel with water as a coolant to provide the specimen edge finish to RMS 64 or better.

For the test specimens that required tabs, the G-11 glass/epoxy tabs were first bonded to the piece. A two-part paste adhesive, Dexter Hysol EA 9309NA, was used as a tabbing and bonding adhesive. Prior to tabbing, the bonded area of the piece was lightly blasted, using 60 grit silica sand, while the tabs were also blasted using 60 grit silica sand. After preparation, the surfaces were rinsed with deionized water and dried in an air circulating oven at 150 ± 5°F for a minimum of 30 minutes. After bonding tabs, the specimens were cut slightly over-sized and then surface ground to the required dimensions.

TEST METHOD :

a. Tension (T):

The tensile specimens were prepared as a dogbone configuration and tested in accordance with ASTM D 638-99. A bi-axial strain gage, Micro Measurements CEA-06-250UT-350, was installed at the center of each specimen using measurements Group M-bond 200. This test was conducted at a crosshead rate of 0.2 inch/minute on a United Calibration universal testing machine, equipped with a pair of serrated mechanical grips. Each specimen was tested for modulus and tensile strength. A PC based data acquisition system was used to monitor load and strain output until failure occurred. Modulus was determined from the linear portion of the stress-strain curve. The tensile properties were calculated using the following equations:

$$\text{Tensile Strength (psi)} = \frac{\mathbf{P}}{\mathbf{wt}}$$

$$\text{Tensile Modulus (psi)} = \frac{1}{\mathbf{wt}}\left(\frac{\Delta \mathbf{P}}{\Delta \varepsilon}\right)$$

and

$$\text{POISSON'S RATIO} = -\frac{\Delta e_t}{\Delta e_a}$$

where P = maximum load (lbf)

$\frac{\Delta P}{\Delta \varepsilon}$ = slope of the initial linear portion of load-strain curve (psi)

w = specimen width (inches)

t = specimen length (inches)

Δe_t = the difference in transverse strain corresponding to the difference in axial strain (in/in);

and Δe_a = the difference in axial strain (in/in).

b. Compression (C):

The compressive specimens were prepared as a dogbone configuration and tested in accordance with ASTM D 695-96. The dimensions were 0.75" x 3.18" x thickness with 0.5" in the reduced section. A uni-axial strain gage, Micro Measurements CEA-06-250UW-350, was bonded at the center of each specimen using Measurements Group M-bond 200. Each specimen was assembled in a compression test fixture, as shown in ASTM D 695-96, Figure 1, but with a cut-out to accommodate the strain gage. The fastener assemblies of the fixture were finger-tightened. This test was conducted on a United Calibration universal testing machine at the crosshead rate of 0.05 inch/minute. A PC based data acquisition system was used to monitor load and strain output until failure. Each specimen was tested to determine compressive strength and modulus, which were calculated using the following equation:

$$\text{Compressive Strength (psi)} = \frac{\mathbf{P}}{\mathbf{wt}}$$

and

$$\text{Compressive Modulus (psi)} = \frac{1}{\mathbf{wt}}\left(\frac{\Delta\mathbf{P}}{\Delta\varepsilon}\right)$$

where P = maximum load (lbf)

$\frac{\Delta P}{\Delta\varepsilon}$ = slope of the initial linear portion of load-strain curve (psi)

w = specimen width (inches)

and t = specimen length (inches)

e. Flexure (F):

The flexural specimens were fabricated and tested in accordance with ASTM D 790-99. The dimensions were 1" wide x the length greater than 16 times the thickness. A three-point loading test fixture with a span of 16 times the thickness was used. Each specimen was tested on a United Calibration universal testing machine at the crosshead rate so that the failure occurred within 3 to 6 minutes. A pin deflectometer was placed beneath the specimen at the mid-span to monitor deflection. A PC based data acquisition system was used to monitor load and mid-span deflection until failure. Each specimen was tested to determine flexural modulus and strength, which were calculated using the following equations:

$$\text{Flexural Strength (psi)} = \frac{\mathbf{3PL}}{\mathbf{2wt}^2}$$

and

$$\text{Flexural Modulus (psi)} = \frac{\mathbf{mL}^3}{\mathbf{4wt}^3}$$

where P = maximum load (lbf)

L = span length (inches)

w = specimen width (inches)

t = specimen thickness (inches)

and m = slope of the initial linear portion of the load-mid-span deflection (lbf/in)

d. Interlaminar (Short Beam) Shear (ILS):

Each specimen was prepared and tested in accordance with ASTM D 2344-84(95). The specimens were fabricated to a length of at least seven times the thickness x 0.25" width. A three-point loading fixture was used to perform the test. The diameter of the loading nose and the diameter of the support noses were 1/4" and 1/8", respectively. The ratio of the span to depth was 5 times the average thickness of the test group. Each specimen was tested on a United Calibration universal testing machine at a crosshead rate of 0.05 inch/minute to determine interlaminar shear strength, which was calculated using the following equation:

$$\text{Interlaminar Shear Strength (psi)} = \frac{3P}{4wt}$$

where P = maximum load (lbf);
w = specimen width (inches);
and t = specimen thickness (inches).

e. V-notch Shear (VNS)

Each V-notched shear specimen was prepared and tested in accordance with ASTM D 5379-98. The dimensions were 3.00" x 0.75" x thickness with 90° notches placed at the middle of the length. G11 glass/epoxy tabs were bonded onto the specimen outside the notched area using a two-part room temperature curing adhesive, Dexter Hysol EA 9309. A ±45° strain gage rosette, Micro-Measurements EA-06-062TV-350, was bonded at the center of the gage area, using Measurements Group M-bond 200. The specimen was centered within the test fixture by using an alignment tool, which indexed from the lower notch to the center of the fixture. The wedge clamps of the fixture were then "finger tightened" to assure that no rotation of the specimen occurred during testing. Each specimen was tested on a United Calibration universal testing machine at a crosshead rate of 0.05 inch/minute. A PC data acquisition system was used to monitor the load and individual strain outputs continuously throughout the test. The specimens were tested for shear strength and shear modulus. Shear modulus was determined as a chord modulus between 1000 and 6000 microstrain. Shear properties were calculated as follows:

$$\text{SHEAR STRENGTH (psi)} = \frac{P}{wt}$$

and

$$\text{SHEAR MODULUS (psi)} = \frac{\Delta\tau_{12}}{\Delta\gamma_{12}}$$

where P = maximum load (lbsf)
w = distance between the notches (inches)
t = thickness (inches)
and $\frac{\Delta\tau_{12}}{\Delta\gamma_{12}}$ = slope of a linear line on the shear stress-shear strain curve between 1000 and 6000 microstrain (psi)

f. Density:

The density of each specimen was tested in accordance with ASTM D792-98. Each specimen was weighed in air and in water on an analytical balance to the nearest 0.0001 gram. When it was weighed in water, the water temperature was also recorded. The material density can be calculated as follows:

$$d_{comp.}\ \text{[Density](grams/c.c.)} = \frac{(W_1)(D_w)}{W_1 + W_2 - W_3}$$

where W_1 = specimen weight in air (grams);
W_2 = tare weight of the weighing assembly (grams);
W_3 = weight of specimen and weighing assembly in water (grams);
and D_w = density of water at the test temperature (grams/c.c.).

It should be noted that the density of water at the test temperature can be found in CRC, "Handbook of Chemistry and Physics", 49th Edition, Page F-4, 1968.

g. Resin & Fiber Content By Weight:

The resin and fiber contents by weight of the specimens were tested in accordance with ASTM D 2584-94 "Standard Test Method for Ignition Loss of Cured Reinforced Resin". The same density specimens were used for this test. The specimens were placed in a muffle furnace at 1050 ± 50°F to remove any organic materials. After burn-off, the resin and fiber content by weight can be calculated with the following equations:

$$f_{fw}\text{[Fiber Content By Weight] (\%)} = \left(\frac{W_2}{W_1}\right)(100)$$

and

$$f_{rw}\text{[Resin Content By Weight] (\%)} = \left(\frac{W_1 - W_2}{W_1}\right)(100)$$

where W_1 = specimen weight in air (grams);
and W_2 = residual weight after burn-off (grams).

h. RESIN & FIBER CONTENT BY VOLUME:

Resin and fiber contents by volume were calculated in accordance with ASTM D 3171-76(90). After obtaining the results of resin and fiber contents by weight and client provided resin and fiber densities, the resin and fiber contents by volume can be calculated using the following equations:

$$f_{fv}\text{[Fiber Content By Volume] (\%)} = \frac{(f_{fw})(d_{comp})}{D_f}$$

and

$$f_{rv}\text{[Resin Content By Volume] (\%)} = \frac{(f_{rw})(d_{comp})}{D_r}$$

where D_f = density of fiber given by Martin Marietta (2.56 grams/c.c.);
and D_r = density of resin given by Martin Marietta (1.23 grams/c.c.).

i. Void Volume:

After obtaining resin and fiber content by volume, the void volume was determined in accordance with ASTM D 2734-94, Paragraph 9.2.1, using the following equation:

$$f_{vv}\text{[Void Volume] (\%)} = [\,100 - (\,f_{rv} + f_{fv}\,)]$$

j. Glass Transition Temperature (TG):

Glass transition temperature was conducted per the outline in ASTM E 1545-95a. This test was performed on a DuPont TMA 943 at a heating rate of 10°C/minute with an applied load of 2.0 grams in a nitrogen environment. Glass transition temperature was determined from the intersection of two linear lines drawn tangent to the deflection-temperature curves before and after an apparent inflection point.

k. Coefficient of Linear Thermal Expansion (CTE):

Coefficients of linear thermal expansion of the composite laminate in the 0° and 90° directions were conducted per ASTM E 831-93 on a DuPont Thermomechanical Analyzer, Model 943, which was operated at a heating rate of 5°C/minute in a nitrogen environment with an applied load of 2.0 grams.

$$\alpha = [\frac{\Delta L}{L_o \Delta T} + \alpha_p] x K$$

where α = coefficient of linear thermal expansion of the test specimen (in/in/°F);
ΔT = difference of two selected temperature points (°F);
ΔL = deflection between two selected temperature points (in);
L_0 = initial length of the specimen measured at room temperature (in);
α_p = coefficient of linear thermal expansion of quartz (0.31×10^{-6} in/in/°F);
and K = a factor determined from NBS given coefficient of linear thermal expansion of copper standard divided by measured coefficient of linear thermal expansion of copper standard between two selected temperature range (1.067).

REMARKS :

1. Test results are presented herein for client evaluation.

2. In this report the 0° direction testing was in the direction parallel to the Z-direction, based on the Cartesian coordinates as shown in Appendix I. The 90° direction testing in the "Lip" area was in the direction parallel to the X-direction and in the "Web" area parallel to the Y-direction. The through the thickness testing in the "Lip" area was parallel to the Y-direction and in the "Web" area parallel to the X-direction.

3. It should be mentioned that the panel machined from the "Lip" area for the 90° tensile and flexural specimens were ground to the uniform thickness.

4. The following appendices are enclosed in this report.

Appendix I	Photographs & drawing of the part
Appendix II	Tensile stress-strain curves
Appendix III	Compressive stress-strain curves
Appendix IV	Flexural load-mid-span deflection curves
Appendix V	V-notch shear stress-strain curves
Appendix VI	T.M.A. thermograms for glass trasition temperature
Appendix VII	T.M.A. thermograms for coefficient of thermal expansion

Respectfully submitted,

Jack H.C. Ching, Ph.D.
Laboratory Director
DELSEN TESTING LABORATORIES, INC.

jhc L1D83 T35845MM

Delsen Testing Laboratories, Inc. is accredited by the American Association for Laboratory Accreditation in the field of mechanical testing, as listed in the current A2LA Directory of Accredited Laboratories and as shown on the A2LA Scope of Accreditation Certificate No. 0096-01.

TENSILE PROPERTIES

Rate of test: 0.20 inch/minute

TEST METHOD	:	ASTM D 638-99, Type I
MATERIAL ID	:	DuraSpan™
PRE-CONDITIONING	:	None
CONDITIONING	:	None
TEST CONDITIONS	:	Tested at room ambient temperature

SPECIMEN	THICKNESS inches	WIDTH inches	MAXIMUM LOAD pounds	POISSON'S RATIO	MODULUS Msi	ULTIMATE STRENGTH Ksi	STRAIN AT FAILURE %
Test Location: Lip, 0° direction							
L-0T-1	0.297	0.498	6,768	0.28	3.93	45.8	1.26
L-0T-2	0.297	0.498	7,021	0.26	4.12	47.5	1.25
L-0T-3	0.297	0.504	7,034	0.29	3.88	47.0	1.33
L-0T-4	0.296	0.507	6,857	0.26	3.71	45.7	1.32
L-0T-5	0.296	0.505	7,176	0.30	4.05	48.0	1.29
			AVERAGE:	0.28	3.94	46.8	1.29
			STANDARD DEVIATION:	0.018	0.159	1.02	0.035
			COEFFICIENT OF VARIATION(%):	6.43	4.04	2.18	2.71
Test Location: Lip, 90°direction							
L-90T-1	0.279	0.500	1,286	0.18	2.71	9.22	0.34
L-90T-2	0.279	0.504	1,294	0.18	1.65	9.20	0.56
L-90T-3	0.277	0.507	1,388	0.18	1.70	9.89	0.58
L-90T-4	0.276	0.506	----	0.22	2.27	----	----
L-90T-5	0.276	0.506	1,292	0.23	2.46	9.25	0.38
			AVERAGE:	0.20	2.16	9.39	0.47
			STANDARD DEVIATION:	0.025	0.468	0.334	0.123
			COEFFICIENT OF VARIATION(%):	12.5	21.7	3.56	26.2

NOTES :

1. Measured thickness was used in calculations.
2. Modulus was determined from the initial linear portion of stress-strain curve.
3. All 0° specimens exhibited tensile failure within the gage area, except Specimen L-0T-2, which failed in the fillet area. Depending on the ply orientation, transverse tensile failure and longitudinal splitting failure were observed and also led to ply separation.
   All 90°specimens exhibited transverse tensile failure within the gage area.
4. Due to premature strain gage failure caused by fiber breaking beneath, strain at failure of 90° specimens was obtained from ultimate strength divided by modulus.
5. Due to computer malfunction, maximum load and strain at failure of Specimen L-90T-4 were not attainable.

TEST REPORT

TENSILE PROPERTIES

Rate of test: 0.20 inch/minute

TEST METHOD : ASTM D 638-99, Type I
MATERIAL ID : DuraSpan™
PRE-CONDITIONING : None
CONDITIONING : None
TEST CONDITIONS : Tested at room ambient temperature

SPECIMEN	THICKNESS inches	WIDTH inches	MAXIMUM LOAD pounds	POISSON'S RATIO	MODULUS Msi	ULTIMATE STRENGTH Ksi	STRAIN AT FAILURE %
Test Location: Web, 0° direction							
W-0T-1	0.205	0.500	3,711	0.31	2.61	36.2	1.40
W-0T-2	0.206	0.499	3,792	0.26	2.66	36.9	1.48
W-0T-3	0.207	0.501	3,493	0.26	2.74	33.7	1.34
W-0T-4	0.205	0.503	3,097	0.25	2.65	30.0	1.35
W-0T-5	0.207	0.502	3,047	0.29	2.84	29.3	1.16
			AVERAGE:	0.27	2.70	33.2	1.35
			STANDARD DEVIATION:	0.025	0.091	3.48	0.118
			COEFFICIENT OF VARIATION(%):	9.26	3.37	10.5	8.74
Test Location: Web, 90°direction							
W-90T-1	0.206	0.501	2,524	0.27	2.23	24.5	1.10
W-90T-2	0.206	0.502	2,652	0.27	2.63	25.6	1.17
W-90T-3	0.206	0.501	2,470	0.24	2.36	23.9	1.01
W-90T-4	0.205	0.502	2,544	0.22	2.32	24.7	1.06
W-90T-5	0.207	0.500	2,341	0.29	2.75	22.6	1.06
			AVERAGE:	0.26	2.46	24.3	1.08
			STANDARD DEVIATION:	0.028	0.221	1.11	0.060
			COEFFICIENT OF VARIATION(%):	10.8	8.98	4.57	5.56

NOTES :
1. Measured thickness was used in calculations.
2. Modulus was determined from the initial linear portion of stress-strain curve.
3. All 0° specimens exhibited tensile failure within the gage area, except Specimen W-0T-3 and -4, which failed in the fillet area. Due to the failure mode, ply separation was also observed in Specimens W-0T-1, -2 and -5.
   All 90° specimens exhibited tensile failure within the gage area,
4. Due to material constrain, W-90T specimens were machined identical to the configuration of the compressive specimens with a gage length of 1.5 inches, but had longer gripping length, with client consent. All other tensile specimen had gage length of 3.0 inches.
5. Due to premature strain gage failure, strain at failure of Specimen W-90T-1, -3 and -4 was obtained from ultimate strength divided by modulus.

COMPRESSIVE PROPERTIES

Rate of test: 0.05 inch/minute

TEST METHOD	:	ASTM D 695-96
MATERIAL ID	:	DuraSpan™
PRE-CONDITIONING	:	None
CONDITIONING	:	None
TEST CONDITIONS	:	Tested at room ambient temperature

SPECIMEN	THICKNESS inches	WIDTH inches	MAXIMUM LOAD pounds	MODULUS Msi	ULTIMATE STRENGTH Ksi	STRAIN AT FAILURE %
Test Location: Lip, 0° direction						
L-0C-1	0.294	0.506	8,874	3.87	59.7	1.55
L-0C-2	0.297	0.506	10,211	3.90	67.9	1.85
L-0C-3	0.297	0.505	9,595	4.25	64.0	1.44
L-0C-4	0.296	0.507	8,335	4.09	55.5	1.36
L-0C-5	0.297	0.505	9,632	4.04	64.2	1.64
			AVERAGE:	4.03	62.3	1.57
			STANDARD DEVIATION:	0.154	4.77	0.190
			COEFFICIENT OF VARIATION(%):	3.82	7.66	12.1
Test Location: Lip, 90°direction						
L-90C-1	0.297	0.507	3,250	1.79	21.6	1.46
L-90C-2	0.298	0.507	3,348	2.09	22.2	1.47
L-90C-3	0.297	0.508	3,242	2.01	21.5	1.42
L-90C-4	0.296	0.505	3,475	1.79	23.2	1.51
L-90C-5	0.296	0.503	3,105	1.89	20.9	1.33
			AVERAGE:	1.91	21.9	1.44
			STANDARD DEVIATION:	0.134	0.87	0.068
			COEFFICIENT OF VARIATION(%):	7.02	3.97	4.72

NOTES :
1. Measured thickness was used in calculations.
2. Modulus was determined from the initial linear portion of stress-strain curve.
3. All 0° specimens exhibited compressive failure within the columnar area, except Specimens L-0C-1, -3 and -5, which exhibited end failure and ply separation. All 90° specimens exhibited compressive failure within the columnar area.

COMPRESSIVE PROPERTIES

Rate of test: 0.05 inch/minute

TEST METHOD : ASTM D 695-96
MATERIAL ID : DuraSpan™
PRE-CONDITIONING : None
CONDITIONING : None
TEST CONDITIONS : Tested at room ambient temperature

SPECIMEN	THICKNESS inches	WIDTH inches	MAXIMUM LOAD pounds	MODULUS Msi	ULTIMATE STRENGTH Ksi	STRAIN AT FAILURE %
Test Location: Web, 0° direction						
W-0C-1	0.208	0.509	4,131	2.92	39.0	1.36
W-0C-2	0.209	0.506	4,150	2.91	39.2	1.38
W-0C-3	0.209	0.507	4,141	2.90	39.1	1.46
W-0C-4	0.208	0.508	4,141	3.09	39.2	1.37
W-0C-5	0.208	0.508	3,694	2.88	35.0	1.30
			AVERAGE:	2.94	38.3	1.37
			STANDARD DEVIATION:	0.085	1.85	0.057
			COEFFICIENT OF VARIATION(%):	2.89	4.83	4.16
Test Location: Web, 90°direction						
W-90C-1	0.207	0.506	2,979	2.79	28.4	1.13
W-90C-2	0.205	0.505	2,852	2.50	27.5	1.21
W-90C-3	0.207	0.505	2,557	2.43	24.5	1.11
W-90C-4	0.207	0.506	2,689	2.54	25.7	1.03
W-90C-5	0.207	0.507	2,927	2.23	27.9	1.29
			AVERAGE:	2.50	26.8	1.15
			STANDARD DEVIATION:	0.202	1.64	0.099
			COEFFICIENT OF VARIATION(%):	8.08	6.12	8.61

NOTES :
1. Measured thickness was used in calculations.
2. Modulus was determined from the initial linear portion of stress-strain curve.
3. All specimens exhibited compressive failure within the columnar area.
4. Strain at failure of W-0C-2 was obtained from extrapolation.

FLEXURAL PROPERTIES

Rate of test: As Noted

TEST METHOD : ASTM D 790-99
MATERIAL ID : DuraSpan™
PRE-CONDITIONING : None
CONDITIONING : None
TEST CONDITIONS : Tested at room ambient temperature

SPECIMEN	THICKNESS inches	WIDTH inches	MAXIMUM LOAD pounds	MODULUS Msi	ULTIMATE STRENGTH Ksi
Test Location: Lip, 0° direction Rate of Test: 0.13 inch/minute Span: 4.736 inches					
L-0F-1	0.296	1.002	684	2.84	55.3
L-0F-2	0.297	1.002	647	2.83	52.0
L-0F-3	0.296	1.001	617	2.74	50.0
L-0F-4	0.296	1.002	648	2.85	52.1
L-0F-5	0.297	1.002	628	2.83	50.5
			AVERAGE:	2.82	52.0
			STANDARD DEVIATION:	0.044	2.07
			COEFFICIENT OF VARIATION(%):	1.56	3.98
Test Location: Lip, 90°direction Rate of Test: 0.11 inch/minute Span: 4.016 inches					
L-90F-1	0.256	1.003	117	2.25	10.7
L-90F-2	0.252	1.002	278	2.11	26.3
L-90F-3	0.250	1.002	124	2.10	11.9
L-90F-4	0.248	1.002	206	1.75	20.1
L-90F-5	0.248	1.002	209	1.70	20.5
			AVERAGE:	1.85	22.3
			STANDARD DEVIATION:	0.224	3.47
			COEFFICIENT OF VARIATION(%):	12.1	15.6

NOTES :

1. Measured thickness was used in calculations.
2. Modulus was determined from the initial linear portion of stress-mid-span deflection curve.
3. All specimens exhibited failure on the tension surface below the loading nose, except Specimens L-90F-1 and -3, which exhibited failure in tension at "Web" to "Lip" connected area.
4. Specimens L-0F-1 through -4 were tested with the outer surface of the "Lip" area in tension and Specimen L-0F-5 was tested with the inner surface in tension.
5. Specimens L-90F-1 and -3 were tested with the inner surface of the "Lip" area in tension. Specimens L-90F-2, -4 and -5 were tested with the outer surface in tension. Specimens L-90F-2, -4 and –5 were included the statistic calculations

FLEXURAL PROPERTIES

Rate of test: 0.09 inch/minute

TEST METHOD	:	ASTM D 790-99
MATERIAL ID	:	DuraSpan™
PRE-CONDITIONING	:	None
CONDITIONING	:	None
TEST CONDITIONS	:	Tested at room ambient temperature

SPECIMEN	THICKNESS inches	WIDTH inches	MAXIMUM LOAD pounds	MODULUS Msi	ULTIMATE STRENGTH Ksi
Test Location: Web, 0° direction					
Span: 3.312 inches					
W-0F-1	0.206	1.003	355	2.30	41.5
W-0F-2	0.208	1.003	267	2.50	30.6
W-0F-3	0.207	1.003	419	2.48	48.4
W-0F-4	0.205	1.003	351	2.20	41.4
W-0F-5	0.209	1.003	356	2.32	40.4
			AVERAGE:	2.36	40.5
			STANDARD DEVIATION:	0.127	6.37
			COEFFICIENT OF VARIATION(%):	5.38	15.7
Test Location: Web, 90°direction					
Span: 3.312 inches					
W-90F-1	0.207	1.002	317	3.07	36.7
W-90F-2	0.207	0.999	296	3.15	34.3
W-90F-3	0.206	1.002	335	3.01	39.1
W-90F-4	0.207	1.001	275	3.08	31.8
W-90F-5	0.208	0.998	324	3.07	37.2
			AVERAGE:	3.08	35.8
			STANDARD DEVIATION:	0.050	2.82
			COEFFICIENT OF VARIATION(%):	1.62	7.88

NOTES :

1. Measured thickness was used in calculations.
2. Modulus was determined from the initial linear portion of stress-mid-span deflection
3. All specimens exhibited failure on tension surface below the loading nose. With exception, Specimen W-0F-5 exhibited failure on both tension and compression surfaces and Specimens W-90F-1, -3 and -5 exhibited failure on compression surface.
4. Specimens W-0F-2 was tested with the outer surface of the "Web" area in tension and Specimens W-0F-1, -3, -4 and -5 were tested with the inner surface in tension.
5. Specimens W-90F-2 and -4 were tested with the outer surface of the "Web" area in tension. Specimens L-90F-1, -3 and -5 were tested with the inner surface in tension.

INTERLAMINAR SHEAR STRENGTH

Rate of test: 0.05 inch/minute

TEST METHOD	:	ASTM D 2344-85(95)
MATERIAL ID	:	DuraSpan™
PRE-CONDITIONING	:	None
CONDITIONING	:	None
TEST CONDITIONS	:	Tested at room ambient temperature

SPECIMEN	THICKNESS inches	WIDTH inches	MAXIMUM LOAD pounds	ULTIMATE STRENGTH Ksi
Test Location: Lip, 0° direction Span: 1.485 inches				
L-0ILS-1	0.297	0.254	297	2.95
L-0ILS-2	0.297	0.253	305	3.04
L-0ILS-3	0.296	0.253	297	2.97
L-0ILS-4	0.297	0.251	301	3.03
L-0ILS-5	0.296	0.253	276	2.76
			AVERAGE:	2.95
			STANDARD DEVIATION:	0.113
			COEFFICIENT OF VARIATION(%):	3.83
Test Location: Lip, 90° direction Span: 1.485 inches				
L-90ILS-1	0.397	0.251	257	2.59
L-90ILS-2	0.397	0.249	232	2.35
L-90ILS-3	0.397	0.248	258	2.63
L-90ILS-4	0.397	0.249	252	2.56
L-90ILS-5	0.397	0.250	247	2.49
			AVERAGE:	2.52
			STANDARD DEVIATION:	0.110
			COEFFICIENT OF VARIATION(%):	4.37

NOTE : All specimens exhibited interlaminar shear failure.

INTERLAMINAR SHEAR STRENGTH

Rate of test: 0.05 inch/minute

TEST METHOD	:	ASTM D 2344-85(95)
MATERIAL ID	:	DuraSpan™
PRE-CONDITIONING	:	None
CONDITIONING	:	None
TEST CONDITIONS	:	Tested at room ambient temperature

SPECIMEN	THICKNESS inches	WIDTH inches	MAXIMUM LOAD pounds	ULTIMATE STRENGTH Ksi
Test Location: Web, 0° direction Span: 1.035 inches				
W-0ILS-1	0.208	0.250	211	3.04
W-0ILS-2	0.209	0.251	186	2.66
W-0ILS-3	0.206	0.251	198	2.87
W-0ILS-4	0.205	0.250	213	3.12
W-0ILS-5	0.207	0.254	205	2.92
			AVERAGE:	2.92
			STANDARD DEVIATION:	0.176
			COEFFICIENT OF VARIATION(%):	6.03
Test Location: Web, 90° direction Span: 1.035 inches				
W-90ILS-1	0.208	0.253	232	3.31
W-90ILS-2	0.207	0.252	237	3.41
W-90ILS-3	0.206	0.252	227	3.28
W-90ILS-4	0.205	0.253	253	3.66
W-90ILS-5	0.205	0.251	235	3.43
			AVERAGE:	3.42
			STANDARD DEVIATION:	0.150
			COEFFICIENT OF VARIATION(%):	4.39

NOTES : All specimens exhibited interlaminar shear failure.

V-NOTCH SHEAR PROPERTIES

Rate of test: 0.05 inch/minutes

TEST METHOD	:	ASTM D5379-94
MATERIAL ID	:	DuraSpan™
PRE-CONDITIONING	:	None
CONDITIONING	:	None
TEST CONDITIONS	:	Tested at room ambient temperature

SPECIMEN	THICKNESS inches	WIDTH inches	DISTANCE BETWEEN NOTCH ROOTS inches	MAXIMUM LOAD pounds	SHEAR MODULUS Msi	ULTIMATE STRENGTH Ksi
Test Location: Lip, 0° direction						
L-0VNS-1	0.297	0.750	0.450	1,789	0.592	13.4
L-0VNS-2	0.298	0.753	0.450	1,978	0.626	14.8
L-0VNS-3	0.297	0.752	0.449	1,914	0.608	14.4
L-0VNS-4	0.297	0.753	0.447	1,987	0.500	15.8
L-0VNS-5	0.298	0.753	0.447	1,972	0.606	14.8
				AVERAGE:	0.586	14.6
				STANDARD DEVIATION:	0.0498	0.87
				COEFFICIENT OF VARIATION(%):	8.50	5.96
Test Location: Lip, 90° direction						
L-90VNS-1	0.298	0.751	0.446	1,929	0.448	14.5
L-90VNS-2	0.297	0.752	0.448	1,791	0.570	13.5
L-90VNS-3	0.297	0.752	0.449	1,783	0.546	13.4
L-90VNS-4	0.296	0.752	0.449	1,810	0.540	13.6
L-90VNS-5	0.297	0.753	0.450	1,870	0.564	14.0
				AVERAGE:	0.534	13.8
				STANDARD DEVIATION:	0.0494	0.45
				COEFFICIENT OF VARIATION(%):	9.25	3.26

NOTES :
1. Measured thickness was used in calculations.
2. Modulus was determined as a secant between 2,000 and 6,000 microstrain, except modulus of Specimen L-90VNS-1, which was determined between 6,500 and 12.500 microstrain.
3. All specimens exhibited shear failure within the shear area.

V-NOTCH SHEAR PROPERTIES

Rate of test: 0.05 inch/minutes

TEST METHOD	:	ASTM D5379-94
MATERIAL ID	:	DuraSpan™
PRE-CONDITIONING	:	None
CONDITIONING	:	None
TEST CONDITIONS	:	Tested at room ambient temperature

SPECIMEN	THICKNESS inches	WIDTH inches	DISTANCE BETWEEN NOTCH ROOTS inches	MAXIMUM LOAD pounds	SHEAR MODULUS Msi	ULTIMATE STRENGTH Ksi
Test Location: Web, 0° direction						
W-0VNS-1	0.209	0.755	0.447	1,919	0.720	20.5
W-0VNS-2	0.211	0.755	0.448	1,899	0.776	20.1
W-0VNS-3	0.209	0.753	0.450	1,984	0.842	21.1
W-0VNS-4	0.210	0.754	0.447	1,916	0.619	20.4
W-0VNS-5	0.210	0.751	0.448	1,896	0.720	20.2
				AVERAGE:	0.735	20.5
				STANDARD DEVIATION:	0.0822	0.39
				COEFFICIENT OF VARIATION(%):	11.2	1.90
Test Location: Web, 90° direction						
W-90VNS-1	0.208	0.754	0.446	1,866	0.821	20.1
W-90VNS-2	0.212	0.753	0.447	1,723	0.754	18.2
W-90VNS-3	0.211	0.752	0.450	1,895	0.723	20.0
W-90VNS-4	0.210	0.755	0.447	1,738	0.742	18.5
W-90VNS-5	0.209	0.754	0.448	1,604	0.640	17.1
				AVERAGE:	0.736	18.8
				STANDARD DEVIATION:	0.0651	1.27
				COEFFICIENT OF VARIATION(%):	8.85	6.76

NOTES :

1. Measured thickness was used in calculations.
2. Modulus was determined as a secant between 2,000 and 6,000 microstrain.
3. All specimens exhibited shear failure within the shear area.

DENSITY, FIBER & RESIN CONTENTS
Tested "as received"

TEST METHOD : ASTM D 792-91, ASTM D 2584-94, ASTM D 3171-76(90), and ASTM D 2734-94, Paragraph 9.2.1

DENSITY : Fiber density = 2.57 grams/c.c. (0.093 lb/in^3)
Resin density = 1.34 grams/c.c. (0.0484 lb/in^3) given by Martin Marietta

SPECIMEN	WEIGHT grams	DENSITY grams/c.c.	FIBER CONTENT BY WEIGHT %	RESIN CONTENT BY WEIGHT %	FIBER CONTENT BY VOLUME %	RESIN CONTENT BY VOLUME %	VOID VOLUME %
DuraSpan™							
L-RC-1	2.9959	1.9873	73.22	26.78	56.62	39.72	3.66
L-RC-2	2.8605	1.9937	73.49	26.51	56.01	39.44	3.55
L-RC-3	3.0364	1.9958	73.91	26.09	57.40	38.86	3.74
AVERAGE:		1.9923	73.54	26.46	57.01	39.34	3.65
STANDARD DEVIATION:		0.0044	0.35	0.35	0.39	0.44	0.10
C.O.V.(%):		0.22	0.48	1.32	0.68	1.12	2.74
W-RC-1	3.0095	1.9810	73.71	26.29	56.82	38.87	4.31
W-RC-2	3.0346	2.0006	74.92	25.08	58.32	37.44	4.24
W-RC-3	3.0005	1.9332	70.19	29.81	52.80	46.01	4.19
AVERAGE:		1.9716	72.94	27.06	55.98	39.77	4.25
STANDARD DEVIATION:		0.0347	2.46	2.46	2.85	2.89	0.06
C.O.V.(%):		1.76	3.37	9.09	5.09	7.27	1.41

NOTE: Specimens 1 and 2 were prepared from one part and Specimen 3 prepared from another part.

THERMAL MECHANICAL ANALYSIS
Tested "as received"
Heating Rate: 10°C/minute
Environment: Nitrogen
Applied Load: 2.0 grams
Mode: Expansion
Test Direction: Through the thickness

TEST METHOD : ASTM E 1545-95a.

SPECIMEN	SPECIMEN THICKNESS mils	GLASS TRANSITION TEMPERATURE °F
DuraSpan™		
L-TG-1	296	165
W-TG-1	209	137

NOTE : Glass transition temperature was determined from the intersection of two linear lines drawn tangent to the deflection-temperature curve before and after the observed inflection point.

THERMAL MECHANICAL ANALYSIS
Tested "as received"
Heating Rate: 5°C/minute
Applied Load: 2.0 grams
Environment: Nitrogen
Mode: Expansion

TEST METHOD : ASTM E 831-93

SPECIMEN	INITIAL LENGTH mils	COEFFICIENT OF LINEAR THERMAL EXPANSION $x10^{-6}$ in/in/°F	REMARK
DuraSpan™			
L-0CTE-1	446	6.1	1st scan (from 50 to 118°F)
		4.9	2nd scan
L-90CTE-1	448	11.3	1st scan (from 50 to 153°F)
		9.4	2nd scan
W-0CTE-1	446	7.0	1st scan (from 50 to 150°F)
		6.1	2nd scan
W-90CTE-1	450	8.7	1st scan (from 50 to 138°F)
		8.2	2nd scan

NOTES:

1. The first scan was terminated at 250°F after observing transition. Coefficient of linear thermal expansion was calculated between the temperature range as indicated.
2. From the second heating scan, average coefficient of thermal expansion was determined over the temperature range between 50°F and 200°F.
3. The specimens, identified as 0, were tested in the direction parallel to the pultruded direction or in the Z direction as shown in the drawing.
4. The specimens, identified as 90, were tested in the direction perpendicular to the pultruded direction or in the X direction and in the Y direction, respectively, for the "Lip" area and for the "Web" area.

Appendix D - Rating Factors by using LFD Method and Rating Comparisons

Table D.1 - TRAP LFD inventory and operating rating of the original design condition

Table D.2 - TRAP LFD rating of the existing condition without considering the members' loss of section

Table D.3 - TRAP LFD rating of the existing condition with the section loss considered

Table D.4 - TRAP LFD truss rating of the new FRP deck without considering the members' loss of section

Table D.5 - TRAP LFD truss rating of the new FRP deck with the section loss considered

Table D.6 - Summary of TRAP LFD rating results for all truss, floorbeam and stringer members

Table D.7 - ANSYS LFD inventory and operating truss rating of the original design condition

Table D.8 - ANSYS LFD truss rating of the new FRP deck.

Figure D.1 - Comparison of safety factors between WSD and LFD

APPENDIX D - RATING FACTORS BY USING LFD METHOD AND RATING COMPARISONS

D.1 Load Factor Rating

The following general expression defined by AASHTO is used to determine the load rating of a structure:

$$RF = \frac{C - A_1 DL}{A_2 (LL + I)}$$

where, on each member, $C =$ capacity of the member, $DL =$ dead load of the member, and $LL + I =$ maximum live load and impact factors induced by the repositioning of the two trucks. For load factor rating, A_1 for dead load is defined as 1.3, and A_2 is 2.17 for Inventory level and 1.3 for Operating level.

Based on the TRAP output, for truss members, Table D.1 contains results of the LFD inventory and operating rating of the original design condition. Table D.2 contains LFD rating results of the existing condition without considering the members' loss of section and Table D.3 contains LFD rating results of the existing condition with the section loss considered. For the truss members, Table D.4 contains LFD rating results of the new FRP deck without considering the members' loss of section and Table D.5 contains LFD rating results of the new FRP deck with the section loss considered. Summary of LFD rating results for all truss, floorbeam and stringer members is shown in Table D.6.

Based on the ANSYS output, for truss members, Table D.7 contains results of the LFD inventory and operating rating of the original design condition. Table D.8 contains LFD rating results of the new FRP deck.

D.2 Differences in Rating Factors between TRAP Analysis and Previous Ratings

The rating factors computed by TRAP are higher than those reported by previous ratings of the bridge. A review of the BAR5 rating performed in 1994 revealed two major differences in assumptions from the TRAP rating. The conservative assumptions made in the BAR5 rating result in significantly lower rating factors.

The first difference involves the use of net sections. The BAR5 rating subtracts the entire area of all bolt/rivet holes to compute the net section of tension members. This is not required by current AASHTO specifications. As per Table 10.32.1A (note *i*) in the 1996 AASHTO Standard Specifications, only the area of holes in excess of 15% of the gross section shall be deducted when rating tension members against yield strength. This specification was followed when computing net sections for the TRAP rating, resulting in higher tension capacities.

The second difference is related to the application of dead loads. In the TRAP analysis, the dead load is distributed to all joints of the truss. The self-weight of each truss member is applied to the adjacent joints. Top bracing loads are applied to the upper chord joints. The weights of the floor steel, deck slab, curb and railing are distributed to all joints of the lower chord, including the supports (L0, L5) which represent the deck loads that go straight to the abutments through the stringer bearings.

In the BAR5 analysis, all of the dead load is applied at the middle four joints of the lower chord (L1, L2, L3, L4). The applied loads are based on two quantities reported on the original plans: the dead load support reaction, and the dead load tension in the first vertical (U1-L1). The vertical tension quantity is applied at L1 and L4. This value is then subtracted from the support reaction, and the difference is applied at L2 and L3. This simplification concentrates the weight of the bridge at the center of the span, increasing the load carried by the truss. The TRAP rating distributes the dead load more evenly across the bridge, resulting in lower dead loads in the truss members.

Conservative assumptions made during previous ratings of the bridge have led to low rating factors. In comparison, the higher capacities and lower dead load forces computed in the TRAP analysis result in higher rating factors.

D.3 Discrepancies in Results between TRAP and ANSYS Finite Element Models

The load rating results from TRAP and ANSYS showed some differences. This is due to several factors, such as the true bridge geometry, where the ANSYS 3D model includes the skew of the bridge. Also, when modeling the live load, a more realistic approach was used in the ANSYS model and the two HS-20 trucks, not automated as the TRAP program does, but simulated as to travel on the bridge in different locations (skewed as the bridge piers), thus giving more realistic results. Also, the type of mesh that was used would affect the loading, as the bridge deck was modeled using a refined mesh, with the truck placed at different locations along the deck, whereas TRAP considers the deck as rigid. In addition, since the bridge was modeled as a space (3D) truss, that also would affect the results of output and would lead to the differences noticed in the submitted runs (for ANSYS and TRAP).

It should be noted that when modeling the HS-20 truck on the bridge in ANSYS, the loading is loaded at the $1/3^{rd}$ and mid-point of the bridge (due to symmetry). This would mean that when applied at the $1/3^{rd}$ point of the bridge, member 29 has a member force of 63.13 kips while member 30 has only 28.55 kips. If the truck is moved to the $2/3^{rd}$ point, member 30 force would switch with member 29 force. The same thing applies to members 33 and 34. For members 35 and 36, one of them will act as a counter and removing it will not overstress the bridge; thus we take them to be equal as they encounter small loads. Due to complicity and symmetry, truck loads are only applied on the first half and the same behavior is expected if truck loads move to the second half.

It should be noted that, if live loading is applied to all critical locations, rating by applying the commonly used 2-D TRAP will give conservative results, while the additional ANSYS modeling and runs were built to be able to approach the true behavior (for load testing) of the MD-24.

D.4 Differences in Rating Factors between WSD and LFD Ratings

The presumption that LFD rating will give a higher rating factor than given by the WSD rating is not always true. The Group I load factors currently in the AASHTO Specifications are:

Maximum Design Load = 1.3[D + (5/3)(L + I)]

This is shown as Curve "A" on Figure D.1 (AASHTO LFD) which relates the factor of safety for bending and tension members to the percent of total load, which is either dead load (upper scale) or live load plus impact (lower scale). The conventional factor of safety against first yield in the service load (WSD) method is 1.82 and this is shown as Curve "B". For long span bridges, 10 percent overstress in members carrying mostly dead load is allowed and its corresponding factor of safety is 1.65, which is shown as Curve "C".

It can be seen from Figure D.1 that if dead to total load ratio is under 45%, AASHTO service load (WSD) method yields a lower safety factor, which can be interpreted as lower rating factors, and vice versa is also true. By comparing the rating factors shown between tables 2.1 through 2.6 and tables D.1 through D.6, there is no constant pattern for the controlling rating factors and their associated members.

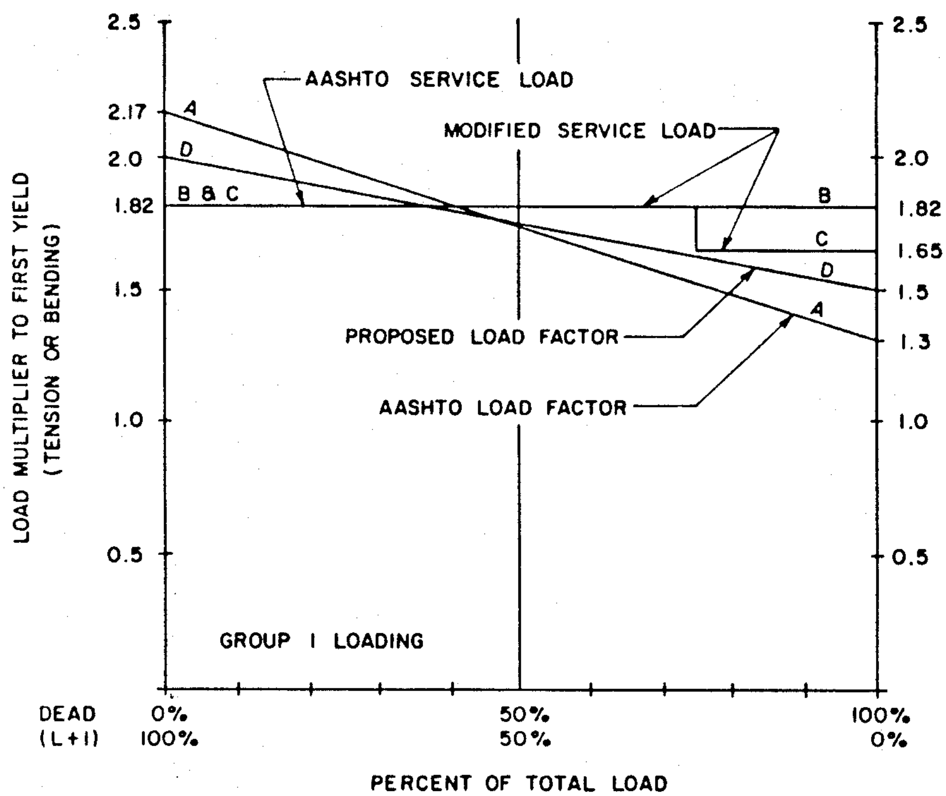

FIGURE D.1 - COMPARISON OF SAFETY FACTORS BETWEEN WSD AND LFD

Table D.1: TRAP-LFD Truss Rating (Original Condition)

TRUSS RATING **(ORIGINAL CONDITION)** **HS20**

All forces in kips **(with AASHTO lanes)**

INVENTORY - LFD

Truss Element	Member Designation	Allowable Tension	Allowable Compr.	1.3 DL	2.17 LL+I Tension	2.17 LL+I Compr.	Rating Tension	Rating Compr.
Bottom Chord	L0-L1	566.18	-475.26	183.17	156.59		2.45	
	L1-L2	566.18	-475.26	183.17	156.59		2.45	
	L2-L3	861.31	-708.76	274.69	214.50		2.73	
	L3-L4	566.18	-475.26	184.47	156.59		2.44	
	L4-L5	566.18	-475.26	184.47	156.59		2.44	
Top Chord	U1-U2	876.15	-714.85	-273.65		-229.39		1.92
	U2-U3	876.15	-714.85	-273.39		-214.72		2.06
	U3-U4	876.15	-714.85	-274.43		-229.39		1.92
Verticals	L1-U1	346.11	-195.55	81.38	158.08		1.67	
	L2-U2	474.55	-315.75	-5.59		-73.93		4.20
	L3-U3	474.55	-315.75	-5.85		-73.93		4.19
	L4-U4	346.11	-195.55	81.38	158.08		1.67	
Diagonals	L0-U1	1613.71	-1234.26	-258.96		-221.64		4.40
	L2-U1	420.20	-133.64	127.92	164.12	-42.01	1.78	6.23
	L2-U3	209.49	-16.15	-1.43	104.53		2.02	
	L3-U2	209.49	-16.15	-0.39	104.53		2.01	
	L3-U4	420.20	-133.64	127.14	164.12	-42.01	1.79	6.21
	L5-U4	1613.71	-1234.26	-260.91		-221.64		4.39

LFD Inventory Rating Factors: **L1-U1** **1.67**

OPERATING - LFD

Truss Element	Member Designation	Allowable Tension	Allowable Compr.	1.3 DL	1.3 LL+I Tension	1.3 LL+I Compr.	Rating Tension	Rating Compr.
Bottom Chord	L0-L1	566.18	-475.26	183.17	93.81		4.08	
	L1-L2	566.18	-475.26	183.17	93.81		4.08	
	L2-L3	861.31	-708.76	274.69	128.51		4.56	
	L3-L4	566.18	-475.26	184.47	93.81		4.07	
	L4-L5	566.18	-475.26	184.47	93.81		4.07	
Top Chord	U1-U2	876.15	-714.85	-273.65		-137.42		3.21
	U2-U3	876.15	-714.85	-273.39		-128.64		3.43
	U3-U4	876.15	-714.85	-274.43		-137.42		3.20
Verticals	L1-U1	346.11	-195.55	81.38	94.71		2.80	
	L2-U2	474.55	-315.75	-5.59		-44.29		7.00
	L3-U3	474.55	-315.75	-5.85		-44.29		7.00
	L4-U4	346.11	-195.55	81.38	94.71		2.80	
Diagonals	L0-U1	1613.71	-1234.26	-258.96		-132.78		7.35
	L2-U1	420.20	-133.64	127.92	98.32	-25.17	2.97	10.39
	L2-U3	209.49	-16.15	-1.43	62.62		3.37	
	L3-U2	209.49	-16.15	-0.39	62.62		3.35	
	L3-U4	420.20	-133.64	127.14	98.32	-25.17	2.98	10.36
	L5-U4	1613.71	-1234.26	-260.91		-132.78		7.33

LFD Operating Rating Factors: **L1-U1** **2.80**

TRUSS RATING **(ORIGINAL CONDITION)**
All forces in kips **(with AASHTO lanes)**

INVENTORY - LFD

Truss Element	Member Designation	Allowable		1.3 DL	State Vehicle Type 3				State Vehicle Type 3S2				State Vehicle Type 3-3			
					2.17 LL+I		Rating		2.17 LL+I		Rating		2.17 LL+I		Rating	
		Tension	Compr.		Tension	Compr.	Tension	Compr.	Tension	Compr.	Tension	Compr.	Tension	Compr.	Tension	Compr.
Bottom Chord	L0-L1	566.18	-475.26	183.17	111.06		3.45		140.20		2.73		146.39		2.62	
	L1-L2	566.18	-475.26	183.17	111.06		3.45		140.20		2.73		146.39		2.62	
	L2-L3	861.31	-708.76	274.69	150.16		3.91		203.33		2.89		208.75		2.81	
	L3-L4	566.18	-475.26	184.47	111.06		3.44		140.20		2.72		146.39		2.61	
	L4-L5	566.18	-475.26	184.47	111.06		3.44		140.20		2.72		146.39		2.61	
Top Chord	U1-U2	876.15	-714.85	-273.65		-163.51		2.70		-207.50		2.13		-211.34		2.09
	U2-U3	876.15	-714.85	-273.39		-150.32		2.94		-203.55		2.17		-208.95		2.11
	U3-U4	876.15	-714.85	-274.43		-163.51		2.69		-207.50		2.12		-211.34		2.08
Verticals	L1-U1	346.11	-195.55	81.38	120.39		2.20		109.30		2.42		100.58		2.63	
	L2-U2	474.55	-315.75	-5.59		-53.77		5.77		-56.62		5.48		-53.51		5.80
	L3-U3	474.55	-315.75	-5.85		-53.77		5.76		-56.62		5.47		-53.51		5.79
	L4-U4	346.11	-195.55	81.38	120.39		2.20		109.30		2.42		100.58		2.63	
Diagonals	L0-U1	1613.71	-1234.26	-258.96		-157.06		6.21		-198.27		4.92		-207.02		4.71
	L2-U1	420.20	-133.64	127.92	117.33	-31.99	2.49	8.18	140.40	-26.15	2.08	10.00	142.40	-26.32	2.05	9.94
	L2-U3	209.49	-16.15	-1.43	76.06		2.77		80.09		2.63		75.71		2.79	
	L3-U2	209.49	-16.15	-0.39	76.06		2.76		80.09		2.62		75.71		2.77	
	L3-U4	420.20	-133.64	127.14	117.33	-31.99	2.50	8.15	140.40	-26.15	2.09	9.97	142.40	-26.32	2.06	9.91
	L5-U4	1613.71	-1234.26	-260.91		-157.06		6.20		-198.27		4.91		-207.02		4.70
LFD Inventory Rating Factors:						**L1-U1**	**2.20**			**L2-U1**	**2.08**			**L2-U1**	**2.05**	

OPERATING - LFD

Truss Element	Member Designation	Allowable		1.3 DL	1.3 LL+I		Rating		1.3 LL+I		Rating		1.3 LL+I		Rating	
		Tension	Compr.		Tension	Compr.	Tension	Compr.	Tension	Compr.	Tension	Compr.	Tension	Compr.	Tension	Compr.
Bottom Chord	L0-L1	566.18	-475.26	183.17	66.53		5.76		83.99		4.56		87.70		4.37	
	L1-L2	566.18	-475.26	183.17	66.53		5.76		83.99		4.56		87.70		4.37	
	L2-L3	861.31	-708.76	274.69	89.96		6.52		121.81		4.82		125.06		4.69	
	L3-L4	566.18	-475.26	184.47	66.53		5.74		83.99		4.54		87.70		4.35	
	L4-L5	566.18	-475.26	184.47	66.53		5.74		83.99		4.54		87.70		4.35	
Top Chord	U1-U2	876.15	-714.85	-273.65		-97.96		4.50		-124.31		3.55		-126.61		3.48
	U2-U3	876.15	-714.85	-273.39		-90.05		4.90		-121.94		3.62		-125.18		3.53
	U3-U4	876.15	-714.85	-274.43		-97.96		4.50		-124.31		3.54		-126.61		3.48
Verticals	L1-U1	346.11	-195.55	81.38	72.12		3.67		65.48		4.04		60.26		4.39	
	L2-U2	474.55	-315.75	-5.59		-32.21		9.63		-33.92		9.14		-32.06		9.67
	L3-U3	474.55	-315.75	-5.85		-32.21		9.62		-33.92		9.14		-32.06		9.67
	L4-U4	346.11	-195.55	81.38	72.12		3.67		65.48		4.04		60.26		4.39	
Diagonals	L0-U1	1613.71	-1234.26	-258.96		-94.09		10.37		-118.78		8.21		-124.02		7.86
	L2-U1	420.20	-133.64	127.92	70.29	-19.16	4.16	13.65	84.11	-15.67	3.47	16.70	85.31	-15.77	3.43	16.59
	L2-U3	209.49	-16.15	-1.43	45.57		4.63		47.98		4.40		45.36		4.65	
	L3-U2	209.49	-16.15	-0.39	45.57		4.61		47.98		4.37		45.36		4.63	
	L3-U4	420.20	-133.64	127.14	70.29	-19.16	4.17	13.61	84.11	-15.67	3.48	16.65	85.31	-15.77	3.44	16.54
	L5-U4	1613.71	-1234.26	-260.91		-94.09		10.34		-118.78		8.19		-124.02		7.85
LFD Operating Rating Factors:						**L1-U1**	**3.67**			**L2-U1**	**3.47**			**L2-U1**	**3.43**	

Table D.2: TRAP-LFD Truss Rating (Existing Condition with Overlay)

TRUSS RATING **(ORIGINAL DECK WITH OVERLAY)** **HS20**

All forces in kips **(with AASHTO lanes)**

INVENTORY - LFD

Truss Element	Member Designation	Allowable Tension	Allowable Compr.	1.3 DL	2.17 LL+I Tension	2.17 LL+I Compr.	Rating Tension	Rating Compr.
Bottom Chord	L0-L1	566.18	-475.26	195.91	156.59		2.36	
	L1-L2	566.18	-475.26	195.91	156.59		2.36	
	L2-L3	861.31	-708.76	293.80	214.50		2.65	
	L3-L4	566.18	-475.26	197.21	156.59		2.36	
	L4-L5	566.18	-475.26	197.21	156.59		2.36	
Top Chord	U1-U2	876.15	-714.85	-292.76		-229.39		1.84
	U2-U3	876.15	-714.85	-292.50		-214.72		1.97
	U3-U4	876.15	-714.85	-293.54		-229.39		1.84
Verticals	L1-U1	346.11	-195.55	87.75	158.08		1.63	
	L2-U2	474.55	-315.75	-5.59		-73.93		4.20
	L3-U3	474.55	-315.75	-5.85		-73.93		4.19
	L4-U4	346.11	-195.55	87.75	158.08		1.63	
Diagonals	L0-U1	1613.71	-1234.26	-277.03		-221.64		4.32
	L2-U1	420.20	-133.64	137.02	164.12	-42.01	1.73	6.44
	L2-U3	209.49	-16.15	-1.43	104.53		2.02	
	L3-U2	209.49	-16.15	-0.39	104.53		2.01	
	L3-U4	420.20	-133.64	136.11	164.12	-42.01	1.73	6.42
	L5-U4	1613.71	-1234.26	-278.98		-221.64		4.31

LFD Inventory Rating Factors: **L1-U1** **1.63**

OPERATING - LFD

Truss Element	Member Designation	Allowable Tension	Allowable Compr.	1.3 DL	1.3 LL+I Tension	1.3 LL+I Compr.	Rating Tension	Rating Compr.
Bottom Chord	L0-L1	566.18	-475.26	195.91	93.81		3.95	
	L1-L2	566.18	-475.26	195.91	93.81		3.95	
	L2-L3	861.31	-708.76	293.80	128.51		4.42	
	L3-L4	566.18	-475.26	197.21	93.81		3.93	
	L4-L5	566.18	-475.26	197.21	93.81		3.93	
Top Chord	U1-U2	876.15	-714.85	-292.76		-137.42		3.07
	U2-U3	876.15	-714.85	-292.50		-128.64		3.28
	U3-U4	876.15	-714.85	-293.54		-137.42		3.07
Verticals	L1-U1	346.11	-195.55	87.75	94.71		2.73	
	L2-U2	474.55	-315.75	-5.59		-44.29		7.00
	L3-U3	474.55	-315.75	-5.85		-44.29		7.00
	L4-U4	346.11	-195.55	87.75	94.71		2.73	
Diagonals	L0-U1	1613.71	-1234.26	-277.03		-132.78		7.21
	L2-U1	420.20	-133.64	137.02	98.32	-25.17	2.88	10.75
	L2-U3	209.49	-16.15	-1.43	62.62		3.37	
	L3-U2	209.49	-16.15	-0.39	62.62		3.35	
	L3-U4	420.20	-133.64	136.11	98.32	-25.17	2.89	10.72
	L5-U4	1613.71	-1234.26	-278.98		-132.78		7.19

LFD Operating Rating Factors: **L1-U1** **2.73**

Table D.2: TRAP-LFD Truss Rating (Existing Condition with Overlay)

TRUSS RATING **(ORIGINAL DECK WITH OVERLAY)**
All forces in kips **(with AASHTO lanes)**

INVENTORY - LFD

Truss Element	Member Designation	Allowable Tension	Allowable Compr.	1.3 DL	State Vehicle Type 3: 2.17 LL+I Tension	State Vehicle Type 3: 2.17 LL+I Compr.	State Vehicle Type 3: Rating Tension	State Vehicle Type 3: Rating Compr.	State Vehicle Type 3S2: 2.17 LL+I Tension	State Vehicle Type 3S2: 2.17 LL+I Compr.	State Vehicle Type 3S2: Rating Tension	State Vehicle Type 3S2: Rating Compr.	State Vehicle Type 3-3: 2.17 LL+I Tension	State Vehicle Type 3-3: 2.17 LL+I Compr.	State Vehicle Type 3-3: Rating Tension	State Vehicle Type 3-3: Rating Compr.
	L0-L1	566.18	-475.26	195.91	111.06		3.33		140.20		2.64		146.39		2.53	
Bottom	L1-L2	566.18	-475.26	195.91	111.06		3.33		140.20		2.64		146.39		2.53	
Chord	L2-L3	861.31	-708.76	293.80	150.16		3.78		203.33		2.79		208.75		2.72	
	L3-L4	566.18	-475.26	197.21	111.06		3.32		140.20		2.63		146.39		2.52	
	L4-L5	566.18	-475.26	197.21	111.06		3.32		140.20		2.63		146.39		2.52	
Top	U1-U2	876.15	-714.85	-292.76		-163.51		2.58		-207.50		2.03		-211.34		2.00
Chord	U2-U3	876.15	-714.85	-292.50		-150.32		2.81		-203.55		2.07		-208.95		2.02
	U3-U4	876.15	-714.85	-293.54		-163.51		2.58		-207.50		2.03		-211.34		1.99
	L1-U1	346.11	-195.55	87.75	120.39		2.15		109.30		2.36		100.58		2.57	
Verticals	L2-U2	474.55	-315.75	-5.59		-53.77		5.77		-56.62		5.48		-53.51		5.80
	L3-U3	474.55	-315.75	-5.85		-53.77		5.76		-56.62		5.47		-53.51		5.79
	L4-U4	346.11	-195.55	87.75	120.39		2.15		109.30		2.36		100.58		2.57	
	L0-U1	1613.71	-1234.26	-277.03		-157.06		6.09		-198.27		4.83		-207.02		4.62
	L2-U1	420.20	-133.64	137.02	117.33	-31.99	2.41	8.46	140.40	-26.15	2.02	10.35	142.40	-26.32	1.99	10.28
Diagonals	L2-U3	209.49	-16.15	-1.43	76.06		2.77		80.09		2.63		75.71		2.79	
	L3-U2	209.49	-16.15	-0.39	76.06		2.76		80.09		2.62		75.71		2.77	
	L3-U4	420.20	-133.64	136.11	117.33	-31.99	2.42	8.43	140.40	-26.15	2.02	10.32	142.40	-26.32	2.00	10.25
	L5-U4	1613.71	-1234.26	-278.98		-157.06		6.08		-198.27		4.82		-207.02		4.61

LFD Inventory Rating Factors: State Vehicle Type 3: **L1-U1 2.15** | State Vehicle Type 3S2: **L2-U1 2.02** | State Vehicle Type 3-3: **L2-U1 1.99**

OPERATING - LFD

Truss Element	Member Designation	Allowable Tension	Allowable Compr.	1.3 DL	State Vehicle Type 3: 1.3 LL+I Tension	State Vehicle Type 3: 1.3 LL+I Compr.	State Vehicle Type 3: Rating Tension	State Vehicle Type 3: Rating Compr.	State Vehicle Type 3S2: 1.3 LL+I Tension	State Vehicle Type 3S2: 1.3 LL+I Compr.	State Vehicle Type 3S2: Rating Tension	State Vehicle Type 3S2: Rating Compr.	State Vehicle Type 3-3: 1.3 LL+I Tension	State Vehicle Type 3-3: 1.3 LL+I Compr.	State Vehicle Type 3-3: Rating Tension	State Vehicle Type 3-3: Rating Compr.
	L0-L1	566.18	-475.26	195.91	66.53		5.57		83.99		4.41		87.70		4.22	
Bottom	L1-L2	566.18	-475.26	195.91	66.53		5.57		83.99		4.41		87.70		4.22	
Chord	L2-L3	861.31	-708.76	293.80	89.96		6.31		121.81		4.66		125.06		4.54	
	L3-L4	566.18	-475.26	197.21	66.53		5.55		83.99		4.39		87.70		4.21	
	L4-L5	566.18	-475.26	197.21	66.53		5.55		83.99		4.39		87.70		4.21	
Top	U1-U2	876.15	-714.85	-292.76		-97.96		4.31		-124.31		3.40		-126.61		3.33
Chord	U2-U3	876.15	-714.85	-292.50		-90.05		4.69		-121.94		3.46		-125.18		3.37
	U3-U4	876.15	-714.85	-293.54		-97.96		4.30		-124.31		3.39		-126.61		3.33
	L1-U1	346.11	-195.55	87.75	72.12		3.58		65.48		3.95		60.26		4.29	
Verticals	L2-U2	474.55	-315.75	-5.59		-32.21		9.63		-33.92		9.14		-32.06		9.67
	L3-U3	474.55	-315.75	-5.85		-32.21		9.62		-33.92		9.14		-32.06		9.67
	L4-U4	346.11	-195.55	87.75	72.12		3.58		65.48		3.95		60.26		4.29	
	L0-U1	1613.71	-1234.26	-277.03		-94.09		10.17		-118.78		8.06		-124.02		7.72
	L2-U1	420.20	-133.64	137.02	70.29	-19.16	4.03	14.12	84.11	-15.67	3.37	17.28	85.31	-15.77	3.32	17.16
Diagonals	L2-U3	209.49	-16.15	-1.43	45.57		4.63		47.98		4.40		45.36		4.65	
	L3-U2	209.49	-16.15	-0.39	45.57		4.61		47.98		4.37		45.36		4.63	
	L3-U4	420.20	-133.64	136.11	70.29	-19.16	4.04	14.08	84.11	-15.67	3.38	17.22	85.31	-15.77	3.33	17.11
	L5-U4	1613.71	-1234.26	-278.98		-94.09		10.15		-118.78		8.04		-124.02		7.70

LFD Operating Rating Factors: State Vehicle Type 3: **L1-U1 3.58** | State Vehicle Type 3S2: **L2-U1 3.37** | State Vehicle Type 3-3: **L2-U1 3.32**

Table D.3: TRAP-LFD Truss Rating (Existing Condition with Overlay, Section Loss)

TRUSS RATING **(ORIGINAL DECK WITH OVERLAY, SECTION LOSS)** **HS20**

All forces in kips **(with AASHTO lanes)**

INVENTORY - LFD

	Truss Element	Member Designation	Allowable Tension	Allowable Compr.	1.3 DL	2.17 LL+I Tension	2.17 LL+I Compr.	Rating Tension	Rating Compr.
	Bottom Chord	L0-L1	566.18	-475.26	195.91	156.59		2.36	
		L1-L2	566.18	-475.26	195.91	156.59		2.36	
		L2-L3	861.31	-708.76	293.80	214.50		2.65	
		L3-L4	566.18	-475.26	197.21	156.59		2.36	
		L4-L5	566.18	-475.26	197.21	156.59		2.36	
	Top Chord	U1-U2	876.15	-714.85	-292.76		-229.39		1.84
		U2-U3	876.15	-714.85	-292.50		-214.72		1.97
		U3-U4	876.15	-714.85	-293.54		-229.39		1.84
SECTION LOSS →	Verticals	L1-U1	251.80	-195.55	87.75	158.08		1.04	
		L2-U2	474.55	-315.75	-5.59		-73.93		4.20
		L3-U3	474.55	-315.75	-5.85		-73.93		4.19
		L4-U4	346.11	-195.55	87.75	158.08		1.63	
	Diagonals	L0-U1	1613.71	-1234.26	-277.03		-221.64		4.32
		L2-U1	420.20	-133.64	137.02	164.12	-42.01	1.73	6.44
		L2-U3	209.49	-16.15	-1.43	104.53		2.02	
		L3-U2	209.49	-16.15	-0.39	104.53		2.01	
		L3-U4	420.20	-133.64	136.11	164.12	-42.01	1.73	6.42
		L5-U4	1613.71	-1234.26	-278.98		-221.64		4.31

LFD Inventory Rating Factors: **L1-U1** **1.04**

OPERATING - LFD

	Truss Element	Member Designation	Allowable Tension	Allowable Compr.	1.3 DL	1.3 LL+I Tension	1.3 LL+I Compr.	Rating Tension	Rating Compr.
	Bottom Chord	L0-L1	566.18	-475.26	195.91	93.81		3.95	
		L1-L2	566.18	-475.26	195.91	93.81		3.95	
		L2-L3	861.31	-708.76	293.80	128.51		4.42	
		L3-L4	566.18	-475.26	197.21	93.81		3.93	
		L4-L5	566.18	-475.26	197.21	93.81		3.93	
	Top Chord	U1-U2	876.15	-714.85	-292.76		-137.42		3.07
		U2-U3	876.15	-714.85	-292.50		-128.64		3.28
		U3-U4	876.15	-714.85	-293.54		-137.42		3.07
SECTION LOSS →	Verticals	L1-U1	251.80	-195.55	87.75	94.71		1.73	
		L2-U2	474.55	-315.75	-5.59		-44.29		7.00
		L3-U3	474.55	-315.75	-5.85		-44.29		7.00
		L4-U4	346.11	-195.55	87.75	94.71		2.73	
	Diagonals	L0-U1	1613.71	-1234.26	-277.03		-132.78		7.21
		L2-U1	420.20	-133.64	137.02	98.32	-25.17	2.88	10.75
		L2-U3	209.49	-16.15	-1.43	62.62		3.37	
		L3-U2	209.49	-16.15	-0.39	62.62		3.35	
		L3-U4	420.20	-133.64	136.11	98.32	-25.17	2.89	10.72
		L5-U4	1613.71	-1234.26	-278.98		-132.78		7.19

LFD Operating Rating Factors: **L1-U1** **1.73**

Table D.3: TRAP-LFD Truss Rating (Existing Condition with Overlay, Section Loss)

TRUSS RATING **(ORIGINAL DECK WITH OVERLAY, SECTION LOSS)**
All forces in kips **(with AASHTO lanes)**

INVENTORY - LFD

	Truss Element	Member Designation	Allowable Tension	Allowable Compr.	1.3 DL	State Vehicle Type 3: 2.17 LL+I Tension	State Vehicle Type 3: 2.17 LL+I Compr.	State Vehicle Type 3: Rating Tension	State Vehicle Type 3: Rating Compr.	State Vehicle Type 3S2: 2.17 LL+I Tension	State Vehicle Type 3S2: 2.17 LL+I Compr.	State Vehicle Type 3S2: Rating Tension	State Vehicle Type 3S2: Rating Compr.	State Vehicle Type 3-3: 2.17 LL+I Tension	State Vehicle Type 3-3: 2.17 LL+I Compr.	State Vehicle Type 3-3: Rating Tension	State Vehicle Type 3-3: Rating Compr.
	Bottom Chord	L0-L1	566.18	-475.26	195.91	111.06		3.33		140.20		2.64		146.39		2.53	
		L1-L2	566.18	-475.26	195.91	111.06		3.33		140.20		2.64		146.39		2.53	
		L2-L3	861.31	-708.76	293.80	150.16		3.78		203.33		2.79		208.75		2.72	
		L3-L4	566.18	-475.26	197.21	111.06		3.32		140.20		2.63		146.39		2.52	
		L4-L5	566.18	-475.26	197.21	111.06		3.32		140.20		2.63		146.39		2.52	
	Top Chord	U1-U2	876.15	-714.85	-292.76		-163.51		2.58		-207.50		2.03		-211.34		2.00
		U2-U3	876.15	-714.85	-292.50		-150.32		2.81		-203.55		2.07		-208.95		2.02
		U3-U4	876.15	-714.85	-293.54		-163.51		2.58		-207.50		2.03		-211.34		1.99
SECTION LOSS →	Verticals	L1-U1	251.80	-195.55	87.75	120.39		1.36		109.30		1.50		100.58		1.63	
		L2-U2	474.55	-315.75	-5.59		-53.77		5.77		-56.62		5.48		-53.51		5.80
		L3-U3	474.55	-315.75	-5.85		-53.77		5.76		-56.62		5.47		-53.51		5.79
		L4-U4	346.11	-195.55	87.75	120.39		2.15		109.30		2.36		100.58		2.57	
	Diagonals	L0-U1	1613.71	-1234.26	-277.03		-157.06		6.09		-198.27		4.83		-207.02		4.62
		L2-U1	420.20	-133.64	137.02	117.33	-31.99	2.41	8.46	140.40	-26.15	2.02	10.35	142.40	-26.32	1.99	10.28
		L2-U3	209.49	-16.15	-1.43	76.06		2.77		80.09		2.63		75.71		2.79	
		L3-U2	209.49	-16.15	-0.39	76.06		2.76		80.09		2.62		75.71		2.77	
		L3-U4	420.20	-133.64	136.11	117.33	-31.99	2.42	8.43	140.40	-26.15	2.02	10.32	142.40	-26.32	2.00	10.25
		L5-U4	1613.71	-1234.26	-278.98		-157.06		6.08		-198.27		4.82		-207.02		4.61
	LFD Inventory Rating Factors:						**L1-U1**	**1.36**			**L1-U1**	**1.50**			**L1-U1**	**1.63**	

OPERATING - LFD

	Truss Element	Member Designation	Allowable Tension	Allowable Compr.	1.3 DL	State Vehicle Type 3: 1.3 LL+I Tension	State Vehicle Type 3: 1.3 LL+I Compr.	State Vehicle Type 3: Rating Tension	State Vehicle Type 3: Rating Compr.	State Vehicle Type 3S2: 1.3 LL+I Tension	State Vehicle Type 3S2: 1.3 LL+I Compr.	State Vehicle Type 3S2: Rating Tension	State Vehicle Type 3S2: Rating Compr.	State Vehicle Type 3-3: 1.3 LL+I Tension	State Vehicle Type 3-3: 1.3 LL+I Compr.	State Vehicle Type 3-3: Rating Tension	State Vehicle Type 3-3: Rating Compr.
	Bottom Chord	L0-L1	566.18	-475.26	195.91	66.53		5.57		83.99		4.41		87.70		4.22	
		L1-L2	566.18	-475.26	195.91	66.53		5.57		83.99		4.41		87.70		4.22	
		L2-L3	861.31	-708.76	293.80	89.96		6.31		121.81		4.66		125.06		4.54	
		L3-L4	566.18	-475.26	197.21	66.53		5.55		83.99		4.39		87.70		4.21	
		L4-L5	566.18	-475.26	197.21	66.53		5.55		83.99		4.39		87.70		4.21	
	Top Chord	U1-U2	876.15	-714.85	-292.76		-97.96		4.31		-124.31		3.40		-126.61		3.33
		U2-U3	876.15	-714.85	-292.50		-90.05		4.69		-121.94		3.46		-125.18		3.37
		U3-U4	876.15	-714.85	-293.54		-97.96		4.30		-124.31		3.39		-126.61		3.33
SECTION LOSS →	Verticals	L1-U1	251.80	-195.55	87.75	72.12		2.27		65.48		2.51		60.26		2.72	
		L2-U2	474.55	-315.75	-5.59		-32.21		9.63		-33.92		9.14		-32.06		9.67
		L3-U3	474.55	-315.75	-5.85		-32.21		9.62		-33.92		9.14		-32.06		9.67
		L4-U4	346.11	-195.55	87.75	72.12		3.58		65.48		3.95		60.26		4.29	
	Diagonals	L0-U1	1613.71	-1234.26	-277.03		-94.09		10.17		-118.78		8.06		-124.02		7.72
		L2-U1	420.20	-133.64	137.02	70.29	-19.16	4.03	14.12	84.11	-15.67	3.37	17.28	85.31	-15.77	3.32	17.16
		L2-U3	209.49	-16.15	-1.43	45.57		4.63		47.98		4.40		45.36		4.65	
		L3-U2	209.49	-16.15	-0.39	45.57		4.61		47.98		4.37		45.36		4.63	
		L3-U4	420.20	-133.64	136.11	70.29	-19.16	4.04	14.08	84.11	-15.67	3.38	17.22	85.31	-15.77	3.33	17.11
		L5-U4	1613.71	-1234.26	-278.98		-94.09		10.15		-118.78		8.04		-124.02		7.70
	LFD Operating Rating Factors:						**L1-U1**	**2.27**			**L1-U1**	**2.51**			**L1-U1**	**2.72**	

Table D.4: TRAP-LFD Truss Rating (with FRP Deck)

TRUSS RATING **(WITH FRP DECK)** **HS20**

All forces in kips **(with AASHTO lanes)**

INVENTORY - LFD

Truss Element	Member Designation	Allowable Tension	Allowable Compr.	1.3 DL	2.17 LL+I Tension	2.17 LL+I Compr.	Rating Tension	Rating Compr.
Bottom Chord	L0-L1	566.18	-475.26	136.11	153.48		2.80	
	L1-L2	566.18	-475.26	136.11	153.48		2.80	
	L2-L3	861.31	-708.76	204.23	210.27		3.12	
	L3-L4	566.18	-475.26	137.54	153.48		2.79	
	L4-L5	566.18	-475.26	137.54	153.48		2.79	
Top Chord	U1-U2	876.15	-714.85	-203.06		-224.86		2.28
	U2-U3	876.15	-714.85	-202.80		-210.49		2.43
	U3-U4	876.15	-714.85	-203.97		-224.86		2.27
Verticals	L1-U1	346.11	-195.55	57.85	154.96		1.86	
	L2-U2	474.55	-315.75	-5.59		-73.19		4.24
	L3-U3	474.55	-315.75	-5.85		-73.19		4.23
	L4-U4	346.11	-195.55	57.85	154.96		1.86	
Diagonals	L0-U1	1613.71	-1234.26	-192.53		-217.26		4.79
	L2-U1	420.20	-133.64	94.77	160.88	-41.16	2.02	5.55
	L2-U3	209.49	-16.15	-1.56	103.51		2.04	
	L3-U2	209.49	-16.15	-0.39	103.51		2.03	
	L3-U4	420.20	-133.64	93.86	160.88	-41.16	2.03	5.53
	L5-U4	1613.71	-1234.26	-194.48		-217.26		4.79

LFD Inventory Rating Factors: **L1-U1** **1.86**

OPERATING - LFD

Truss Element	Member Designation	Allowable Tension	Allowable Compr.	1.3 DL	1.3 LL+I Tension	1.3 LL+I Compr.	Rating Tension	Rating Compr.
Bottom Chord	L0-L1	566.18	-475.26	136.11	91.95		4.68	
	L1-L2	566.18	-475.26	136.11	91.95		4.68	
	L2-L3	861.31	-708.76	204.23	125.97		5.22	
	L3-L4	566.18	-475.26	137.54	91.95		4.66	
	L4-L5	566.18	-475.26	137.54	91.95		4.66	
Top Chord	U1-U2	876.15	-714.85	-203.06		-134.71		3.80
	U2-U3	876.15	-714.85	-202.80		-126.10		4.06
	U3-U4	876.15	-714.85	-203.97		-134.71		3.79
Verticals	L1-U1	346.11	-195.55	57.85	92.83		3.11	
	L2-U2	474.55	-315.75	-5.59		-43.85		7.07
	L3-U3	474.55	-315.75	-5.85		-43.85		7.07
	L4-U4	346.11	-195.55	57.85	92.83		3.11	
Diagonals	L0-U1	1613.71	-1234.26	-192.53		-130.16		8.00
	L2-U1	420.20	-133.64	94.77	96.38	-24.66	3.38	9.26
	L2-U3	209.49	-16.15	-1.56	62.01		3.40	
	L3-U2	209.49	-16.15	-0.39	62.01		3.38	
	L3-U4	420.20	-133.64	93.86	96.38	-24.66	3.39	9.22
	L5-U4	1613.71	-1234.26	-194.48		-130.16		7.99

LFD Operating Rating Factors: **L1-U1** **3.11**

Table D.4: TRAP-LFD Truss Rating (with FRP Deck)

TRUSS RATING **(WITH FRP DECK)**
All forces in kips **(with AASHTO lanes)**

INVENTORY - LFD

Truss Element	Member Designation	Allowable Tension	Allowable Compr.	1.3 DL	State Vehicle Type 3: 2.17 LL+I Tension	2.17 LL+I Compr.	Rating Tension	Rating Compr.	State Vehicle Type 3S2: 2.17 LL+I Tension	2.17 LL+I Compr.	Rating Tension	Rating Compr.	State Vehicle Type 3-3: 2.17 LL+I Tension	2.17 LL+I Compr.	Rating Tension	Rating Compr.
Bottom Chord	L0-L1	566.18	-475.26	136.11	108.87		3.95		137.43		3.13		143.48		3.00	
	L1-L2	566.18	-475.26	136.11	108.87		3.95		137.43		3.13		143.48		3.00	
	L2-L3	861.31	-708.76	204.23	147.19		4.46		199.31		3.30		204.63		3.21	
	L3-L4	566.18	-475.26	137.54	108.87		3.94		137.43		3.12		143.48		2.99	
	L4-L5	566.18	-475.26	137.54	108.87		3.94		137.43		3.12		143.48		2.99	
Top Chord	U1-U2	876.15	-714.85	-203.06		-160.28		3.19		-203.42		2.52		-207.15		2.47
	U2-U3	876.15	-714.85	-202.80		-147.34		3.48		-199.53		2.57		-204.83		2.50
	U3-U4	876.15	-714.85	-203.97		-160.28		3.19		-203.42		2.51		-207.15		2.47
Verticals	L1-U1	346.11	-195.55	57.85	118.03		2.44		107.15		2.69		98.58		2.92	
	L2-U2	474.55	-315.75	-5.59		-53.25		5.82		-56.07		5.53		-52.99		5.85
	L3-U3	474.55	-315.75	-5.85		-53.25		5.82		-56.07		5.53		-52.99		5.85
	L4-U4	346.11	-195.55	57.85	118.03		2.44		107.15		2.69		98.58		2.92	
Diagonals	L0-U1	1613.71	-1234.26	-192.53		-153.96		6.77		-194.37		5.36		-202.92		5.13
	L2-U1	420.20	-133.64	94.77	115.03	-31.36	2.83	7.28	137.62	-25.65	2.36	8.90	139.57	-25.80	2.33	8.85
	L2-U3	209.49	-16.15	-1.56	75.32		2.80		79.29		2.66		74.95		2.82	
	L3-U2	209.49	-16.15	-0.39	75.32		2.79		79.29		2.65		74.95		2.80	
	L3-U4	420.20	-133.64	93.86	115.03	-31.36	2.84	7.26	137.62	-25.65	2.37	8.87	139.57	-25.80	2.34	8.82
	L5-U4	1613.71	-1234.26	-194.48		-153.96		6.75		-194.37		5.35		-202.92		5.12

LFD Inventory Rating Factors: State Vehicle Type 3: **L1-U1 2.44**; State Vehicle Type 3S2: **L2-U1 2.36**; State Vehicle Type 3-3: **L2-U1 2.33**

OPERATING - LFD

Truss Element	Member Designation	Allowable Tension	Allowable Compr.	1.3 DL	State Vehicle Type 3: 1.3 LL+I Tension	1.3 LL+I Compr.	Rating Tension	Rating Compr.	State Vehicle Type 3S2: 1.3 LL+I Tension	1.3 LL+I Compr.	Rating Tension	Rating Compr.	State Vehicle Type 3-3: 1.3 LL+I Tension	1.3 LL+I Compr.	Rating Tension	Rating Compr.
Bottom Chord	L0-L1	566.18	-475.26	136.11	65.22		6.59		82.33		5.22		85.96		5.00	
	L1-L2	566.18	-475.26	136.11	65.22		6.59		82.33		5.22		85.96		5.00	
	L2-L3	861.31	-708.76	204.23	88.18		7.45		119.41		5.50		122.59		5.36	
	L3-L4	566.18	-475.26	137.54	65.22		6.57		82.33		5.21		85.96		4.99	
	L4-L5	566.18	-475.26	137.54	65.22		6.57		82.33		5.21		85.96		4.99	
Top Chord	U1-U2	876.15	-714.85	-203.06		-96.02		5.33		-121.86		4.20		-124.10		4.12
	U2-U3	876.15	-714.85	-202.80		-88.27		5.80		-119.54		4.28		-122.71		4.17
	U3-U4	876.15	-714.85	-203.97		-96.02		5.32		-121.86		4.19		-124.10		4.12
Verticals	L1-U1	346.11	-195.55	57.85	70.71		4.08		64.19		4.49		59.06		4.88	
	L2-U2	474.55	-315.75	-5.59		-31.90		9.72		-33.59		9.23		-31.75		9.77
	L3-U3	474.55	-315.75	-5.85		-31.90		9.71		-33.59		9.23		-31.75		9.76
	L4-U4	346.11	-195.55	57.85	70.71		4.08		64.19		4.49		59.06		4.88	
Diagonals	L0-U1	1613.71	-1234.26	-192.53		-92.24		11.29		-116.44		8.95		-121.56		8.57
	L2-U1	420.20	-133.64	94.77	68.91	-18.79	4.72	12.16	82.45	-15.37	3.95	14.86	83.62	-15.46	3.89	14.78
	L2-U3	209.49	-16.15	-1.56	45.12		4.68		47.50		4.44		44.90		4.70	
	L3-U2	209.49	-16.15	-0.39	45.12		4.65		47.50		4.42		44.90		4.67	
	L3-U4	420.20	-133.64	93.86	68.91	-18.79	4.74	12.11	82.45	-15.37	3.96	14.81	83.62	-15.46	3.90	14.72
	L5-U4	1613.71	-1234.26	-194.48		-92.24		11.27		-116.44		8.93		-121.56		8.55

LFD Operating Rating Factors: State Vehicle Type 3: **L1-U1 4.08**; State Vehicle Type 3S2: **L2-U1 3.95**; State Vehicle Type 3-3: **L2-U1 3.89**

Table D.5: TRAP-LFD Truss Rating (with FRP Deck, Section Loss)

TRUSS RATING **(WITH FRP DECK, SECTION LOSS)** **HS20**
All forces in kips **(with AASHTO lanes)**

INVENTORY - LFD	Truss Element	Member Designation	Allowable Tension	Allowable Compr.	1.3 DL	2.17 LL+I Tension	2.17 LL+I Compr.	Rating Tension	Rating Compr.
	Bottom Chord	L0-L1	566.18	-475.26	136.11	153.48		2.80	
		L1-L2	566.18	-475.26	136.11	153.48		2.80	
		L2-L3	861.31	-708.76	204.23	210.27		3.12	
		L3-L4	566.18	-475.26	137.54	153.48		2.79	
		L4-L5	566.18	-475.26	137.54	153.48		2.79	
	Top Chord	U1-U2	876.15	-714.85	-203.06		-224.86		2.28
		U2-U3	876.15	-714.85	-202.80		-210.49		2.43
		U3-U4	876.15	-714.85	-203.97		-224.86		2.27
SECTION LOSS →	Verticals	L1-U1	251.80	-195.55	57.85	154.96		1.25	
		L2-U2	474.55	-315.75	-5.59		-73.19		4.24
		L3-U3	474.55	-315.75	-5.85		-73.19		4.23
		L4-U4	346.11	-195.55	57.85	154.96		1.86	
	Diagonals	L0-U1	1613.71	-1234.26	-192.53		-217.26		4.79
		L2-U1	420.20	-133.64	94.77	160.88	-41.16	2.02	5.55
		L2-U3	209.49	-16.15	-1.56	103.51		2.04	
		L3-U2	209.49	-16.15	-0.39	103.51		2.03	
		L3-U4	420.20	-133.64	93.86	160.88	-41.16	2.03	5.53
		L5-U4	1613.71	-1234.26	-194.48		-217.26		4.79

LFD Inventory Rating Factors: **L1-U1** **1.25**

OPERATING - LFD	Truss Element	Member Designation	Allowable Tension	Allowable Compr.	1.3 DL	1.3 LL+I Tension	1.3 LL+I Compr.	Rating Tension	Rating Compr.
	Bottom Chord	L0-L1	566.18	-475.26	136.11	91.95		4.68	
		L1-L2	566.18	-475.26	136.11	91.95		4.68	
		L2-L3	861.31	-708.76	204.23	125.97		5.22	
		L3-L4	566.18	-475.26	137.54	91.95		4.66	
		L4-L5	566.18	-475.26	137.54	91.95		4.66	
	Top Chord	U1-U2	876.15	-714.85	-203.06		-134.71		3.80
		U2-U3	876.15	-714.85	-202.80		-126.10		4.06
		U3-U4	876.15	-714.85	-203.97		-134.71		3.79
SECTION LOSS →	Verticals	L1-U1	251.80	-195.55	57.85	92.83		2.09	
		L2-U2	474.55	-315.75	-5.59		-43.85		7.07
		L3-U3	474.55	-315.75	-5.85		-43.85		7.07
		L4-U4	346.11	-195.55	57.85	92.83		3.11	
	Diagonals	L0-U1	1613.71	-1234.26	-192.53		-130.16		8.00
		L2-U1	420.20	-133.64	94.77	96.38	-24.66	3.38	9.26
		L2-U3	209.49	-16.15	-1.56	62.01		3.40	
		L3-U2	209.49	-16.15	-0.39	62.01		3.38	
		L3-U4	420.20	-133.64	93.86	96.38	-24.66	3.39	9.22
		L5-U4	1613.71	-1234.26	-194.48		-130.16		7.99

LFD Operating Rating Factors: **L1-U1** **2.09**

Table D.5: TRAP-LFD Truss Rating (with FRP Deck, Section Loss)

TRUSS RATING **(WITH FRP DECK, SECTION LOSS)**
All forces in kips **(with AASHTO lanes)**

INVENTORY - LFD	Truss Element	Member Designation	Allowable Tension	Allowable Compr.	1.3 DL	**State Vehicle Type 3** 2.17 LL+I Tension	2.17 LL+I Compr.	Rating Tension	Rating Compr.	**State Vehicle Type 3S2** 2.17 LL+I Tension	2.17 LL+I Compr.	Rating Tension	Rating Compr.	**State Vehicle Type 3-3** 2.17 LL+I Tension	2.17 LL+I Compr.	Rating Tension	Rating Compr.
	Bottom Chord	L0-L1	566.18	-475.26	136.11	108.87		3.95		137.43		3.13		143.48		3.00	
		L1-L2	566.18	-475.26	136.11	108.87		3.95		137.43		3.13		143.48		3.00	
		L2-L3	861.31	-708.76	204.23	147.19		4.46		199.31		3.30		204.63		3.21	
		L3-L4	566.18	-475.26	137.54	108.87		3.94		137.43		3.12		143.48		2.99	
		L4-L5	566.18	-475.26	137.54	108.87		3.94		137.43		3.12		143.48		2.99	
	Top Chord	U1-U2	876.15	-714.85	-203.06		-160.28		3.19		-203.42		2.52		-207.15		2.47
		U2-U3	876.15	-714.85	-202.80		-147.34		3.48		-199.53		2.57		-204.83		2.50
		U3-U4	876.15	-714.85	-203.97		-160.28		3.19		-203.42		2.51		-207.15		2.47
SECTION LOSS →	Verticals	L1-U1	251.80	-195.55	57.85	118.03		1.64		107.15		1.81		98.58		1.97	
		L2-U2	474.55	-315.75	-5.59		-53.25		5.82		-56.07		5.53		-52.99		5.85
		L3-U3	474.55	-315.75	-5.85		-53.25		5.82		-56.07		5.53		-52.99		5.85
		L4-U4	346.11	-195.55	57.85	118.03		2.44		107.15		2.69		98.58		2.92	
	Diagonals	L0-U1	1613.71	-1234.26	-192.53		-153.96		6.77		-194.37		5.36		-202.92		5.13
		L2-U1	420.20	-133.64	94.77	115.03	-31.36	2.83	7.28	137.62	-25.65	2.36	8.90	139.57	-25.80	2.33	8.85
		L2-U3	209.49	-16.15	-1.56	75.32		2.80		79.29		2.66		74.95		2.82	
		L3-U2	209.49	-16.15	-0.39	75.32		2.79		79.29		2.65		74.95		2.80	
		L3-U4	420.20	-133.64	93.86	115.03	-31.36	2.84	7.26	137.62	-25.65	2.37	8.87	139.57	-25.80	2.34	8.82
		L5-U4	1613.71	-1234.26	-194.48		-153.96		6.75		-194.37		5.35		-202.92		5.12

LFD Inventory Rating Factors: Type 3: **L1-U1 1.64** | Type 3S2: **L1-U1 1.81** | Type 3-3: **L1-U1 1.97**

OPERATING - LFD	Truss Element	Member Designation	Allowable Tension	Allowable Compr.	1.3 DL	**State Vehicle Type 3** 1.3 LL+I Tension	1.3 LL+I Compr.	Rating Tension	Rating Compr.	**State Vehicle Type 3S2** 1.3 LL+I Tension	1.3 LL+I Compr.	Rating Tension	Rating Compr.	**State Vehicle Type 3-3** 1.3 LL+I Tension	1.3 LL+I Compr.	Rating Tension	Rating Compr.
	Bottom Chord	L0-L1	566.18	-475.26	136.11	65.22		6.59		82.33		5.22		85.96		5.00	
		L1-L2	566.18	-475.26	136.11	65.22		6.59		82.33		5.22		85.96		5.00	
		L2-L3	861.31	-708.76	204.23	88.18		7.45		119.41		5.50		122.59		5.36	
		L3-L4	566.18	-475.26	137.54	65.22		6.57		82.33		5.21		85.96		4.99	
		L4-L5	566.18	-475.26	137.54	65.22		6.57		82.33		5.21		85.96		4.99	
	Top Chord	U1-U2	876.15	-714.85	-203.06		-96.02		5.33		-121.86		4.20		-124.10		4.12
		U2-U3	876.15	-714.85	-202.80		-88.27		5.80		-119.54		4.28		-122.71		4.17
		U3-U4	876.15	-714.85	-203.97		-96.02		5.32		-121.86		4.19		-124.10		4.12
SECTION LOSS →	Verticals	L1-U1	251.80	-195.55	57.85	70.71		2.74		64.19		3.02		59.06		3.28	
		L2-U2	474.55	-315.75	-5.59		-31.90		9.72		-33.59		9.23		-31.75		9.77
		L3-U3	474.55	-315.75	-5.85		-31.90		9.71		-33.59		9.23		-31.75		9.76
		L4-U4	346.11	-195.55	57.85	70.71		4.08		64.19		4.49		59.06		4.88	
	Diagonals	L0-U1	1613.71	-1234.26	-192.53		-92.24		11.29		-116.44		8.95		-121.56		8.57
		L2-U1	420.20	-133.64	94.77	68.91	-18.79	4.72	12.16	82.45	-15.37	3.95	14.86	83.62	-15.46	3.89	14.78
		L2-U3	209.49	-16.15	-1.56	45.12		4.68		47.50		4.44		44.90		4.70	
		L3-U2	209.49	-16.15	-0.39	45.12		4.65		47.50		4.42		44.90		4.67	
		L3-U4	420.20	-133.64	93.86	68.91	-18.79	4.74	12.11	82.45	-15.37	3.96	14.81	83.62	-15.46	3.90	14.72
		L5-U4	1613.71	-1234.26	-194.48		-92.24		11.27		-116.44		8.93		-121.56		8.55

LFD Operating Rating Factors: Type 3: **L1-U1 2.74** | Type 3S2: **L1-U1 3.02** | Type 3-3: **L1-U1 3.28**

Table D.6 - Summary of TRAP LFD Rating Results for All Truss, Floorbeam and Stringer Members

Summary of Rating Factors - LFD Method

								WITH SECTION LOSS *			
TRUSS	Vehicle	Original Condition		Existing Deck with Overlay		FRP Deck		Existing Deck with Overlay		FRP Deck	
INVENTORY	HS20	1.67	L1-U1	1.63	L1-U1	1.89	L1-U1	1.04	L1-U1	1.28	L1-U1
	State Vehicle Type 3	2.20	L1-U1	2.15	L1-U1	2.48	L1-U1	1.36	L1-U1	1.69	L1-U1
	State Vehicle Type 3S2	2.08	L2-U1	2.02	L2-U1	2.42	L2-U1	1.50	L1-U1	1.86	L1-U1
	State Vehicle Type 3-3	2.05	L2-U1	1.99	L2-U1	2.38	L2-U1	1.63	L1-U1	2.02	L1-U1
OPERATING	HS20	2.80	L1-U1	2.73	L1-U1	3.16	L1-U1	1.73	L1-U1	2.14	L1-U1
	State Vehicle Type 3	3.67	L1-U1	3.58	L1-U1	4.15	L1-U1	2.27	L1-U1	2.81	L1-U1
	State Vehicle Type 3S2	3.47	L2-U1	3.37	L2-U1	4.03	L2-U1	2.51	L1-U1	3.10	L1-U1
	State Vehicle Type 3-3	3.43	L2-U1	3.32	L2-U1	3.98	L2-U1	2.72	L1-U1	3.37	L1-U1
INVENTORY	HS20	1.48	L1-U1	1.44	L1-U1	1.70	L1-U1	0.92	L1-U1	1.15	L1-U1
(with 10' lanes)	State Vehicle Type 3	1.94	L1-U1	1.90	L1-U1	2.23	L1-U1	1.20	L1-U1	1.51	L1-U1
	State Vehicle Type 3S2	1.84	L2-U1	1.78	L2-U1	2.17	L2-U1	1.33	L1-U1	1.67	L1-U1
	State Vehicle Type 3-3	1.81	L2-U1	1.76	L2-U1	2.14	L2-U1	1.44	L1-U1	1.81	L1-U1
OPERATING	HS20	2.47	L1-U1	2.41	L1-U1	2.83	L1-U1	1.53	L1-U1	1.92	L1-U1
(with 10' lanes)	State Vehicle Type 3	3.24	L1-U1	3.17	L1-U1	3.72	L1-U1	2.01	L1-U1	2.52	L1-U1
	State Vehicle Type 3S2	3.07	L2-U1	2.98	L2-U1	3.62	L2-U1	2.21	L1-U1	2.78	L1-U1
	State Vehicle Type 3-3	3.03	L2-U1	2.93	L2-U1	3.57	L2-U1	2.41	L1-U1	3.02	L1-U1

Truss Designations:

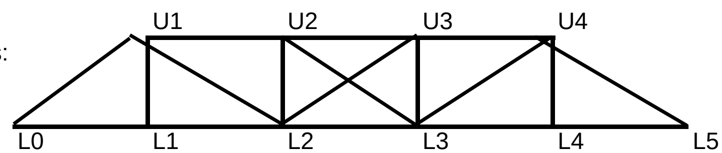

* These ratings take into account section loss at L1-U1 (east truss).

Table D.7 - ANSYS LFD Inventory and Operating Truss Rating of the Orriginal Design Condition

Left Truss, Concrete Slab										LFD RATING	
								Allowable			
Element Number	**Bridge E.NB**	**1.3*DL-ANSYS**	**DL-TRAP**	**3.00**	**4.00**	**2.17*Max LL+I**	**2.17*Min LL+I**	**T/0.55**	**C*0.85*2.12**	**RF,+ve**	**RF,-ve**
19	**L0-L1**	155.35	183.17		177.20	125.21		566.18		3.28	
20	**L1-L2**	150.23	183.17		172.20	122.91		566.18		3.38	
21	**L2-L3**	217.20	274.69		253.20	186.89		861.31		3.45	
22	**L3-L4**	126.75	184.47		136.00	83.55		566.18		5.26	
23	**L4-L5**	139.49	184.47		150.40	93.53		566.18		4.56	
24	**U1-U2**	-240.34	-273.65		-285.00		-217.27		-714.85		2.18
25	**U2-U3**	-238.25	-273.39		-273.00		-194.72		-714.85		2.45
26	**U3-U4**	-231.56	-274.43		-264.60		-187.65		-714.85		2.58
29	**L1-U1**	82.15	81.38	109.60		100.70		346.11		2.62	
33	**L2-U2**	-11.22	-5.59	-20.00			-24.67	474.55	-315.75		24.31
34	**L3-U3**	-11.22	-5.85	-20.00			-24.67	474.55	-315.75		13.25
30	**L4-U4**	37.12	81.38	29.20		1.40		346.11		220.37	
27	**L0-U1**	-240.21	-258.96		-276.20		-198.39		-1234.26		5.01
31	**L2-U1**	107.26	127.92		134.00	111.74		420.20		2.80	
36	**L2-U3**	9.47	-1.43	18.00		23.25		209.49	-16.15	8.60	
35	**L3-U2**	9.47	-1.43	18.00		23.25		209.49	-16.15	8.60	
32	**L3-U4**	130.98	127.14		162.00	132.90		420.20		2.18	
28	**L5-U4**	-197.26	-260.91		-213.00		-132.94		-1234.26		7.80

Table D.8 - ANSYS LFD Truss Rating of the New FRP Deck

	Left Truss, FRP Slab								LFD RATING	
							Allowable			
	Element Number	**Bridge E.NB**	**1.3*DL-ANSYS**	**DL-TRAP**	**2.17*Max LL+I**	**2.17*Min LL+I**	**T/0.55**	**C*0.85*2.12**	**RF,+ve**	**RF,-ve**
Bottom Chord	**19**	**L0-L1**	77.11	16.10	125.21		566.18		3.91	
	20	**L1-L2**	74.52	126.10	122.91		566.18		4.00	
	21	**L2-L3**	108.95	189.28	186.89		861.31		4.03	
	22	**L3-L4**	66.25	127.53	83.55		566.18		5.98	
	23	**L4-L5**	72.45	127.53	93.53		566.18		5.28	
Top Chord	**24**	**U1-U2**	-118.95	-188.11		-217.27		-714.85		2.74
	25	**U2-U3**	-118.31	-187.85		-194.72		-714.85		3.06
	26	**U3-U4**	-116.07	-188.89		-187.65		-714.85		3.19
Verticals	**29**	**L1-U1**	34.82	52.91	100.70		346.11		3.09	
	33	**L2-U2**	-7.08	-5.59		-24.67	474.55	-315.75		18.35
	34	**L3-U3**	-7.08	-5.85		-24.67	474.55	-315.75		13.09
	30	**L4-U4**	18.96	52.91	1.40		346.11		233.32	
Diagonals	**27**	**L0-U1**	-118.86	-178.36		-198.39		-1234.26		5.62
	31	**L2-U1**	53.36	87.62	111.74		420.20		3.28	
	36	**L2-U3**	3.17	-1.56	23.25		209.49	-16.15	8.87	
	35	**L3-U2**	3.17	-0.39	23.25		209.49	-16.15	8.87	
	32	**L3-U4**	62.07	86.84	132.90		420.20		2.69	
	28	**L5-U4**	-102.46	-180.31		-132.94		-1234.26		8.51